THREE-BODY ABRASION SENSITIVITY
OF TRIBO-MECHANICAL COMPONENTS
UNDER FLUID FILM LUBRICATION

By

JIA-LUO XUAN

Diploma
Shanghai University of Technology
Shanghai, China
1979

Master of Engineering Science
Shanghai University of Technology
Shanghai, China
1981

Submitted to the Faculty of the
Graduate College of the
Oklahoma State University
in partial fulfillment of
the requirements for
the Degree of
DOCTOR OF PHILOSOPHY
May, 1988

THREE-BODY ABRASION SENSITIVITY

OF TRIBO-MECHANICAL COMPONENTS

UNDER FLUID FILM LUBRICATION

Thesis Approved:

E. C. Fitch

Thesis Adviser

David G. Lilley

Peter M. Moretti

M. J. Folk

Norman N. Durham

Dean of the Graduate College

PREFACE

This thesis is concerned with a topic fundamental to both tribology and contamination control : the investigation of the time-dependent performance degradation process caused by contaminant particles in most tribo-mechanical components which work under fluid film lubrication. The component is sensitive to particulate contaminants since such a three-body abrasive wear process does occur and can critically jeopardize the service life of the component, even the system. To solve this problem -- to be able to predict, prevent, and diagnose the degradation process -- requires a comprehensive base, both theoretical and experimental, upon which new concepts and useful techniques can be developed. I truly feel fortunate that I can work with Dr. E.C.Fitch at the Fluid Power Research Center, Oklahoma State University, where he initiated the Basic Fluid Power Research Program 21 years ago and the Tribological System Fluid Program 8 years ago. It is these programs that have provided an excellent research base upon which to build this thesis.

It gives me great pleasure to acknowledge my gratitude to Dr. E.C. Fitch, my major advisor and graduate committee chairman, whose personal efforts made my formal education feasible. His contagious enthusiasm for engineering endeavors, his guidance based on his rich engineering experience, and his support through my doctoral program are extremely appreciated.

To the other members of my graduate committee, composed of Dr. P.M. Moretti, Dr. D.G. Lilley, and Dr. M.J. Folk, I extend my sincere thanks for their guidance, critiques, and patience during my research.

I am very grateful to Dr. I.T. Hong, Technical Director of FPRC, who unselfishly shared his time to discuss the Omega theory and give other help.

I want to thank my other colleagues at the FPRC, OSU, for their willing cooperation and help in this research. Mr. J.G. Eleftherakis, Dr. Gabriel Silva, Mr.Ibrahim Khalil, Mr. David LeNorman, Mr. Mark Torbett, Mr. Pat Nealon, and Mr. Rueben Brown, deserve thanks for their assistance in pump test preparation and particle counter work. Thanks are also to Ms.Stacey Sanderlin for her editing of this dissertation.

To Ms. Ruo-Ling Hu, I extend my appreciation for her assistance in typing part of this final manuscript and for her encouragement during this research.

In addition, I want to acknowledge the support received from various organizations as follows :

To Shanghai University of Technology who has supported the initial expense for my doctoral study;

To sponsoring companies of the Basic Fluid Power

Research Program and the Tribological System Fluid Program who have furnished financial support during my research.

Finally, I must thank my parents. The confidence and encouragement shown by my mother, Mrs. Ci Jia Xuan, and my father, Mr. Sun-Tung Xuan, have provided great incentive. To my two brothers, Mr. Jiaji Xuan and Mr. Xiang Xuan, I extend my thanks for their encouragement. Most of all, I would like to thank my wife, Xing Zhou, and my son, Lan Xuan, for their sacrifices, encouragement, and understanding during my graduate study at OSU.

TABLE OF CONTENTS

LIST OF TABLES

Table		Page
XX.	Comparison of Wear and Flow Degradation.	147
XXI.	Comparison of Pump Contaminant Sensitivity . . .	153
XXII.	Particle Counting Data in Test using ACFTD . . .	183
XXIII.	Particle Counting Data in Test using Iron Powder.	184
XXIV.	Particle Counting Data in Test using Glass Beads.	185
XXV.	Particle Counting Data in Test using Al_2O_3 . . .	186

TABLE OF FIGURES

Figure		Page

Figure		Page

Figure		Page

CHAPTER I

INTRODUCTION

Basically, any component with internal surfaces that move relative to one another, and particularly on these surfaces minimal wear and friction should occur, can be classified as a tribo-mechanical component. A system consisting of such components is a tribo-mechanical system. Tribo-mechanical systems include most modern machines, such as hydraulic and pneumatic power, lubrication, fuel, and coolant type systems. It is known that the great majority of failures of tribo-mechanical systems occur as a result of a deterioration process. In many cases, when hydraulic or lubrication components contain two metal surfaces in relative motion that are separated by a fluid film, three-body abrasive wear due to contaminant particles in the fluid is the predominant failure mechanism. In this situation, component performance degrades because of deterioration of critical surfaces and change of clearance (1). Therefore, wear of components in a contaminated environment has been widely recognized as a serious problem and as a primary factor in the life and reliability of hydraulic and lubrication systems (2-7).

Until now, there were two ways to investigate the particulate-induced wear. The first was to study the fundamental wear mechanisms through experiments on various laboratory wear testers. This traditional research approach in the field of tribology provided basic understanding of three-body abrasion. The second approach, on the other hand, is to research the contaminant tolerance of fluid components. By conducting contaminant sensitivity tests on actual components, this method illustrates the wear-induced performance deterioration process in a component exposed to a contaminated environment. This approach leads to the theory of particulate contaminant control which has been widely accepted by the military and the fluid power industry.

A thorough literature survey shows that although many researchers have attempted to investigate the process of abrasive wear, theoretical analysis of three-body abrasion under fluid film lubrication is very limited. It has only been in recent years that this subject has become attractive in tribology. The effect of entrained contaminant particles on surface wear needs to be studied when modeling tribo-systems (8). Furthermore, the relationship between contaminant wear and system performance degradation could not be analyzed theoretically in the past because of the lack of basic understanding of particle effect and the difficulty in identifying the wear-dependence of sensitivity coefficient.

Recently there has been a growing demand from the users of fluid tribo-mechanical systems to develop an effective method which can be applied to estimate the characteristics of performance degradation for a component subjected to an environment with known contamination level. It is clear that in order to achieve such a goal, fundamental theories of processes of both lubricated three-body abrasive wear and performance degradation are necessary.

The purpose of this research is twofold : to develop a theoretical model for simulating the lubricated three-body abrasive wear process, and to establish a three-body abrasion sensitivity theory for analysis of system reliability, contamination control, and component design. In this research, the wear mechanism is investigated with emphasis on the effects of particle properties and the interactions in a "metal-fluid-particle-metal" tribo-system. A generic concept of component performance degradation is presented based on "wear-leakage-degradation" analysis. By incorporating the wear model with degradation analysis, the three-body abrasion sensitivity theory is formulated to predict the contaminant tolerance of a tribo-mechanical component under fluid film lubrication. Experimental tests are conducted to validate these theoretical models.

The next chapter provides background about three-body abrasive wear and component contaminant tolerance (or sensitivity) and outlines previous investigations. Chapter

III is devoted to the development of the wear model and component sensitivity theory. Chapters IV and V delineate the results of the experimental programs to evaluate the wear model and contaminant sensitivity theory, respectively. Finally, in chapter VI the significance of the research is discussed and recommendations for further studies are presented. Chapter VII is a summary along with specific conclusions resulting from this research investigation. The appendices contains typical test data and experiment procedures.

CHAPTER II

BACKGROUND

Previously, wear research was dominated by phenomenological studies. The cost of wear was rarely appreciated by researchers and workers (9) until the Jost Report (10) was published in 1966; this report brought wear to a recognizable level of technology. One branch of wear technology, the research of three-body abrasive wear under fluid film lubrication, has been more active recently because of the ever-increasing demand for contamination control in industries. In this chapter, research in two contaminant-related aspects -- wear analysis and contaminant tolerance of components, will be reviewed in detail.

Three-body Abrasive Wear Investigation

General View of Abrasive Wear

According to a recent survey by the Canada Associate Committee on Tribology (11) abrasive wear is responsible for the largest amount of wear in industrial machinery. Traditionally, abrasive wear processes are divided into two groups: two-body and three-body abrasive wear, depending on

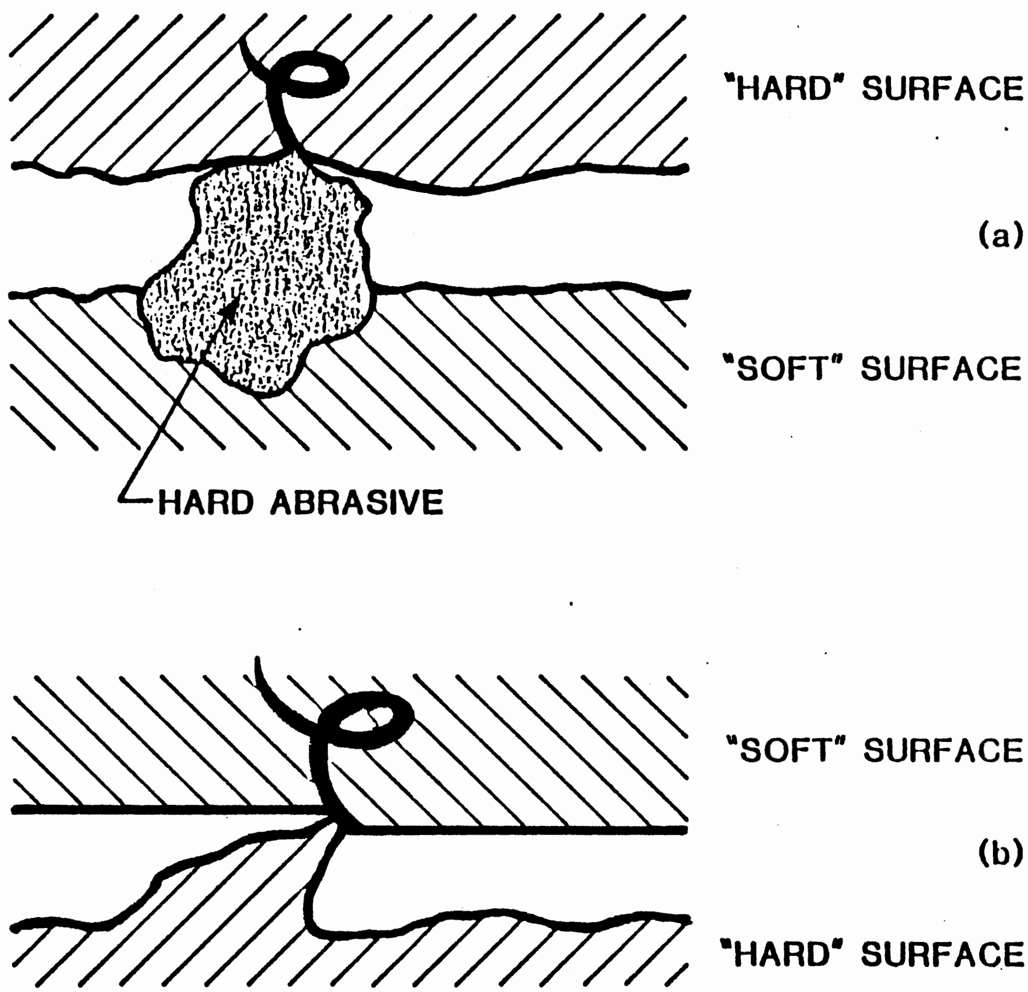

Fig.1 Three-body(a) and Two-body Abrasive Wear

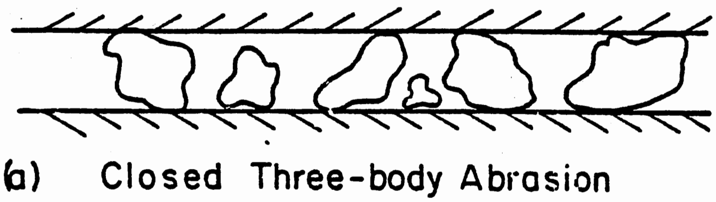

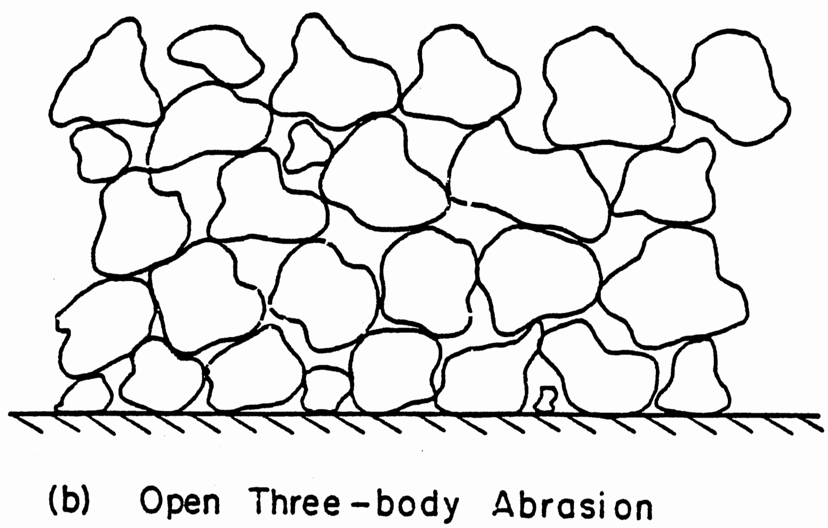

Fig.2 Closed (a) and Open (b) Three-Body Abrasive Wear (36)(1979)

whether the wear is produced by hard asperities or by hard particles which cut or groove one of the rubbing surfaces (Fig.1)(12). According to Misra (36), the three-body case can be further divided into "closed" and "open" three-body abrasion as presented in Fig.2. Most of the abrasive wear problems that arise in industrial and agricultural equipment are caused by closed three-body abrasion, either lubricated or unlubricated.

Development of Three-body Abrasion Research

The historical development of research related to three-body abrasion can be divided into an initial period (before 1978) and a period of fast development after that.

During the first period, relatively few papers were published on this subject (12-32). Most of the papers that were published discuss experimental research concentrated on identifying basic wear parameters. Based on the fundamental works by Archard, Scott, Hirano, Khrushchov, Rabinowicz, Richardson, and Halling, et al., some important observations were obtained.

Among those early studies, results from Khrushchov's pin-on-disc tests (13) are significant because he found that wear resistance is directly proportional to the material hardness for pure annealed metals and some alloys while different relations apply for hardened and tempered steels. In addition, this resistance is found to increase with carbon content. But these observations are basically applicable to two-body abrasion situations.

An early systematic investigation on closed three-body abrasive wear under wet condition was performed by Hirano and Yamamoto (14). They studied tne effects of hardness, size, and concentration of particles and viscosity of oil on wear by using a four-ball machine. They confirmed the influence of particle hardness. Softer abrasives like metal powder do not penetrate into the contact surface but accumulate at the front of the contact area and disturb the formation of an oil film in point contact, causing a slight amount of abrasion. On the other hand, harder particles such as quartz powder are easily introduced into the contact area, causing marked increase in abrasion. The effect of particle hardness on ball wear is presented in Fig.3. The effect of particle size is shown in Fig.4. From this figure it is seen that the intermediate size #500 gives the highest wear value (impression area $A-A_0$), while the finest particles #1000 shows much less abrasion. Particles #120 are presumably too coarse to be introduced into the rubbing surfaces. A straightforward relation is found between wear and particle concentration, as depicted in Fig.4.

Toporov (15) conducted one of the earliest experiments for closed, dry three-body abrasive wear on cast iron. Afterwards, a more detailed study of this problem was carried out by Rabinowicz et al (16). By using the

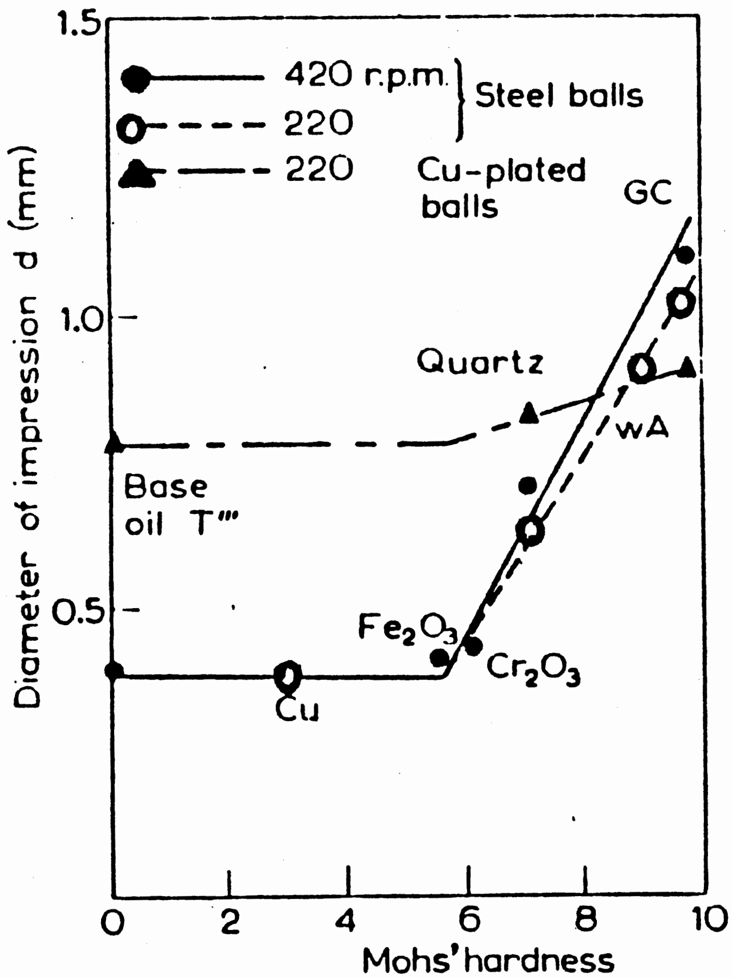

Fig.3 Effect of Particle Hardness on Abrasive Wear (14)(1958)

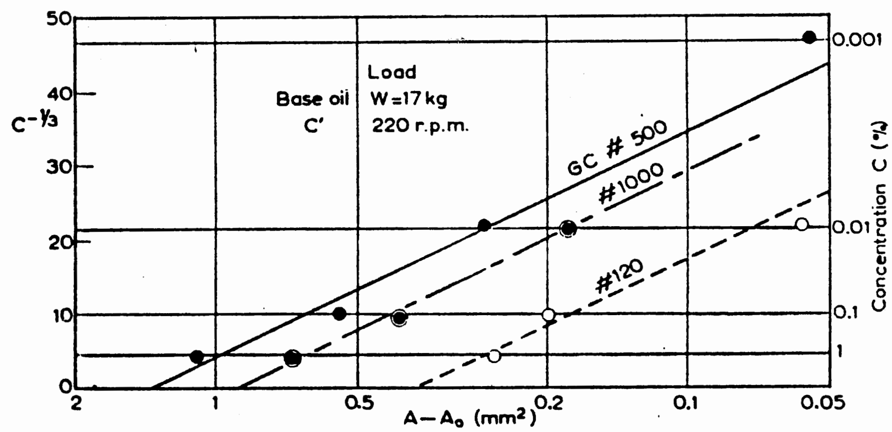

Fig.4 Relation between $A-A_0$ and Concentration of Particles. Also Effect of Particle Size (14) (1958)

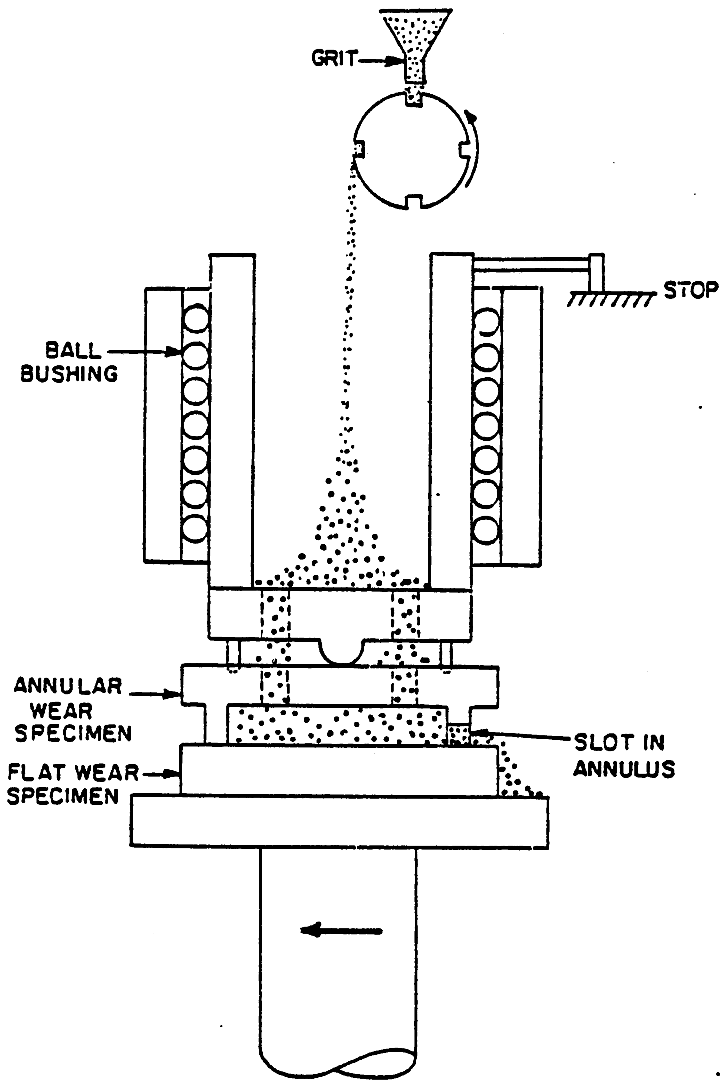

Fig.5 Rabinowicz's Closed Three-Body Abrasive Wear Tester (16) (1961)

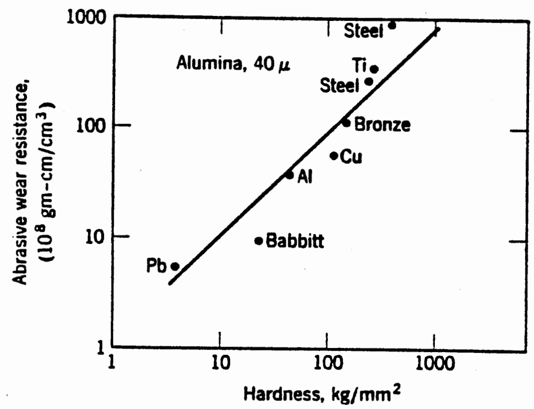

(a) Metals Annealed

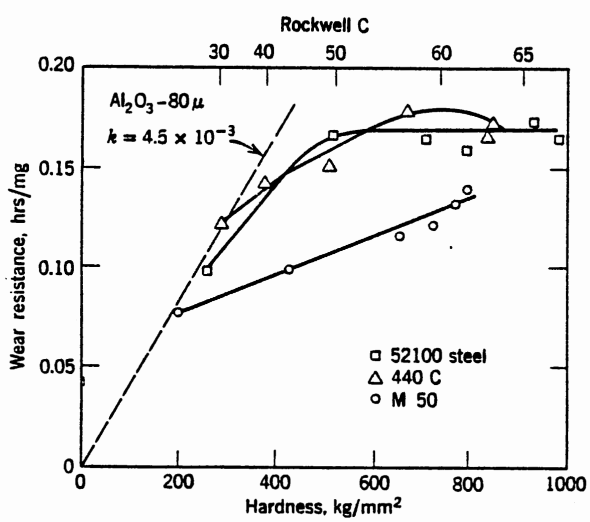

(b) Bearing Steels Heat Treated
in Various Ways

Fig.6 Effect of Metal Hardness on
Dry Three-Body Abrasion
(16) (1961)

apparatus shown in Fig.5, they found a similar relationship exists between wear resistance and metal surface hardness: linear for "technically pure" metals annealed and abraded by alumina particles (Fig.6-a) but nonlinear for quenched and tempered steels (Fig.6-b). To explain the lower wear resistance of harder surfaces, Rabinowicz (17) concluded that brittleness makes wear debris larger than the wear groove size.

The particle size effect was also investigated by Rabinowicz and his colleagues (Fig.7). They verified the phenomenon of critical size. If particles tested are smaller than this size, wear strongly depends on the particle sizes. However, wear is almost constant when the test particles are larger than the critical size. They explained that the reduction of wear with decreasing size is due to the interruption of an adhesive wear process.

A similar critical phenomenon of particle hardness has been known since Wahl (18) reported his wear results (Fig.8). Khruschov (19) and Richardson (20,21,24,25) had attempted to define this relationship with greater precision. According to Khruschov, the wear rate is very low when metal is harder than abrasive ($H_m/H_a > 1$). As the ratio decreases, the wear rate starts to increase and reaches a maximum value when $H_m/H_a < k$, where k lies between 0.6 and 0.7. Nathan and Jones (22) indicated k to be about 0.5. Richardson quoted a higher k value of 0.8 based a fully

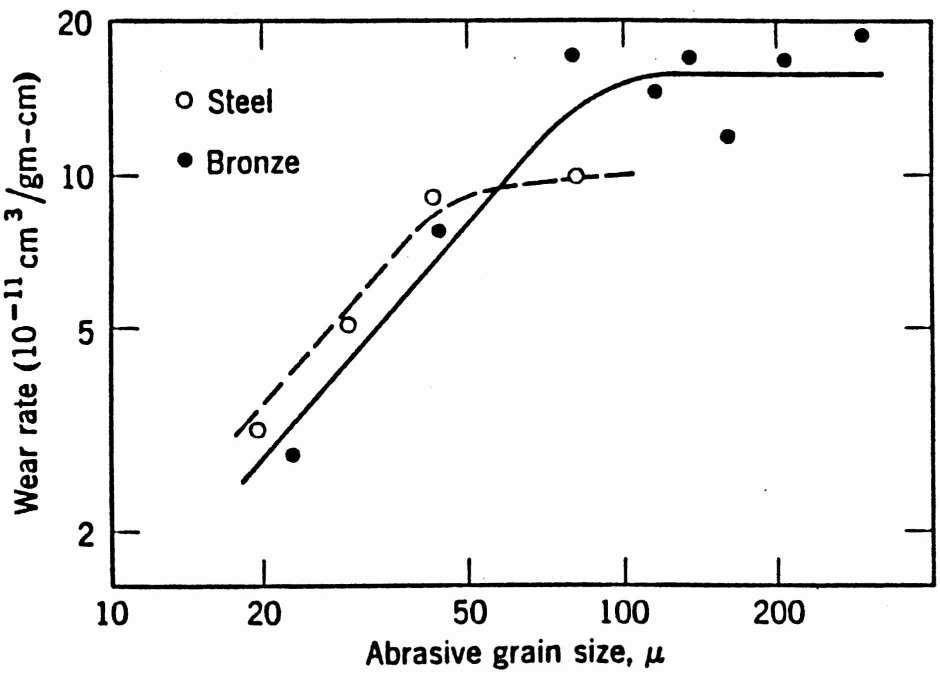

Fig.7 Wear Rate of Two Metals as a Function of Abrasive Grain Size (16) (1961)

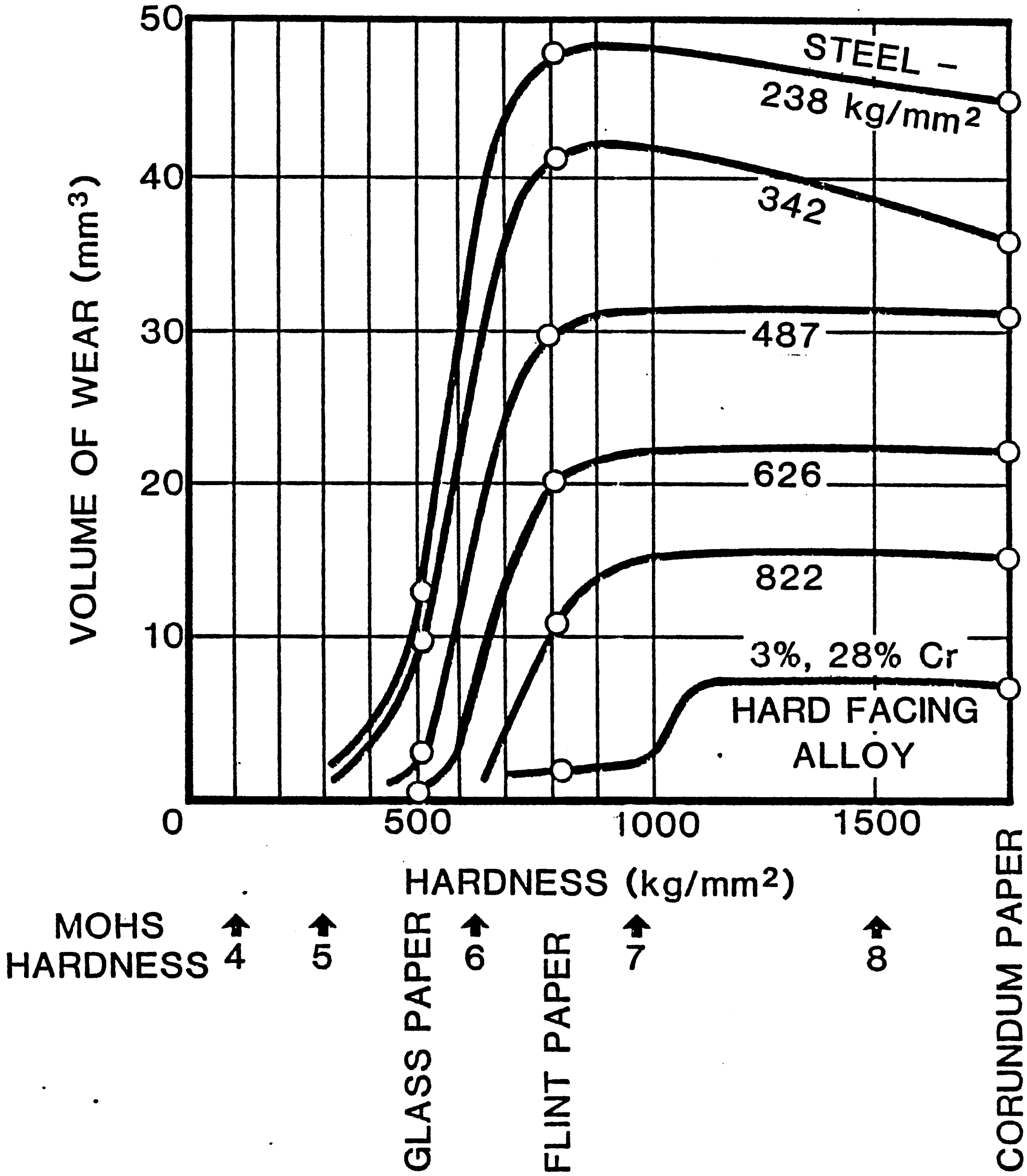

Fig.8 Wear of Several Steels against the Hardness of Abrasives (18) (1954)

strained hardness H_u. Tabor (23) observed that abrasive wear could occur only if the particle was at least 20 percent harder than the worn surface.

Broeder and Heijnekamp (28) experimentally studied abrasive wear in a plain journal-bearing by introducing silicon particles into the oil mixture. Embedding of particles was observed at various places in the softer bushes. They concluded that a soft metal bush does not guarantee low shaft wear.

Both Larsen-Badse (27) and Wright (29) analyzed the effect of surface plastic deformation on cutting efficiency in abrasion. They estimated that only 15 to 20 percent of the groove volume is actually removed during a single abrasive passage. This estimation agrees with results of Mulhearn and Samuels (30) and Stroud and Wilman (31) for cold-drawn steels. However, for silver the percentage of metal removal increases up to 40.

The general relationship between particle size and fluid film thickness under lubricated condition was discussed by Scott (32). He concluded that particles smaller than the minimum oil film thickness have no serious effect on bearing performance but larger particles might become embedded in the softer material or be crushed. He suggested an increase of abrasive wear when lubricant is present in comparison to the dry condition; however, no experiment details or further explanation was provided.

Basically, researchers in the first period were aware of wear failure due to contaminant and studies of both dry and wet abrasive wear were initiated. Important factors revealed were surface hardness, surface deformation, abrasive hardness, grit size, and particle concentration. Some transition phenomena, such as the critical size and critical hardness, were observed. However, none of these explanations for the above phenomena is satisfactory, since the physical basis is unclear. No theoretical model of three-body abrasive wear under fluid film lubrication was proposed. This situation has changed since 1978, as many systematic investigations on three-body abrasion have been published in the second period.

Tessmann (33) and Fitch (34) summarized wear studies conducted in 1977 for The Naval Research Office by the Fluid Power Research Center of Oklahoma State University. The effects of particle size, particle concentration, and material combination on contaminant wear in two different fundamental mechanisms -- a rotating device (Fig.9-a) and a linear reciprocating apparatus (Fig.9-b), were analyzed. Wear was evaluated using the Ferrographic Oil Analysis Technique and represented by the D54 reading (optical density at 54mm location on ferrogram), shown in Fig.10. A comparison between Fig.10-a and 10-b reveals that in rotary mechanisms, more wear was generated with the brass-steel combination than with the aluminum-steel at all

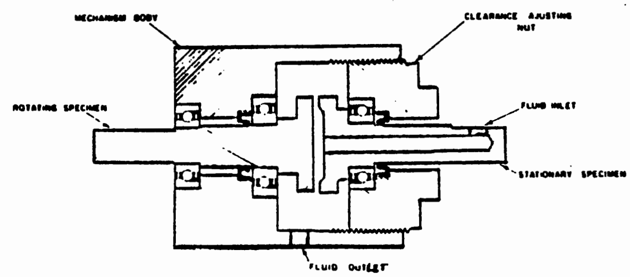

(a)

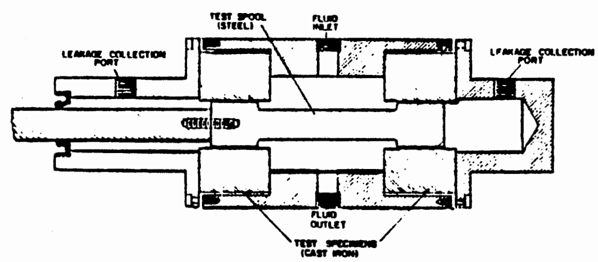

(b)

Fig.9 Schematic of Rotary (a) and Linear (b) Mechanisms (33) (1977)

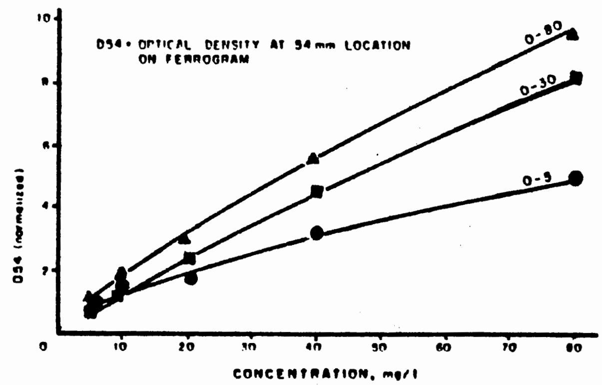

(a) Rotary Mechanism (Brass/Steel)

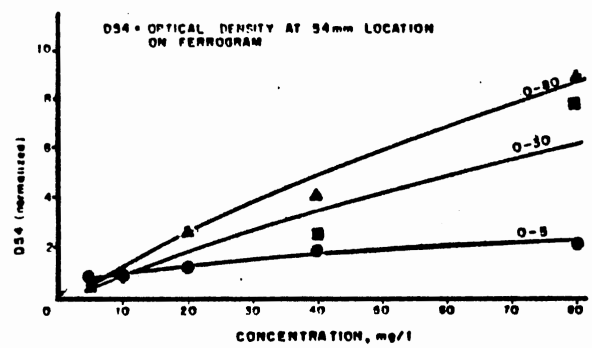

(b) Rotary Mechanism (Aluminium/Steel)

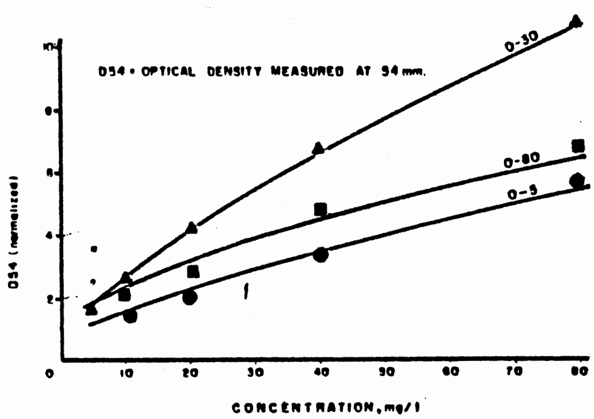

(c) Linear Mechanism

Fig.10 Effects of Particle Size and Concentration on Abrasive Wear (33)

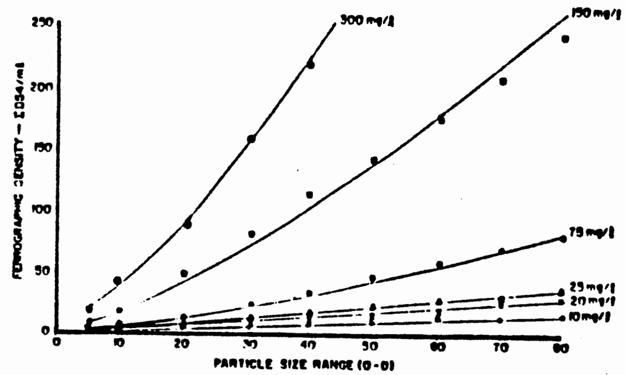

(a) Pump Wear Test (138 bar)

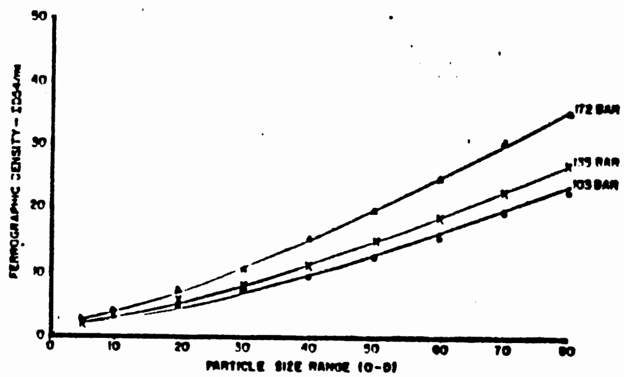

(b) Pump Wear Test (20 mg/L)

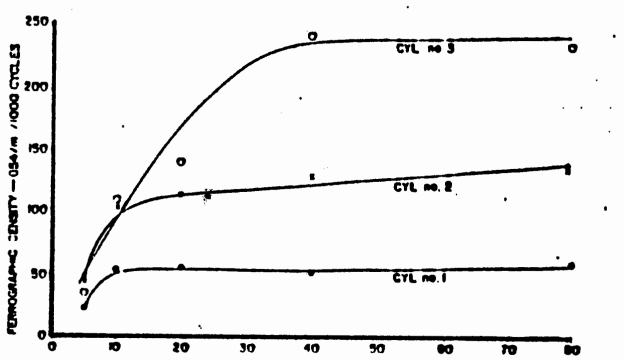

(c) Cylinder Wear Test (172 bar, 300 mg/L)

Fig.11 Abrasive Wear in Hydraulic Pump and Cylinder (34) concentration levels of small size (0-5 μm ACFTD particle). However, the same wear was generated with both metal combinations when using coarse particles (0-80 um). In linear mechanisms (Fig.10-c), the highest wear occurred with intermediate size, (0-30 um). This result agrees with the previous study and is normally attributed to a wedging action of critical size particles that are close to the clearance dimension. Abrasive wear tests on realistic hydraulic pumps and cylinders were also carried out (Fig.11).

A semi-quantitative analysis on three-body wear was presented by Suh and his colleague (35) at the Massachusetts Institute of Technology. They explained why using Rabinowicz and coworkers' (17) two-body wear model of a rigid conical asperity would predict a three-body wear coefficient of one or two orders higher than experimental values. The reason is that the subsurface deformation causes less material to be removed. They further postulated that the three-body wear coefficient is a function of cutting energy, plowing energy, and subsurface deformation energy. Because with a conical particle model, the cutting energy will decrease with decreasing width-to-depth ratio in indentation (Fig.12), the wear will decrease with smaller grits accordingly.

In 1979, Misra and Finnie (36-41), at the University of California, Berkeley, systematically compared two wear

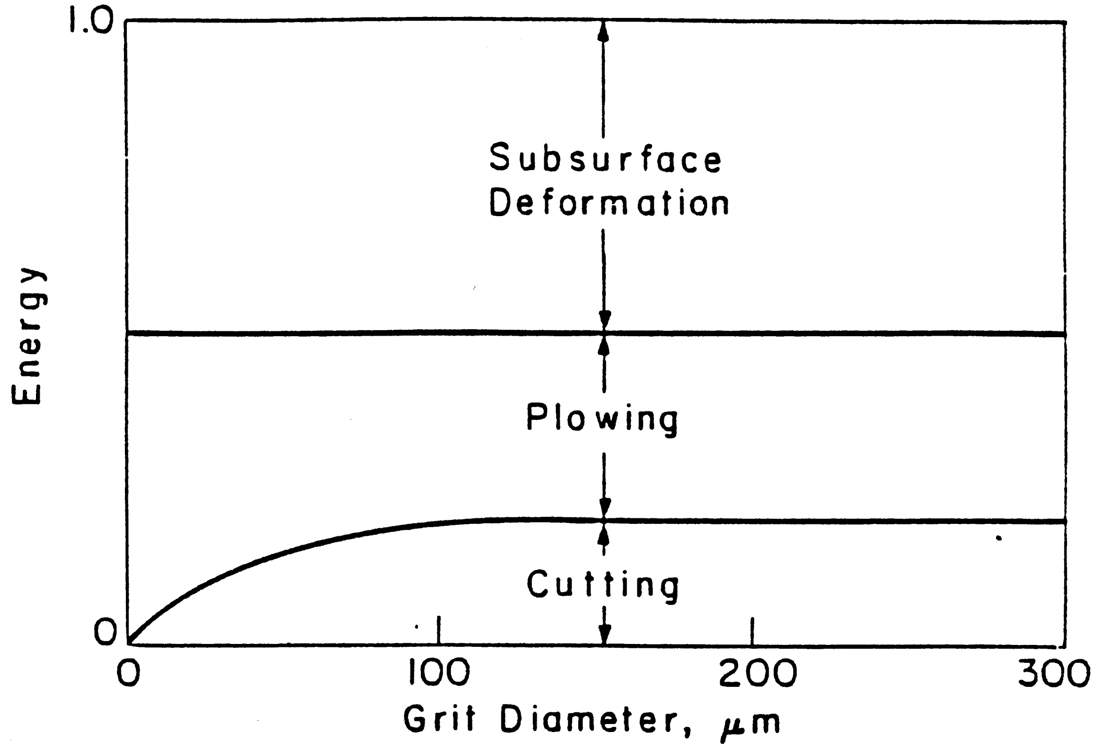

Fig.12 Schematic of Energy Components in Abrasion
(35) (1978)

cases: low-stress, open, three-body abrasion, and two-body abrasion under dry condition. Misra (36) made two major observations. One is that the critical size is about 100um for both cases. Another is that the wear rate depends on the metal-to-abrasive hardness ratio H_m/H_a. Wear rate is a constant for $H_m/H_a<0.8$ and is very low for $H_m/H_a>1.2$.

In the "Wear Control Handbook" published by ASME in 1980, both Peterson (42) and Archard (43) pointed out the importance of dirt or solid particles in wear research. Based on experiments, Rabinowicz (44) estimated that the wear coefficient is typically about 0.001 for dry three-body abrasion and 0.002 for lubricated conditions. He believed that this coefficient is determined mainly by the sharpness of the abrasive.

In the last five years, a number of papers (45-71) have been published, covering various topics in particle-induced three-body abrasive wear from the effects of wearing surface properties -- microstructure (46,47); shear strength (48,49); alloy composition (50); and hardness (51) -- to influences of particulate parameters -- size (52,53,54); shape(55,56,57); hardness (58,59); and toughness (60,61). Studies in the later category were reviewed by Hong (65) in 1982 and by Xuan (71) in 1987. It is found that the present knowledge is inadequate for predicting three-body abrasive wear under fluid film lubrication. The dependence of wear on particle properties needs to be further investigated.

Lubricated Three-body Abrasion

As stated in preceding sections, this problem has long been addressed and studied experimentally; however, actual analysis of the wear mechanism is very limited. It is only in recent years that some theoretical models have been developed for the purpose of wear prediction.

One such model was developed by Ikraov (62) based on a systematic concept of "material/lubricant/abrasive/material" and considered from forces acting upon the friction surfaces and abrasive particles. However, this model is still too simple to simulate the field wear process since neither the particle concentration nor the size distribution is included.

Actually, because of the continuous processes of filtration and ingression of abrasives in the field, a certain contaminant level or distribution (particle number vs. size) corresponds to each application; this level often takes the form of increasing number with decreasing size rather than the uniform size assumed in most earlier investigations. The inaccuracy in control and prediction of this distribution has been a major obstacle in wear studies. In the last twenty years, the FPRC succeeded in identifying and controlling the particle size distributions. therefore, theoretical analysis on lubricated three-body abrasive wear can be performed quantitatively (63-71).

Hong (66) correlated the wear rate with the filtration ratio, which determines the concentration-size distribution of particles in the field. Based on a discrete distribution concept such that the number of particles of size d_i might be defined as the difference between two consequential inversely cumulative values, the model of total accumulative wear volume at time t is Equation (2.1),

$$V(t) = \sum_{t=0}^{t} \cdot \sum_{d_i=0}^{\infty} (N_{c,d_i} - N_{c,d_i+1}) \cdot k_d \cdot d_i^2 \tag{2.1}$$

where $N_{c,di}$ = concentration of particle greater than d_i

k_d = constant

Subsequent to this model, Ito, Khalil, and Hong (67,68) studied the dependence of cutting depth on particle size to calculate wear on a journal surface, shown in Fig.13. A wear equation similar to Eq.(2.1) was developed, which takes into account hydrodynamic lubrication, indenting and cutting mechanisms, and particle concentration-size effect.

Contaminant Tolerance Investigation

Contamination Control

Contamination control is a developing engineering science (72) and it is receiving more attention today (73-77). In order to improve efficiency and accuracy, machines today have much closer component tolerances, making them more vulnerable to contaminants. Contaminant-induced wear

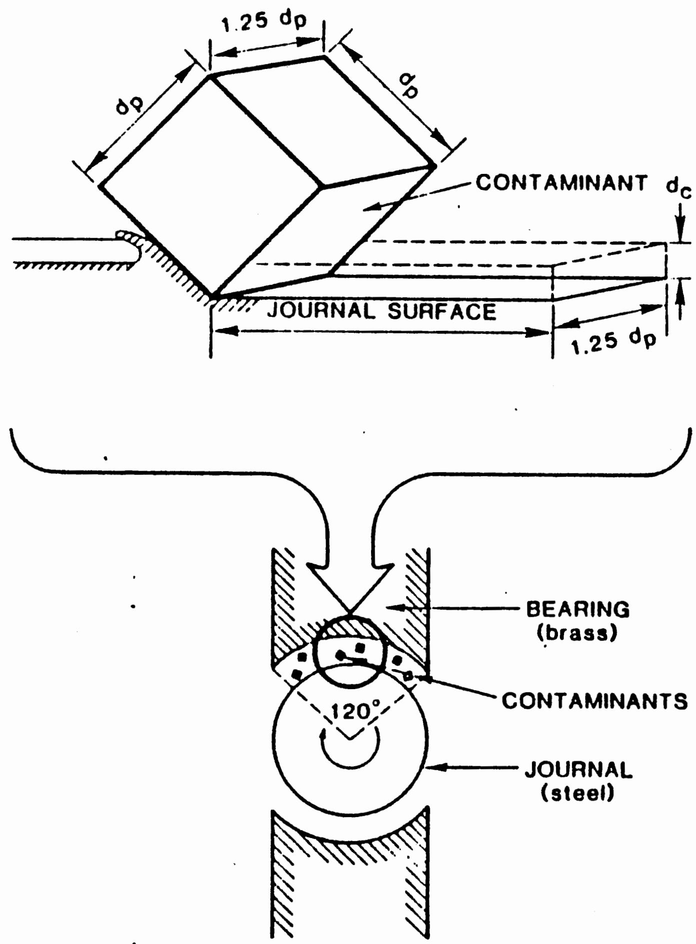

Fig.13 The Cutting Model (67)(1984)

has been reported in various machineries, such as hydrodynamic bearings (78), cylinder lines (79,80), turbomachinery oil systems (81), paper and pulp components (82), jet engines (83), and aircraft hydraulic systems (84). According to Peterson's (75) estimation of cost and frequency attributed to each item in field maintenance, contaminant-caused wear costs the most (Table I). Therefore contaminant monitoring is becoming more important in reliability and service life assessment (85,86). However, contamination control does not only mean monitoring methods but also includes all techniques in contaminant analysis, removal processes, and ingression prevention. Most importantly, however, it includes developing fundamental theories that direct those techniques (1,87). Fitch initiated the research of contamination control for fluid power systems in the early 1960s. Based on experiments conducted at the FPRC in the past two decades, basic theories on major contamination phenomena have been established, and a number of assessment methods developed by the FPRC have gained the approval of NFPA, SAE, ANSI, and ISO (88). According to Fitch (63), the basic consideration of contaminant wear in a fluid component can be expressed in Fig.14, where he shows the wear caused by contaminants is a function of three factors: the system contaminant level, the contaminant abrasivity, and the lubrication mode, which in turn depends on the fluid and component applied. Fitch

TABLE I

COSTS OF CORRECTIVE MAINTENANCE (75) (1982)

Wear	$ 1,420,513
Contamination Given Corrosion	2,373,797
Leaks	505,590
Viberation	579,756
Corrosion	973,820
Broken	481,922
Contamination Given Wear	3,674,622
Misalignment	282,482
Design Faults Given Wear	32,930
Viberation Given Wear	33,549
Contamination Control	565,939
Calibration	88,802
Total	$ 11,013,722

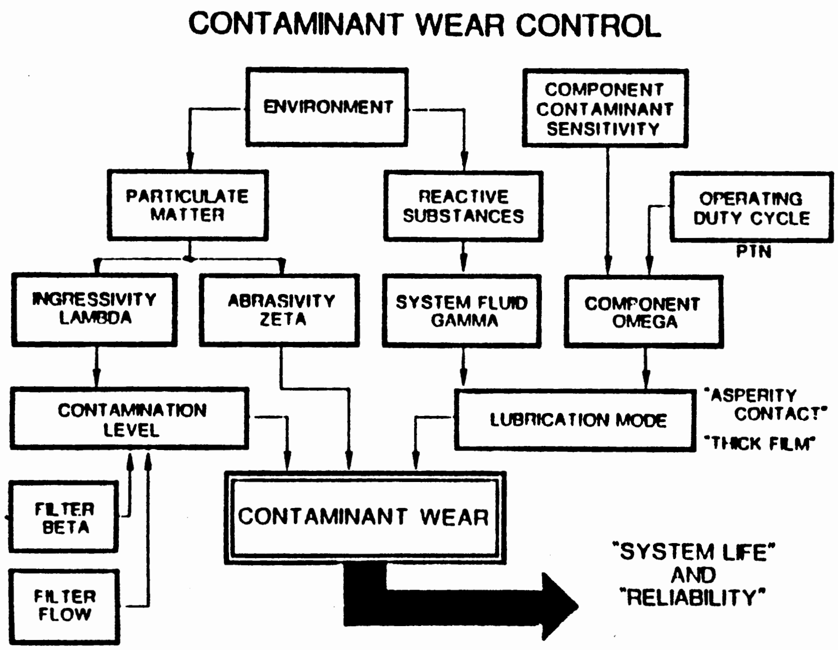

Fig.14 Basic Consideration of Contaminant Wear (63) (1984)

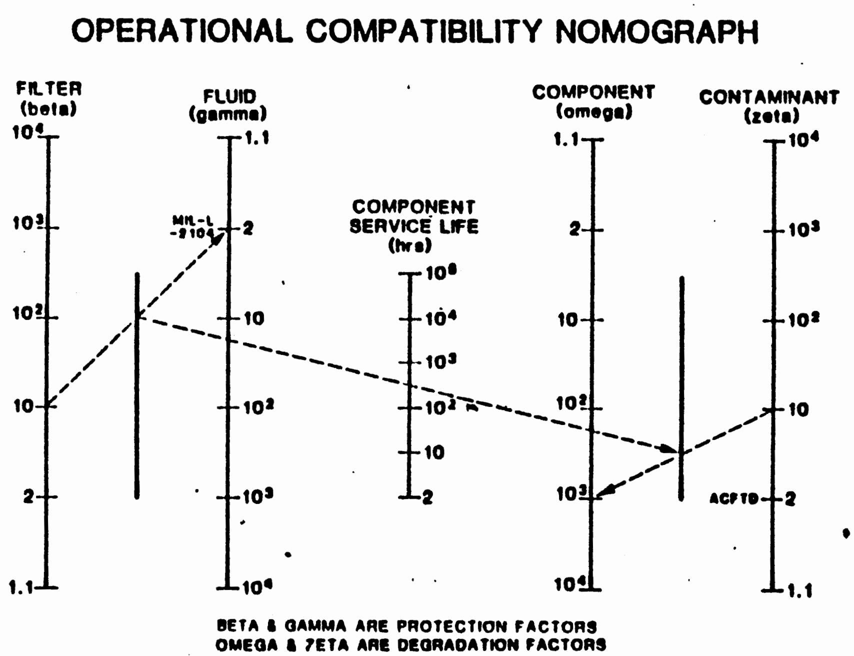

Fig.15 Basic Theory of Contaminant Wear Control (63) (1984)

further explained the wear control theory by using an operational compatibility nomograph, shown in Fig.15. In a fluid system, the filter (its efficiency rating called Beta) and the fluid (its anti-contaminant rating called Gamma) are two protection factors, whereas the component (its contaminant sensitivity rating called Omega) and the contaminant (its abrasivity rating called Zeta) are two factors that cause performance degradation. Therefore, the service life of a component is determined by the balance among the four factors and would be predictable if the four ratings were known. Because theories on the protection factors have been well established (89-119), studies regarding the two degradation factors will be reviewed in the following parts.

Component Sensitivity

It is recognized that the presence of particulate contaminants cause gradual but persistent deterioration of critical surfaces and changes of clearance within a component. Accordingly, these contaminants lead to degradation in a responsive performance parameter (flow-degradation for a pump, speed-degradation for a motor, etc). Therefore, all tribo-mechanical elements are sensitive in some degree to particulate contaminant entrained in the system fluid (1). The term "contaminant sensitivity" refers to the degree of performance degradation that occurs when a component is exposed to a specific contamination environment. The inverse of contaminant sensitivity is the contaminant tolerance, or resistance, which reflects the maximum contaminant level above which performance degrades significantly. Based on these concepts, the sensitivity or tolerance of a component could be experimentally determined. The first contaminant sensitivity test at the FPRC was conducted by Wolf (91) on pumps in 1964. Ten years later, 69 pumps had been tested and a repeatable and reproducible method developed (92-97). The pump contaminant sensitivity test procedure was one of the early documents on the Army's priority list. It also gained approval from NFPA (National Fluid Power Association) in 1976 and from ISO/TC-131/SC-6/WG-6 in 1979 (104).

As regards the interpretation of test results, two things are important. The first is how to define the sensitivity and how to determine it from the degradation test. The second is how to correlate the sensitivity rating with contaminant control.

Bensch and Fitch (94) postulated a sensitivity model based on the premise that for every critical size particle that passes through the component, there is a measurable amount of damage which degrades the performance. Under similar conditions, component exposure to identical critical size particles produces the same amount of performance damage. With this background, they suggested that the pump flow degradation rate (dQ/dt) directly depends on a contaminant sensitivity coefficient (S_i) of the pump to each particle size interval (i) and the particle concentration ($n_i(t)$), as

$$\frac{dQ_i(t)}{dt} = - S_i \cdot Q_i(t) \cdot n_i(t). \tag{2.2}$$

This set of sensitivity coefficients is determined from the pump test. By further assuming that each S_i is proportional to a wear coefficient ${}_i$, Bensch and Fitch derived a pump life model:

$$t = \frac{\ln(Q_0/Q_t)}{\sum_{i=1}^{max} \alpha_i \cdot n_{f,i}^2} \tag{2.3}$$

where t = service life or operating time

Q_0 = initial flow rate

Q_t = flow rate at time t

$n_{f,i}$ = particle concentration at size interval i

Equation (2.3) is used to establish a pump tolerance profile based on a given t.

In order to make the sensitivity results more meaningful, Inoue and Fitch (99,100) superimposed the contaminant tolerance profile of the pump on the standard filter (Beta Ten) profile (Fig.16). Thus it is very clear that any Beta Ten filter below the pump tolerance profile can provide an environment required by the pumps, but the

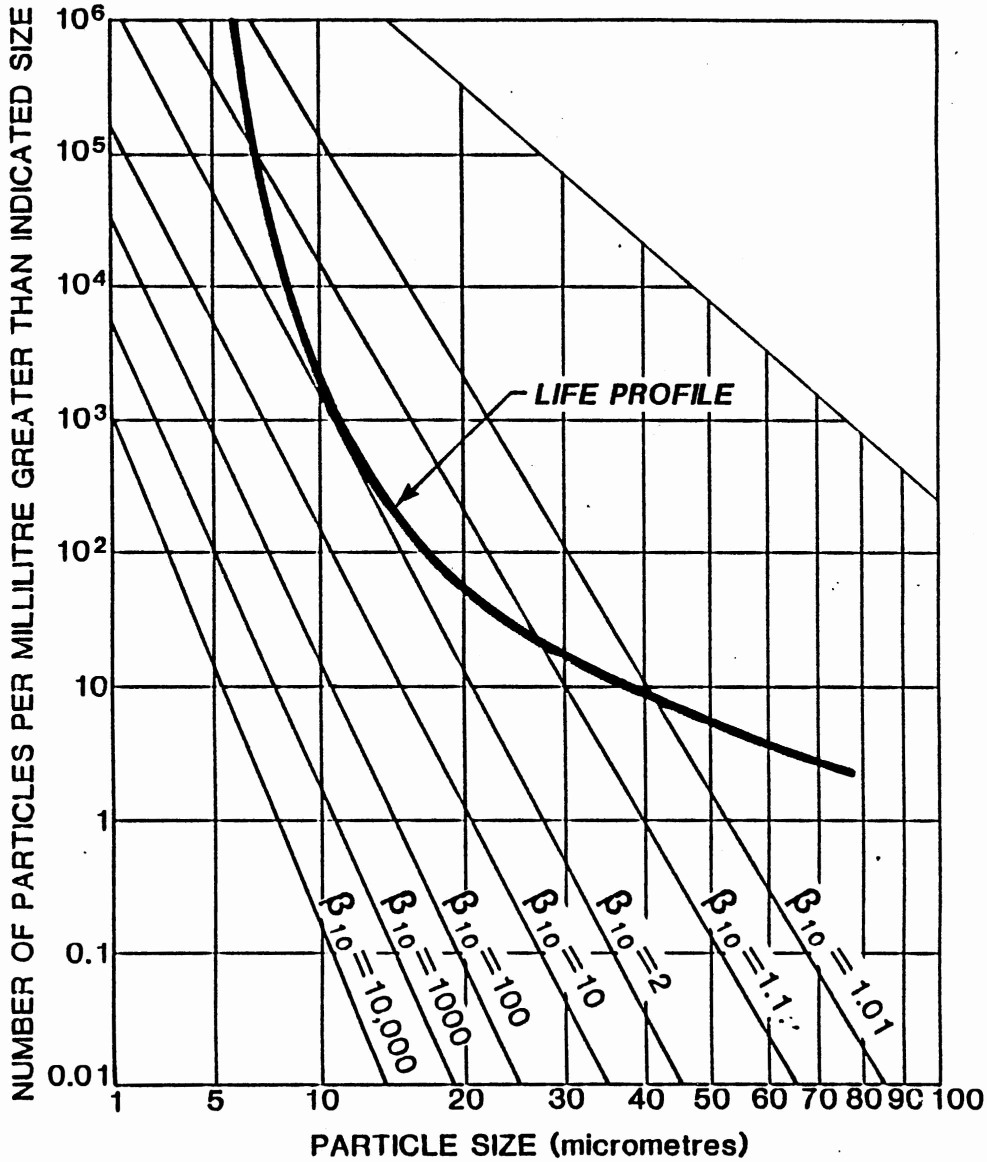

Fig.16 Selection of Filter to Protect a Pump for 1000-Hour Service Life (99)(1979)

optimal one is the one most closely below or tangentially contacting the pump tolerance profile. The value of this optimal Beta Ten filter is termed the "Omega rating" of the pump. A pump with a higher Omega rating is thus more sensitive to particulate attack and requires a better filter to protect it. This result has significantly promoted the application of theoretical research on component contaminant sensitivity and system contaminant control.

From 1974 to 1984, research on contaminant sensitivity of major hydraulic components -- such as pumps, servovalves, relife valves, spool valves, cylinders, seals, motors, gear-transmissions, and bearings, -- has been comprehensively carried out at FPRC (108-110). More than three hundred pumps from twelve different countries have been tested. After comparing these data with the previous model (Eq.2.3), Hong and Fitch (107) found that a linear particle concentration relationship should be adopted as the analytical base. Their linear pump life model is expressed in Equation (2.4),

$$t = \frac{\ln(Q_0/Q_t)}{\sum_{i=1}^{max} S_i \cdot n_{f,i}} \qquad (2.4)$$

where S_i = contaminant sensitivity coefficient at size interval i

Contaminant Abrasivity

As one of the two degradation factors, the particle abrasivity is important since contaminants in the field are often different from AC Fine Test Dust (ACFTD), which is commonly used in standard sensitivity tests. The service life of a tribo-mechanical component, therefore, also depends on the type of contaminants the component is exposed to. Fitch (72) emphasized the significance of developing a technique to differentiate the abrasivity of different contaminants for the ultimate purpose of contaminant life prediction.

Inoue (119) addressed this problem and suggested that the abrasivity of field contaminants be measured relative to the abrasivity of ACFTD.

Hong and Fitch (88) briefly discussed the dependence of the contaminant sensitivity coefficient S_i on particle properties. They introduced a concept of relative contaminant sensitivity, which includes the effect of abrasivity. However, the resultant coefficient $S_{r,i}$ is not available until the involved abrasivity coefficient is solved.

Fundamental investigations on the particle abrasivity rating (Zeta rating) have been conducted at the FPRC in the last two years by Xuan (70,120) and Eleftherakis (61). Xuan attempted to theoretically analyze the effects of critical particle parameters and to establish proper test procedures. During the preliminary stage, more than fifty tests were carried out to qualify the sensitivity and repeatability of an abrasivity test system designed to provide required fluid film condition. Eleftherakis carefully examined the numbers per milliliter for ACFTD and Carbonyl Iron Powder (Grade E). He indicated that the particle abrasivity rating should be a dimensionless quantity on a per particle basis. In this way, he rated that iron powder has an abrasivity of 0.371 compared with one for ACFTD.

Summary of Literature Review

The thorough literature survey shows that contaminant-induced performance degradation in tribo-mechanical elements under fluid film lubrication is a typical three-body abrasive wear phenomenon. The study of wear is necessary to the theory and practice of particulate contaminant control.

But this wear study is incomplete at this stage since the wear process in a "metal-fluid-particle-metal" system is so complicated that there is no theoretical model which can estimate three-body abrasive wear behavior based on available information of surfaces, fluid, and particles. One major obstacle in the development of wear theories is inadequate data and a lack of understanding of the particle property effects on wear under lubricated conditions. Another obstacle is the lack of a system method which can properly correlate the functions of metal, fluid, and particle.

In addition, the research of contaminant tolerance is also incomplete since the physical meaning of those sensitivity coefficients has not been well interpreted. Therefore, the contaminant sensitivity of a component has to be determined experimentally, as its sensitivity coefficients can not be obtained through analysis. Also, the data of particle abrasivity are seriously lacking, leading to inaccurate estimations of wear and performance degradation.

CHAPTER III

DEVELOPMENT OF THEORETICAL MODELS

Model of Three-body Abrasive Wear under Fluid Film Lubrication

Under conditions of fluid film lubrication, three-body abrasive wear occurs when loose abrasive particles or wear debris in the lubricant roll, indent, and cut metal surfaces. Many papers (63-71) have shown that material is removed in this process by abrasives indented into the softer surface and supported by this surface to cut the harder surface. Only strong particles larger than the local fluid film thickness (as shown in Fig.17) can indent and cut. Other particles just roll between the surfaces and do not remove material from surfaces. For this type of abrasion, the actual film thickness, abrasive properties (size, shape, hardness, and toughness), and metal-to-abrasive hardness ratio are most important.

Particle Size Effect

Fluid film lubrication is found in the cylinder bores and valve plates of axial pistons or radial pumps (or motors), in the vane cavities of vane pumps (or motors), in

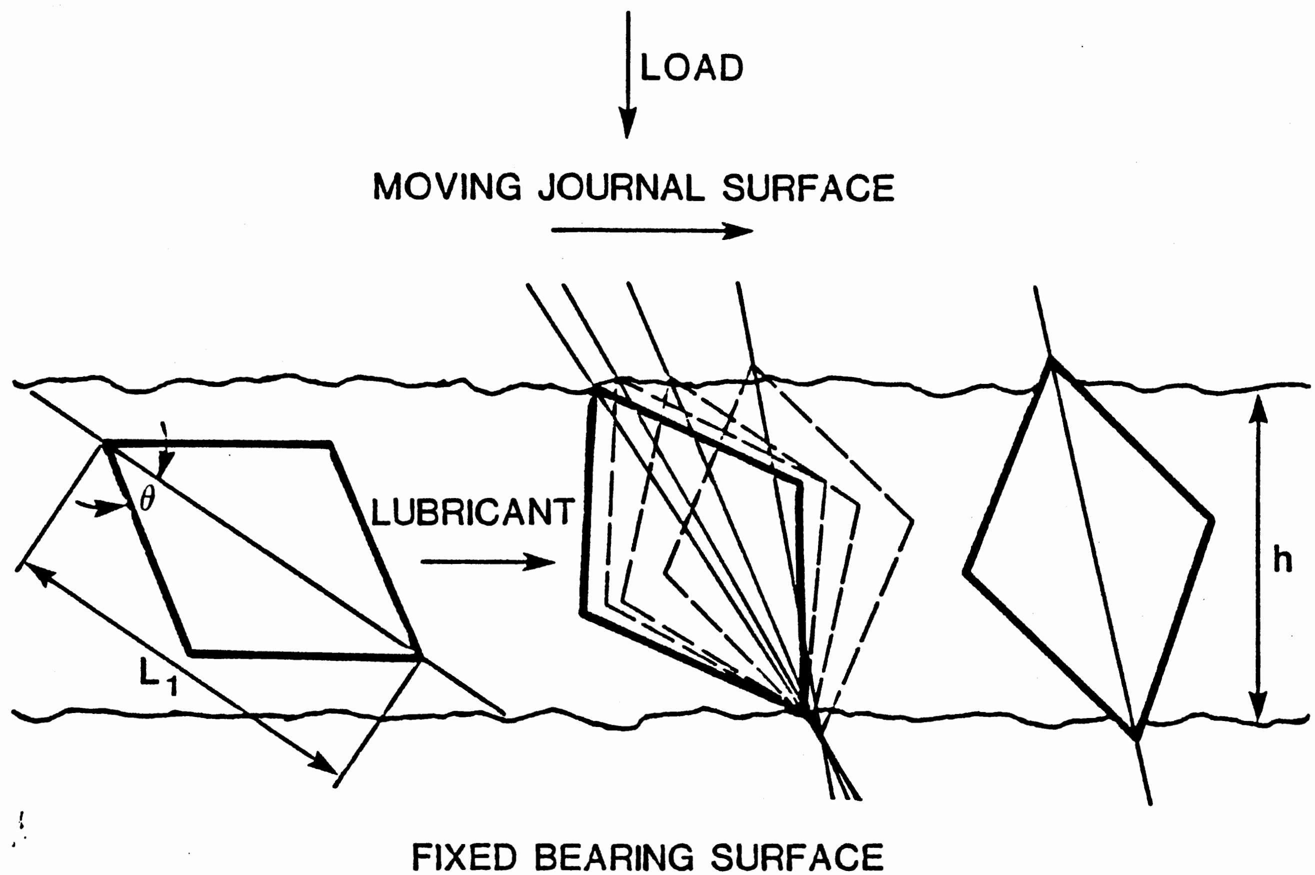

Fig.17 The Motion of an Abrasive Particle in Journal-Bearing Clearance

the shell bearings, and between pistons and walls of jacks. In this lubrication mode, the particle size effect is much different from that under dry conditions since a load-carrying fluid film is created between two metal surfaces, and the film thickness is directly related to the size of a particle which can indent and cut the critical surface. Therefore, the actual thickness of the fluid film needs to be considered first.

The fluid film thickness depends upon both the geometry of surfaces and the operating condition. For a finite journal-bearing configuration, shown in Fig.18, the governing differential equation is the Reynold's equation (121,122). Its non-dimensional form is Eq.(3.1),

$$\frac{\partial}{\partial\beta}\left((1+\epsilon\cos\beta)^3\frac{\partial P^*}{\partial\beta}\right) + \left(\frac{R}{C}\right)^2 \cdot \frac{\partial}{\partial r}\left((1+\epsilon\cos\beta)^3\frac{\partial P^*}{\partial r^3}\right) = -\epsilon\sin\beta \quad (3.1)$$

where P^* = non-dimensional local pressure in oil film

R = journal radius (in)

L = journal axis length (in)

ϵ = bearing eccentricity

β, γ = non-dimensional coordinate

The load W supported by the fluid film can be calculated by Eq.(3.2),

$$W = D \cdot L \cdot N \cdot \mu \cdot \left(\frac{R}{C}\right)^2 \cdot \left(\frac{1}{S}\right) \quad (3.2)$$

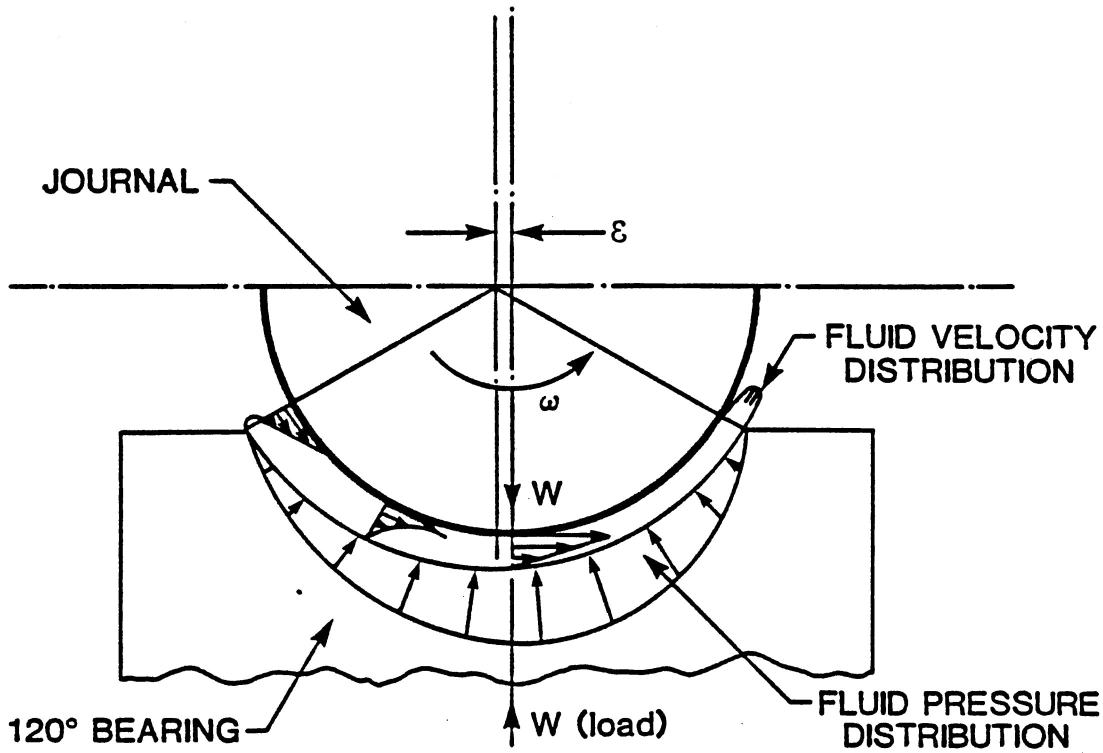

Fig.18 A Finite Journal-Bearing under Fluid Film Lubrication

where W = load (lbf)

D = bearing diameter (in)

N = journal rotation speed (rev/sec)

μ = lubricant viscosity (cSt)

C = journal-bearing radial clearance (in)

S = non-dimensional Sommerfeld number

Here the Sommerfeld number S is a known value for a given journal-bearing under specified operating conditions. Thus, by the S-ϵ bearing characteristics curve (Fig.19) (123), the film thickness h with its two extremities is known from Eqs.(3.3), (3.4), and (3.5)

$$h = C\,(\,1 + \epsilon \cos\beta\,) \tag{3.3}$$

$$h_{min} = C\,(\,1 - \epsilon\,) \tag{3.4}$$

$$h_{max} = C\,(\,1 + \epsilon\,) \tag{3.5}$$

In general, dust from the environment and wear debris from a system exhibit particle dimensions that are approximately equal; that is, length, width, and thickness are approximately the same, with one dimension no more than two or three times larger or smaller than another dimension. Thus, the size of a particle can be given by a single number. Furthermore, for a given quantity of the same kind of particle, a size distribution can be found which presents the percentage of the total number of particles larger than each subsize range. The effect of particle size depends on

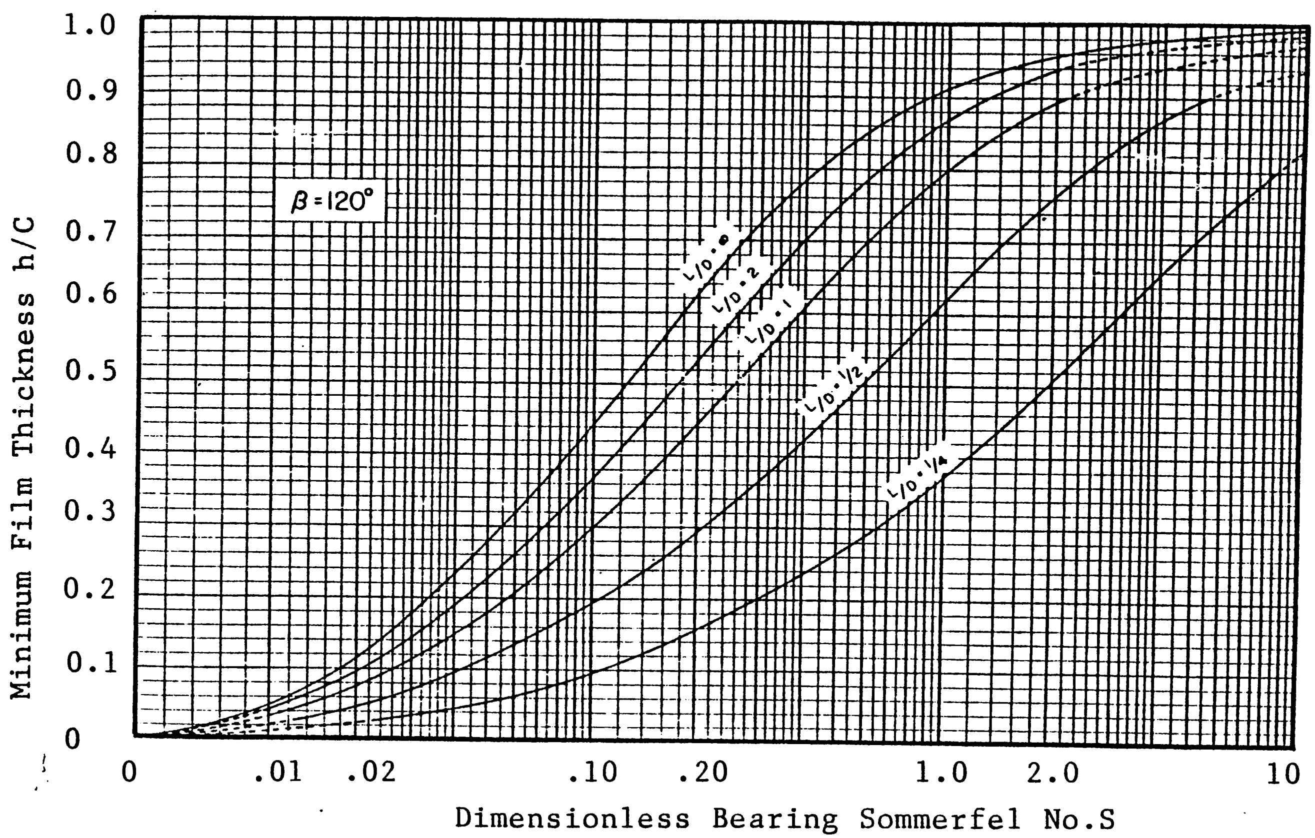

Fig.19 Minimum Film Thickness vs. Sommerfeld Number (121)(1958)

the thickness of the fluid film, since these extremities of the fluid film thickness can specify the possible sizes of particles that may entrain into the journal-bearing clearance and cause abrasive wear. The particles that will contribute to abrasion are those within a certain size range, indicated as the "harmful particle range" in Fig.20. In this figure, h_{min} and h_{max} represent the minimum and maximum film thickness. It shows that if a particle has a longer diagonal or maximum dimension within that size range, it will very likely cause contaminant abrasion wear.

Theoretically, in order to satisfy the balance requirement for forces and momentums in microcutting and indenting, the minimum size of a harmful particle should be larger than the minimum film thickness, and a larger particle is supposed to make a deeper groove. Thus, the wear rate will increase with an increasing harmful size up to the maximum fluid film thickness, and then decrease since larger particles cannot enter the clearance. Experiments using different size ACFTD particles were conducted. Fluid film thickness ranged from 12 um to 27 um. It is seen from Fig.21 (also, Hirano and Yamamoto (14)(Fig.4); Tessmann and Fitch (34)(Fig.10); Odi-owei and Roylance (54)(Fig.22)) that the prediction of a reduction in wear due to particles larger than the film thickness is correct. Particle size's effect on wear under fluid film lubrication is dependent upon the thickness and different from that under dry condition. To

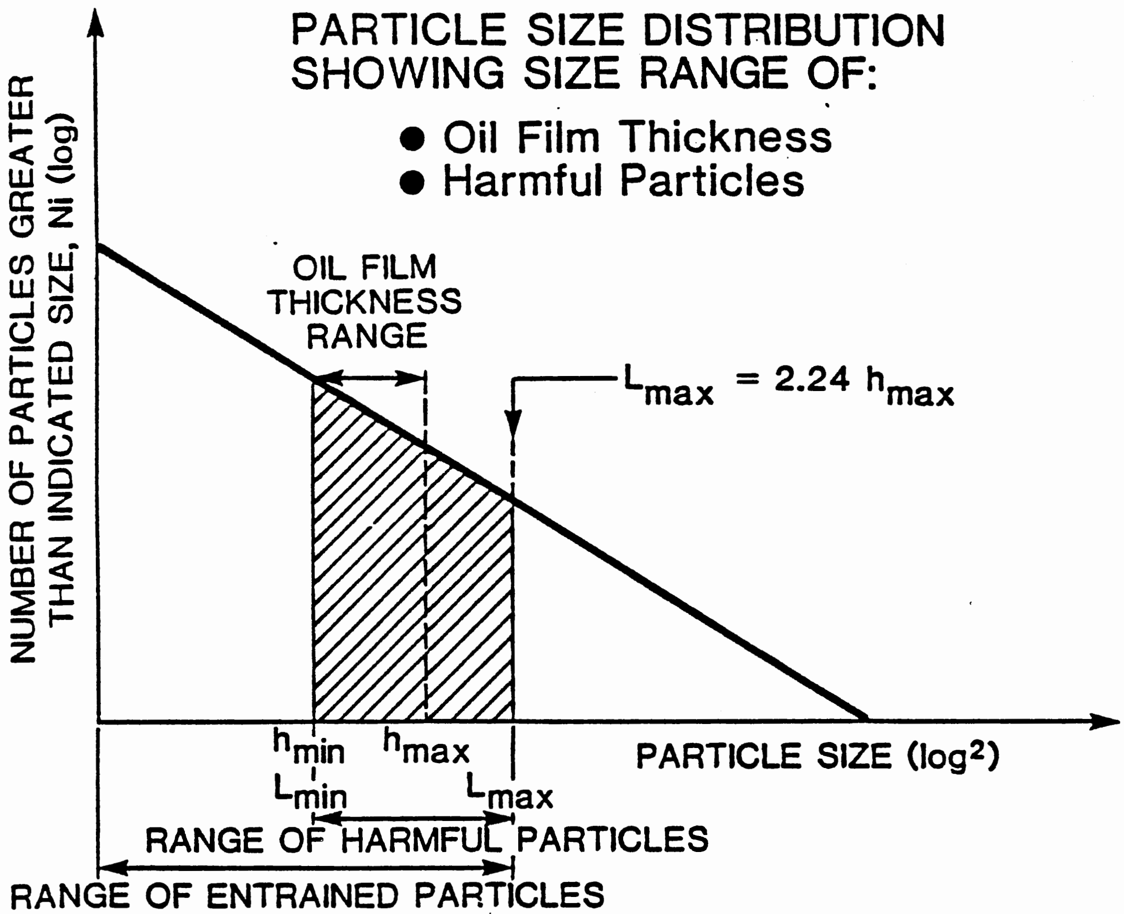

Fig.20 Size Ranges of Oil Film Thickness and Harmful Particles

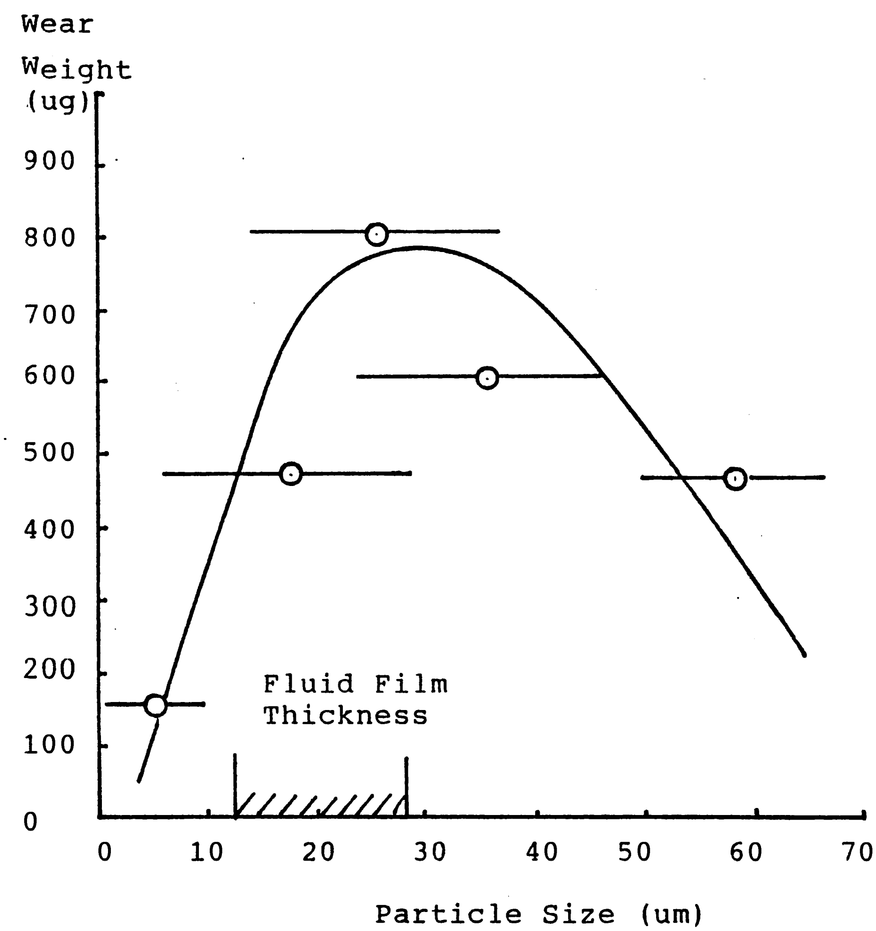

Fig.21 Effect of Particle Size on Three-Body Abrasive Wear under Fluid Film Lubrication

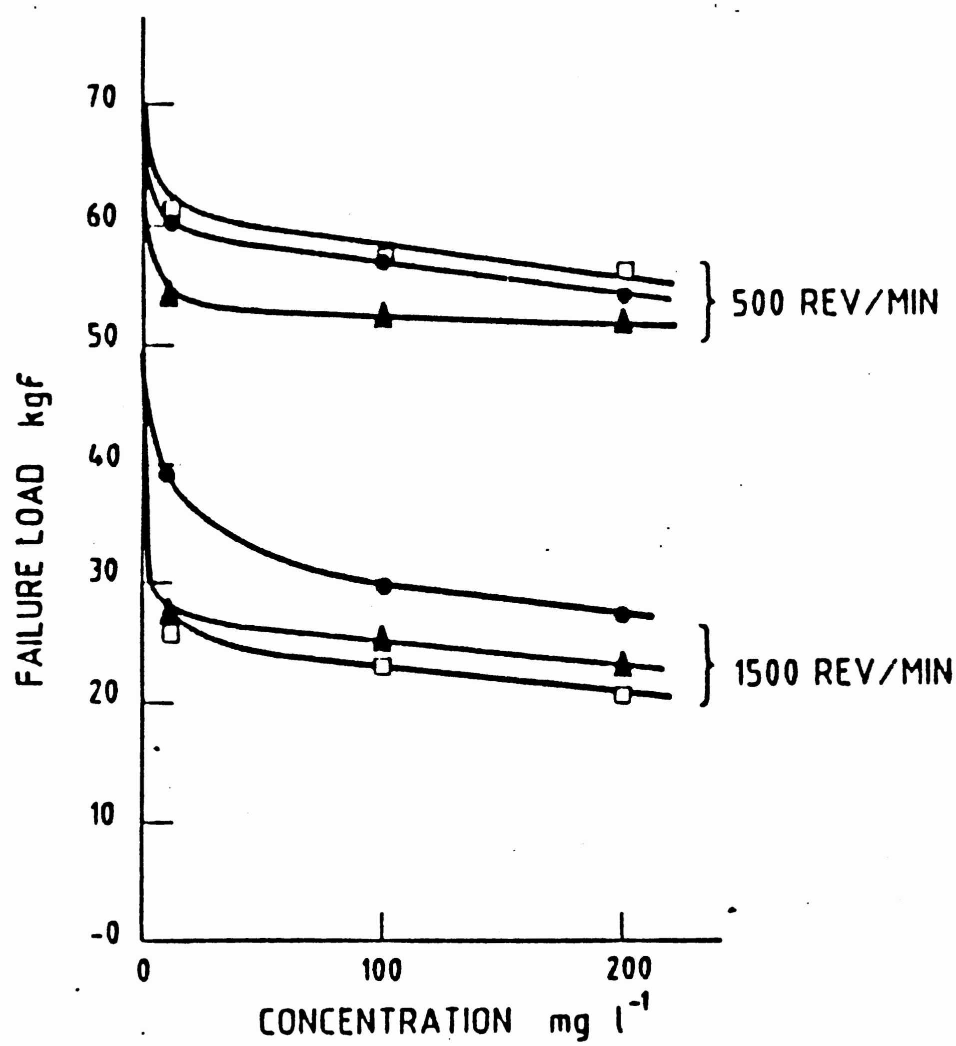

Fig.22 Effect of Contaminant Particle Size and Concentration on the Critical Failure Load (54) (1987)

determine the harmful size range, the effect of particle shape is also to be considered. This will be discussed in a later part of this section. In general, the size limits can be expressed in terms of film thickness and shape factor,

$$\text{Upper Limit} \quad D_{max} = K_{max} \cdot h_{max} \tag{3.6}$$

$$\text{Lower Limit} \quad D_{min} = K_{min} \cdot h_{min} \tag{3.7}$$

where k_{max} , k_{min} = shape factors

Hardness Effect in Three-body Contact

The effect of particle hardness or surface hardness in three-body abrasion has never been well understood. In this case, the hardness effect is much complex than in two-body abrasion and the hardness ratio is more important. There are two hardness ratios : the ratio of harder surface to softer surface (H_m/H_f) and the ratio of harder surface to abrasives (H_m/H_a). The former can affect the ratio of cutting depth to indenting depth. This phenomenon is easy to explain; when this ratio approaches one, the abrasive particle will indent into both surfaces the same depth if it is hard enough, or will be crushed if it is too soft. Therefore, usually a rather soft material is chosen for bushes. The hardness ratio of shaft-to-bush must be above three to reduce cutting damage on shaft surface (17). Fig.23 illustrates the

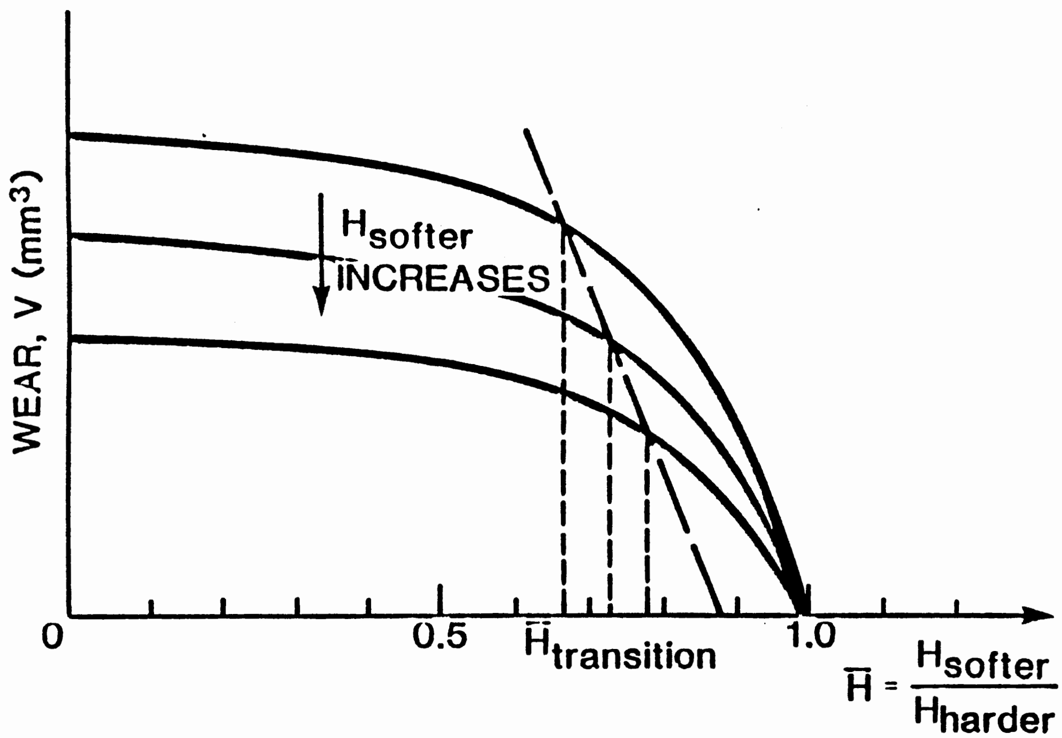

Fig.23 Effect of Hardness Ratio between Metals on Abrasive Wear

relations among surface wear and surface hardness ratio. It is seen that when the hardness ratio is smaller than a critical value $\overline{H}c$, the wear will be independent of the metal hardness ratio but dependent on the hardness of the softer surface. When the hardness ratio is above the critical value but below a maximum value, the wear damage will decrease on the softer surface but increase on the harder surface. Above $\overline{H}_{max}$, the wear damage will be the same on both surfaces. The $\overline{H}_c$ is estimated to be about 0.7 to 0.85 and the $\overline{H}_{max}$ is one.

The hardness ratio of surface-to-abrasive is more significant since it determines if the surface will be abraded or not. Based on previous experiments (18)(Fig.8), a similar hardness ratio effect is shown in Fig.24. Below $\overline{H}_c$, surface wear is independent of hardness ratio but dependent on metal hardness; above $\overline{H}_c$, wear decreases with increasing $\overline{H}_c$ until $\overline{H}_{max}$. The wear behavior can be formulated using Eq.(3.8) and is illustrated in Fig.24-b,

$$F(H) = \begin{cases} 1 & , \quad 0 < \overline{H} \leq \overline{H}_c \\ \dfrac{\overline{H} - \overline{H}_{max}}{\overline{H}_c - \overline{H}_{max}} & , \quad \overline{H}_c < \overline{H} \leq \overline{H}_{max} \\ 0 & , \quad \overline{H}_{max} < \overline{H} \end{cases} \tag{3.8}$$

Here both $\overline{H}_c$ and $\overline{H}_{max}$ vary in a wider range depending on the materials. From Fig.24-a, it is estimated that $\overline{H}_c$ is about 0.4 to 1.0 and $\overline{H}_{max}$ is about 0.5 to 1.4.

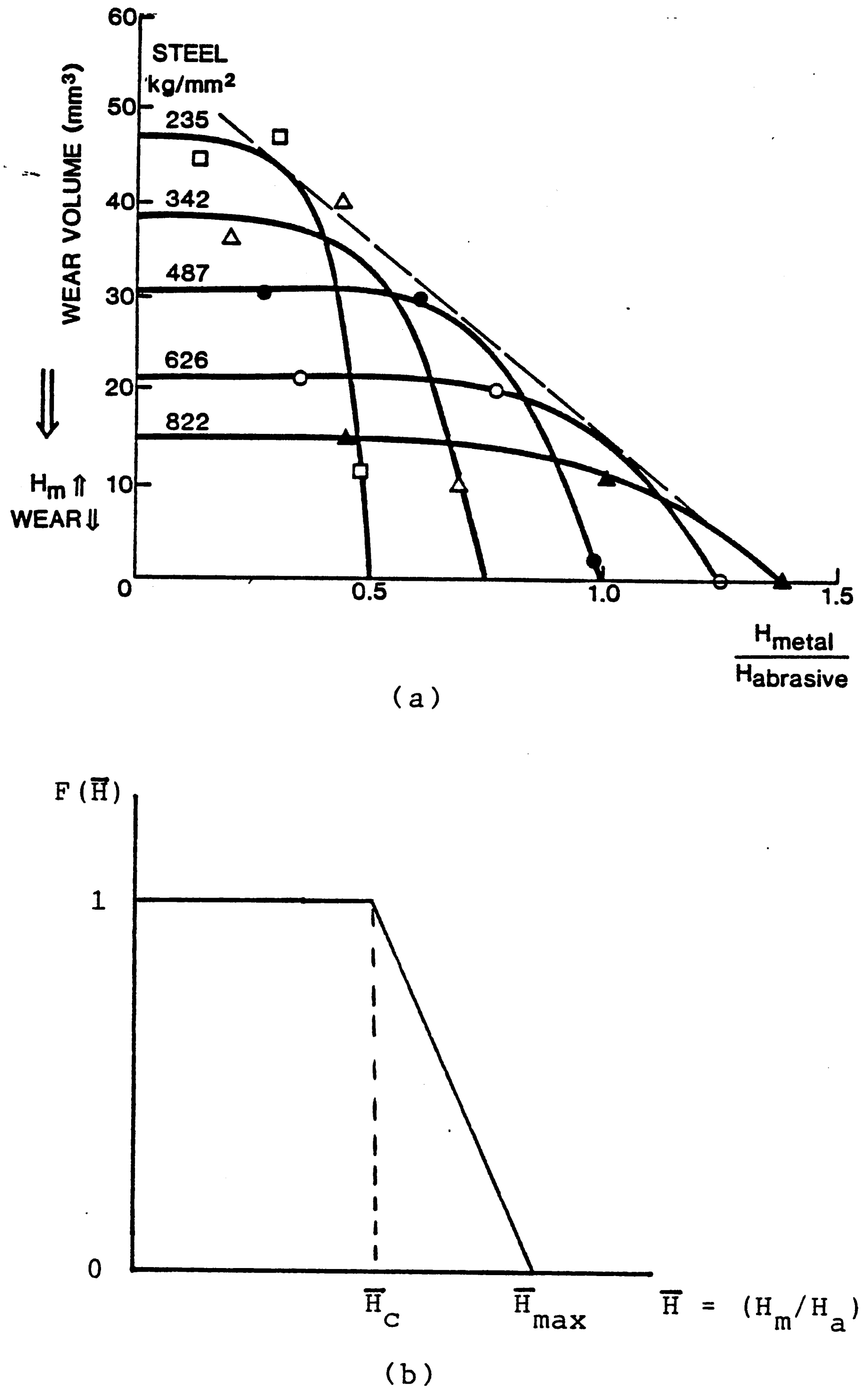

Fig.24 Effect of Metal-to-Abrasive Hardness Ratio on Three-Body Abrasive Wear

TABLE II

ENGINEERING PROPERTIES OF MAJOR TYPES OF ROCK

ROCK TYPE		UNCONFINED COMPRESSIVE STRENGTH (MPa)	HARDNESS		YOUNG'S MODULUS (x 10^3 MPa)
			SHORE SCLEROSCOPE	SCHMIDT HAMMER	
IGNEOUS AND METAMORPHIC ROCKS (* TESTED NORMAL TO CLEAVAGE OR SCHISTOCITY)	MOUNT SORREL GRANITE	176.4	77	54	60.6
	ESKDALE GRANITE	198.3	80	50	56.6
	DALBEATLIE GRANITE	147.8	74	69	41.1
	MARK FIELDITE	185.2	78	66	56.2
	GRANOPHYRE (CUMBRIA)	204.7	85	52	84.3
	ANDESITE (SOMERSET)	204.3	82	67	77
	BASALT (DERBYSHIRE)	321	86	61	93.6
	SLATE* (NORTH WALES)	96.4	41	42	31.2
	SCHIST* (ABERDEENHSIRE)	82.7	47	31	35.5
	GNEISS	162	68	49	46
	HORNFELS (CUMBRIA)	303.1	79	61	109.3
ARENACEOUS SEDIMENTARY ROCKS	FELL SANDSTONE (ROTHBURY)	74.1	42	37	32.7
	CHATSWORTH GRIT (SANDSTONE IN PEAK)	39.2	34	28	25.8
	BUNTER SANDSTONE (EDWINSTOWE)	11.6	18	10	6.4
	KEUPER WATERSTONE (EDWINSTOWE)	42	28	21	21.3
	HORTON FLAGS (HELWITH BRIDGE)	194.8	67	62	67.4
	BRONLLWYN GRIT (LLANBERIS)	197.5	88	54	51.1
CARBONATE ROCKS	CARBONIFEROUS LIMESTONE (BUXTON)	106.2	53	51	66.9
	MAGNESIUM LIMESTONE (ANSTON)	54.6	43	35	41.3
	ANCASTER FIRESTONE (ANCASTER)	28.4	38	30	19.5
	BATH STONE (CORSHAM)	15.6	23	15	16.1
	MIDDLE CHALK (HILLINGTON)	27.2	17	20	30.0
	UPPER CHALK (NORTH-FLEET)	5.5	6	9	4.4
EVAPORITIC ROCKS	GYPSUM (SHERBUM IN ELMET)	27.5	27	25	24.8
	ANHYDRITE (SANDWITH)	97.5	38	40	63.9
	ROCK SALT (WINSFORD)	11.7	12	8	3.8
	POTASH (LOFTUS)	25.8	9	11	7.9
COAL MEASURE ROCKS	MUDSTONE	45.6	32	27	25
	SILTSTONE	83.1	49	39	45
	SHALE	20.2	–	–	5.2
	BARNSLEY HARDS COAL	54.0	–	–	26.5
	DEEP DUFFRYN COAL	18.1	–	–	–

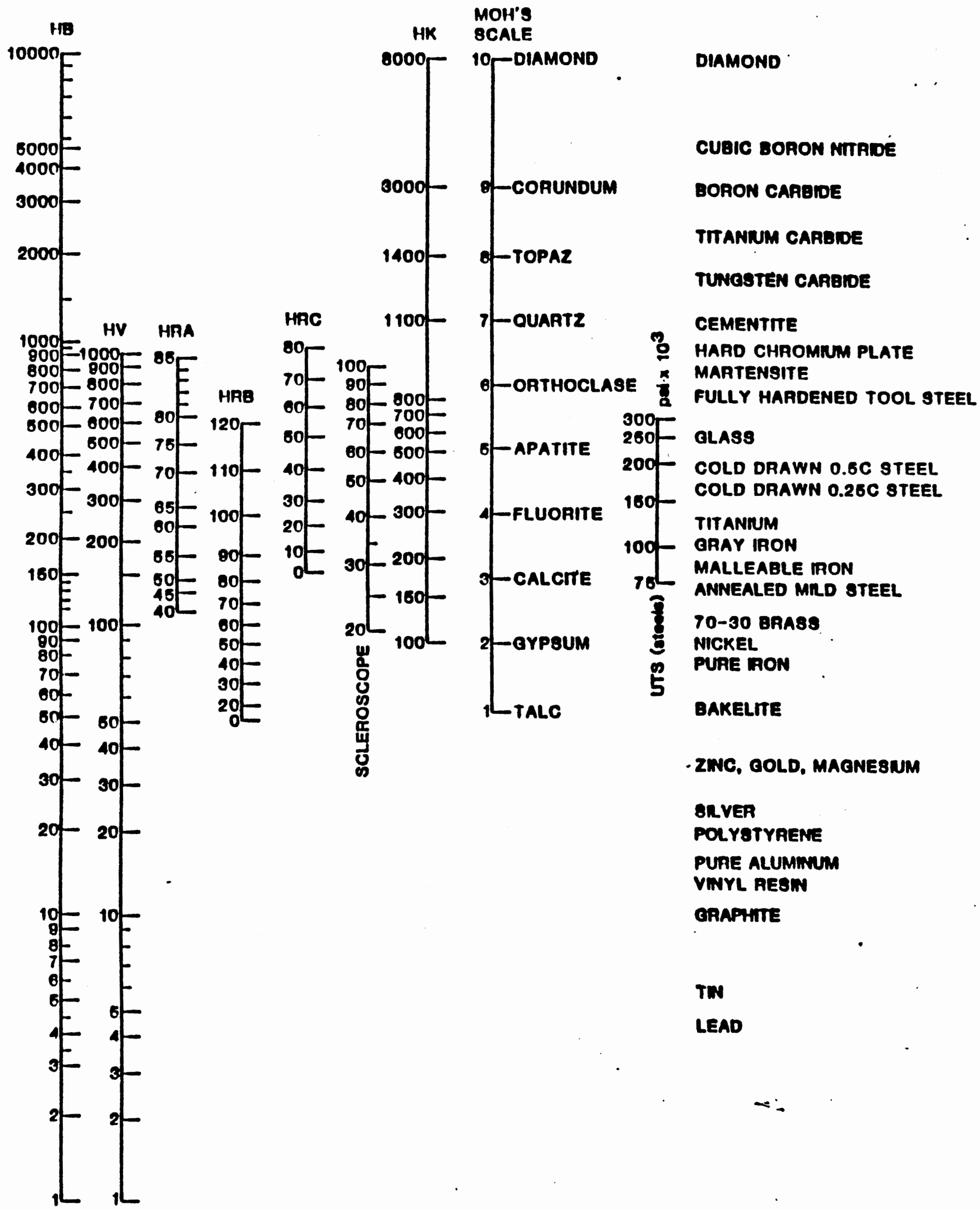

Fig.25 Material Hardness and Scale Conversion (125) (1985)

Table II shows the engineering properties of major soils and rocks. The relative hardness of a kind of particle can be determined on the basis of its chemical composition. Charts for hardness conversion are available in the technical literature; an example chart is given as Fig.25.

Particle Shape Effect

The shape of abrasive particles is also found to affect abrasion significantly. As might be expected, angular particles will produce more wear than round ones. Sharp angular particles result in more chips, whereas spherical particles lead to more plastic deformation (36). Since the dust from the environment is a major cause of abrasive wear, the differences among contaminants result in the large variability in wear mechanisms. Several shapes (sphere, ellipsoid, spheroid, cylinder, cube, square, prism, pyramid, and paraboloid) have been proposed as particle models. Generally, abrasive particles found in hydraulic and lubricating systems have angular shapes with sharp wedge angles that are abrasive to sliding surfaces (64,66,126). Often people use the degree of roundness to refer to the sharpness of a particle. The five stages of shape transition, or five levels of degree of roundness -- angular, subangular, subrounded, rounded, and well rounded -- are illustrated in Fig.26 (127,128). Most kinds of dust particles can be expressed in terms of one of these shape

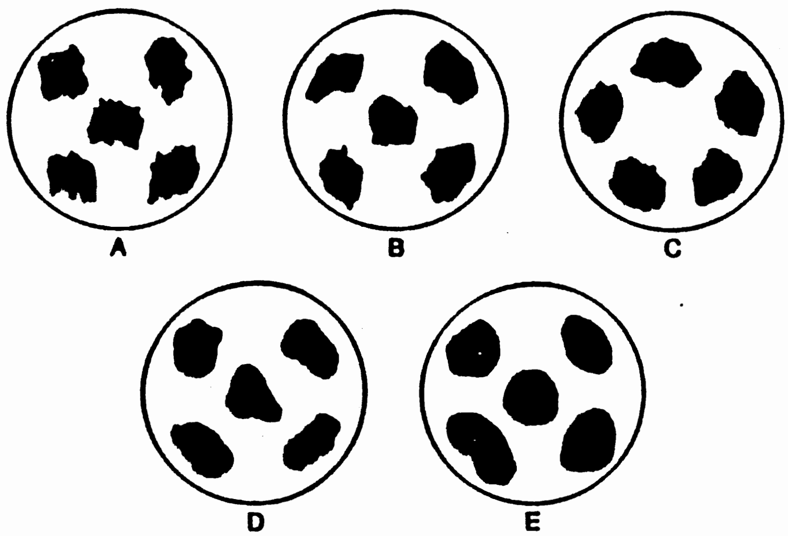

CHART TO SHOW ROUNDNESS CLASSES. A-ANGULAR, B-SUBANGULAR, C-SUBROUNDED, D-ROUNDED, E-WELL ROUNDED.

Fig.26 Particle Shape Stages (Roughness Degrees) (127) (1969) stages, each roundness level is represented by a wedge angle range. In this study, ACFTD, which has been universally used as a standard test dust, is selected as the abrasive particle in the development of the wear model. The shape of ACFTD particles is assumed to be a prism square with two rhombic side planes as shown in Fig.27-a. According to Iwanaga's observation, a 1.5 normal length ratio for the longer axis of the rhombic plane to the shorter axis is chosen. Since the two opposite angle pairs have values 2θ and ($\pi - 2\theta$) respectively, the value of the angle corresponding to the 1.5 axis ratio is 33.7. By further assumption, if the axis length ratio has a normal distribution, then the variation range of particle shape can be determined as

$$1 < L_1/L_2 < 2 \qquad (3.9)$$

corresponding to

$$27^\circ < \theta < 63^\circ \qquad (3.10)$$

Fig.27-b illustrates a more realistic particle shape. When the cutting depth t is much smaller than the height of the particle itself, Eq.(3.11) is valid:

$$B' \doteq B \qquad (3.11)$$

Therefore, the approximation of the model in Fig.27-a to that in Fig.27-b is close and reasonable. The shape factors are calculated as

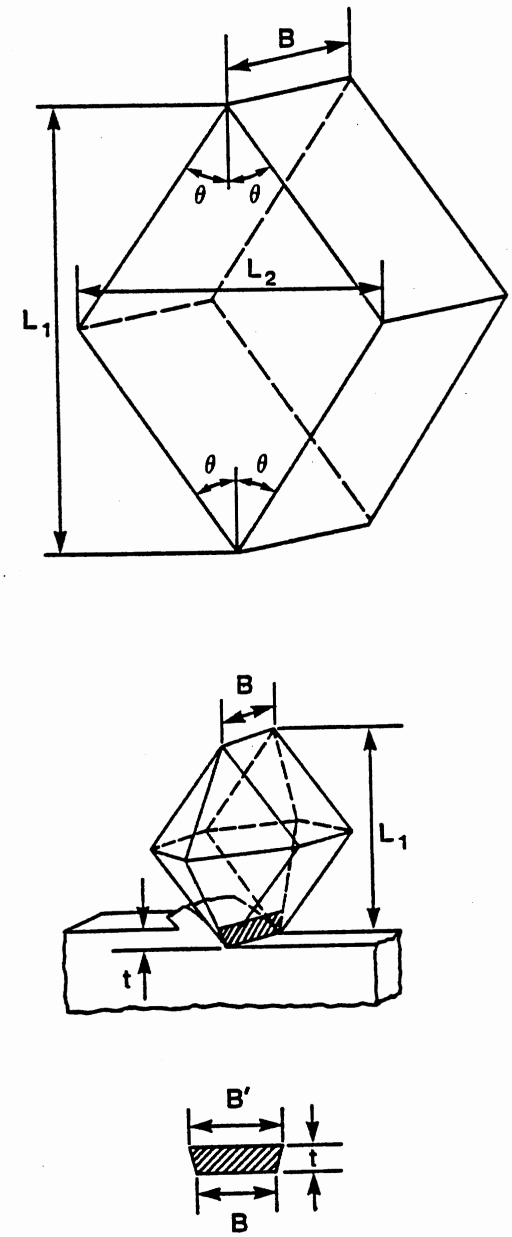

Fig.27 Particle Model

$$K_{max} = \frac{L_{1\ max}}{h_{max}} = 2.24 \tag{3.12}$$

$$K_{min} = \frac{L_{1\ min}}{h_{min}} = 1 \tag{3.13}$$

The size distribution of ACFTD particles is shown in Fig.28. A suggested fluid film and corresponding size range of harmful particles are also illustrated in this figure for modeling purposes.

Particle Toughness Effect

The toughness or shear strength of abrasives is the least discussed among those major particle parameters. There has been little information in the literature about analyzing or testing for this effect. However, this property is important to particles that undergo multipass abrasion processes, such as pump contaminant sensitivity tests (Fig.29) (104). The destruction characteristics of a particle depend on particle's toughness which can be represented by a time constant to reflect the break-down period of the particle. This constant is to be determined experimentally for analysis. Based on previous data, the destruction time of ACFTD particles at all size intervals is estimated to be about nine minutes.

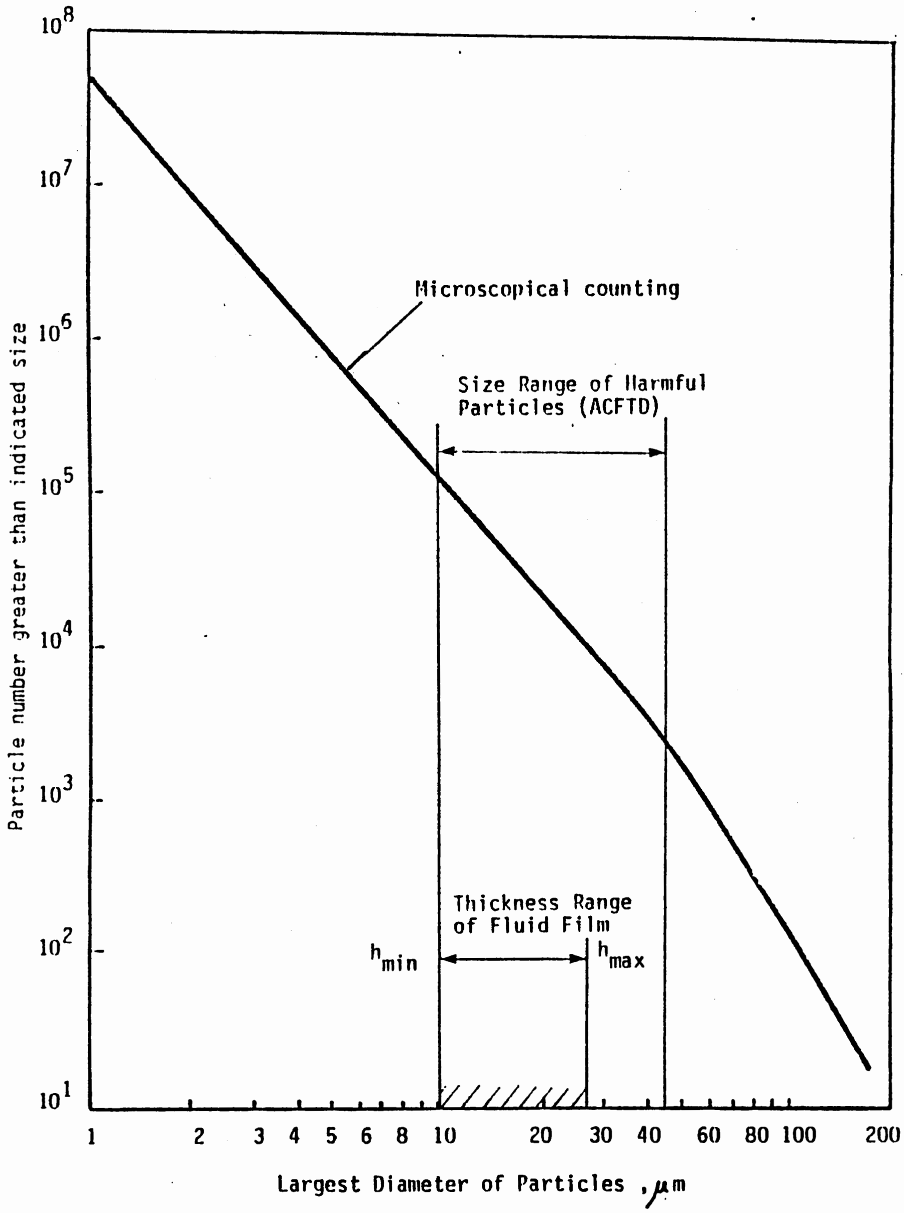

Fig.28 ACFTD Particle Distribution

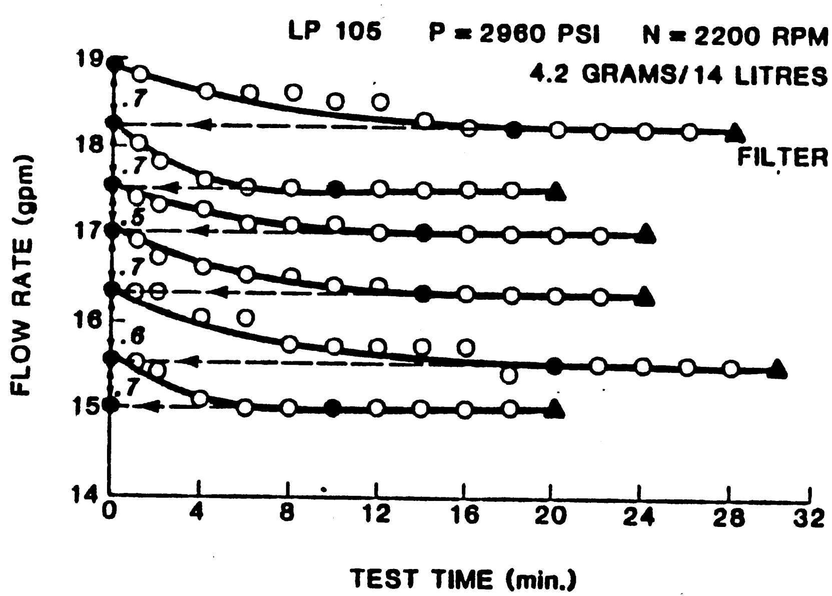

Fig.29 Flow Degradation from Multiple Injections (104) (1985)

Wear Model

The wear process in the "metal-fluid-particle-metal" tribo-system can be analyzed as follows. If a particle has a longer diameter D within the harmful size range, it will very likely cause three-body abrasive wear. Once a particle has entrained into the narrow gap, forced by the moving lubricant, it will go forward and rotate simultaneously until it reaches a critical location where the actual fluid film thickness is too thin to let it pass. At this point, because of the roughness of the metal surfaces, one of the particle's wedge angles that contacts the fixed surface will stop motion, whereas the other end, in contact with the moving surface, will continue to be driven forward. Thus, if the hardness ratio H_m/H_a is above the maximum value $\overline{H}_{max}$, no abrasive wear occurs on the surface since the particle will be crushed(if both surfaces are hard) or completely indented into the softer surface. On the other hand, if H_m/H_a is below the $\overline{H}_{max}$, three-body abrasive wear occurs.

A steady microcutting process is illustrated in Fig.30. Here, the cutting depth is of interest for calculating the rate of material removal on the wearing surface. Since the particle is harder than the harder surface, it can indent into both surfaces under a normal force. Also, the particle undergoes a tangential force. Fig.31 shows that the indenting and cutting forces are balanced along the diagonal in an equilibrium state. In addition, the algebraic sum of

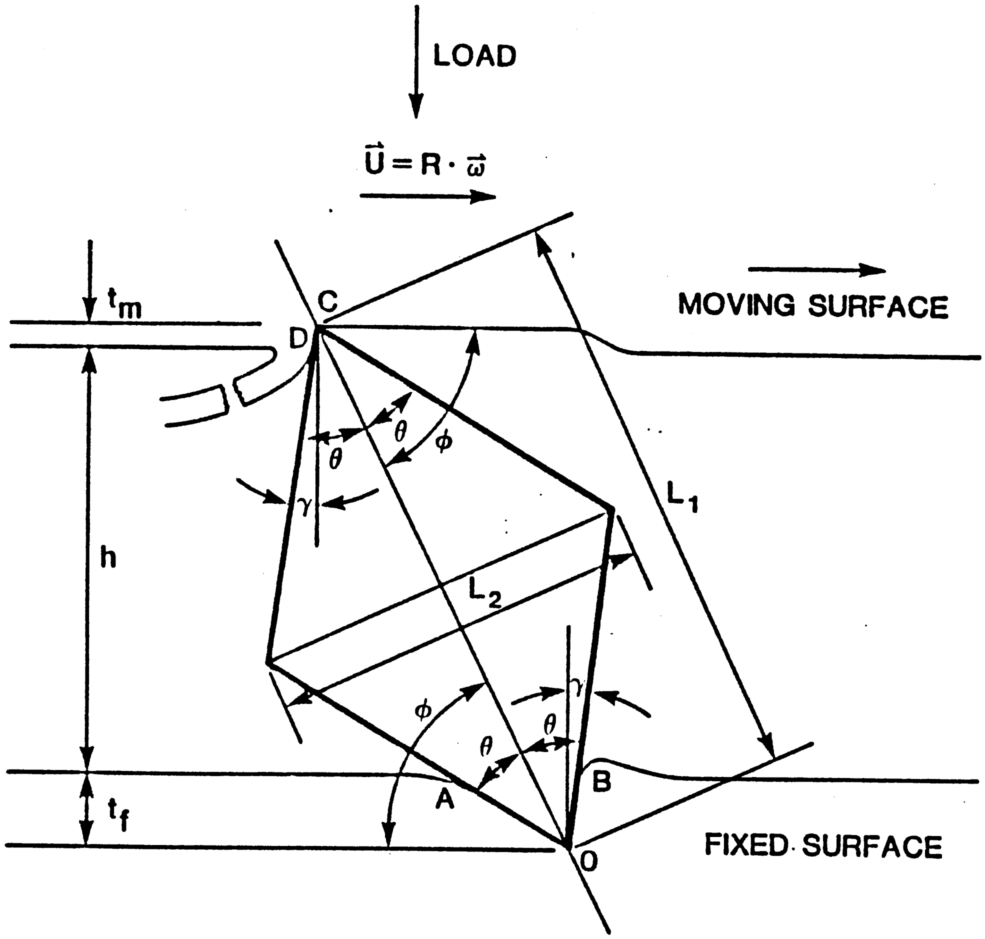

Fig.30 Three-body Abrasive Wear Model

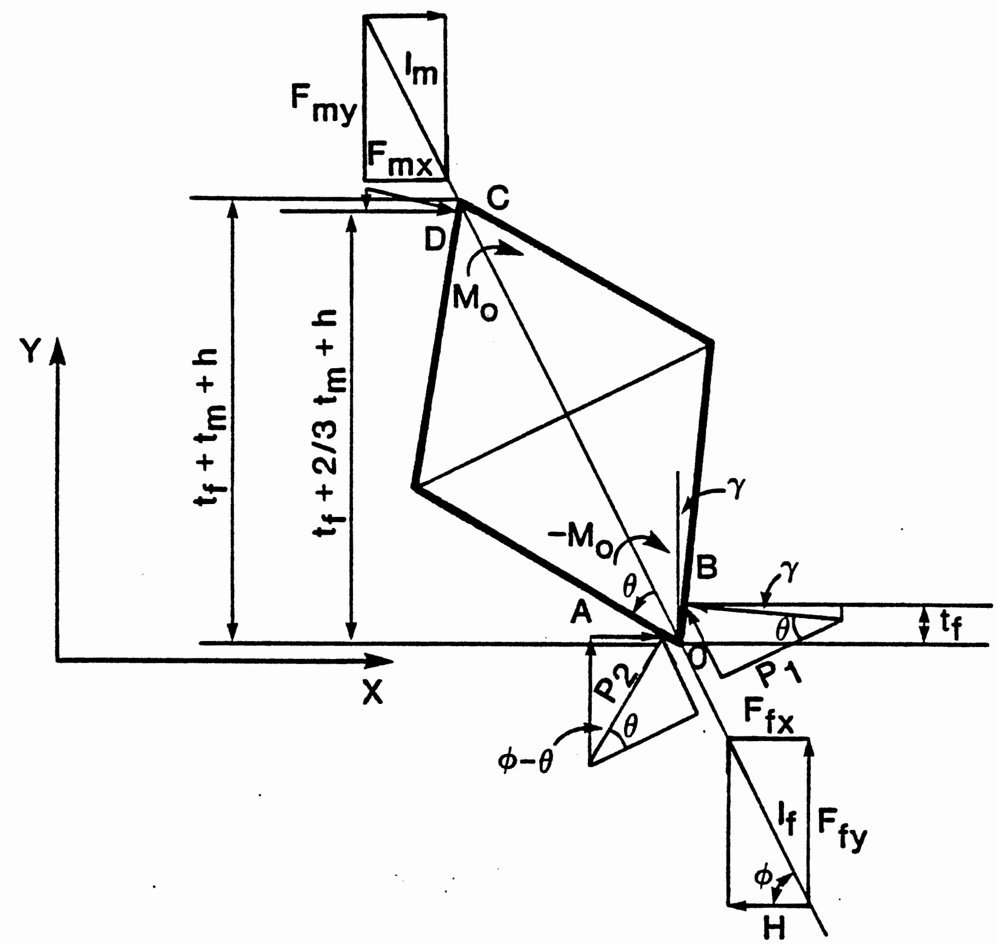

Fig.31 Free-Body Diagram for Analysis of Three-Body Abrasive Wear

the force moments about point o must be zero. Thus, the force and moment equilibrium equations for the free-body of a particle are Eqs.(3.14), (3.15), and (3.16)

$$F_x = 0 \tag{3.14}$$

$$F_y = 0 \tag{3.15}$$

$$M_x(O) = 0 \tag{3.16}$$

where F = acting force

M = force moment

subscripts x and y are Cartesian coordinates

To solve these balance equations, the indenting force and the cutting force need to be calculated separately.

According to Ernst-Merchant's theory (129), the force required to achieve cutting on the moving surface is

$$F_{mx} = 2 \cdot H_m \cdot t_m \cdot B \cdot \cot\left(\frac{\pi}{4} + \frac{\gamma}{2} - \tan^{-1}\frac{\mu_m}{2}\right) \tag{3.17}$$

and on the fixed surface is

$$F_{fx} = 2 \cdot H_f \cdot t_f \cdot B \cdot \cot\left(\frac{\pi}{4} + \frac{\gamma}{2} - \tan^{-1}\frac{\mu_f}{2}\right) \tag{3.18}$$

where F = cutting force

H = surface hardness

t = cutting or indenting depth

B = cutting width

μ = friction coefficient

subscripts m and f stand for moving and fixed surfaces, respectively.

Using Eqs.(3.17) and (3.18), the moment balance Eq.(3.16) can be approximately written as

$$C_1 \cdot t_m^2 + h \cdot t_m + t_f \cdot t_m - \frac{H_f}{H_m} t_f^2 = 0 \tag{3.19}$$

or

$$F_{mx} \cdot (C_1 \cdot t_m + h + t_f) = F_{fx} \cdot t_f \tag{3.20}$$

where c_1 = a constant for approximating the acting point for force F_{mx}, 0.6 to 0.7

To figure the presumed indentation on the softer surface, the total normal stress on each side of the indented wedge of the particle is expressed in terms of the mean normal pressure. This pressure is a function of the wedge angle, yield strength of the material, and friction coefficient (130). In addition, since it is in an equilibrium state, the resultant force along the diagonal should be equal. That is,

$$I_m = I_f \tag{3.21}$$

Using Grumzweig's method (131), the force required to achieve the present unbalanced indentation can be estimated as

$$P = K_s f(\theta , \mu) \tag{3.22}$$

where P = pressure on the wedge

k_s = shear yield strength, $k_s = k_1 H_f$

The wedge pressure P is plotted in Fig.32 as a function of wedge angle and friction coefficient . Now Eq.(3.21) is rewritten:

$$A = \frac{t_f \cdot B}{\cos(\phi + \theta - \pi/2)} \tag{3.23}$$

with

$$2 \cdot P \cdot A \cdot \sin\theta = F_{mx} \cdot \frac{1}{\cos\phi} \tag{3.24}$$

$$P = k_s \cdot H_f \cdot f(\theta, \mu) \tag{3.25}$$

Thus the indenting depth is

$$t_f = \left(\frac{H_m}{H_f}\right) \cdot F_1 \cdot t_m \tag{3.26}$$

with

$$F_1 = \frac{\cos(\phi+\theta-\frac{\pi}{2}) \cdot \tan(\frac{\pi}{4} + \frac{\phi+\theta-\pi/2}{2} - \tan^{-1}\frac{\mu}{2}) \cdot \sin\theta}{k_1 \cdot f(\mu, \theta) \cdot \cos\phi} \tag{3.27}$$

Luo (69) analyzed the interaction between cutting and indenting. He defined R as the ratio of the required cutting force (parallel to the moving direction) to the required indenting force component (parallel to the moving direction). He found that R depends on the inclination angle. When R is larger than one, no cutting, only indenting, occurs. Thus, if the wedge angle and friction

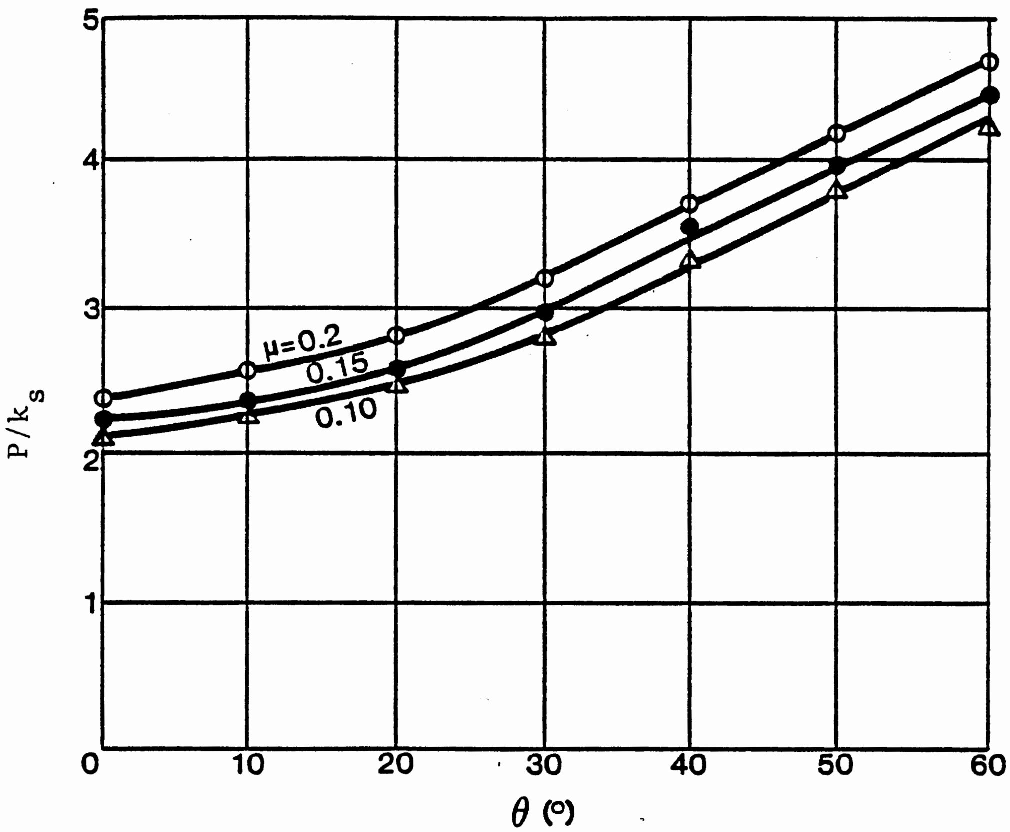

Fig.32 Relationship between Wedge Pressure and Wedge Angle and Friction Coefficient. (131) (1954)

coefficient are estimated, the critical inclination angle can be obtained from Fig.33. Then the function F_1 may be calculated by Eq.(3.27).

From Fig.31, the geometry condition for three-body abrasion is derived as,

$$t_m + t_f + h - D\cdot\sin\phi = 0 \tag{3.28}$$

Substituting Eq.(3.26) into the geometry equation (3.28) and the moment equation (3.20) and combining these two balance requirements, the cutting depth corresponding to a particle of size D is obtained:

$$t_m = \frac{D\cdot\sin\phi}{(H_m/H_f)F_1^2 + 1 - C_1} \tag{3.29}$$

Since the cutting depth (Eq.(3.29)) is derived based on the assumption that the particle is harder than the harder surface, a modification can be made to include the effect of hardness ratio as analyzed before. That is,

$$t_m = \frac{D\cdot\sin\phi\cdot F_2}{(H_m/H_f)F_1^2 + 1 - C_1} \tag{3.30}$$

where

$$F_2 = \begin{cases} 1 & , \quad 0 < \overline{H} \leqslant \overline{H}_c \\ \dfrac{\overline{H} - \overline{H}_{max}}{\overline{H}_c - \overline{H}_{max}} & , \quad \overline{H}_c < \overline{H} \leqslant \overline{H}_{max} \\ 0 & , \quad \overline{H}_{max} \leqslant \overline{H} \end{cases} \tag{3.31}$$

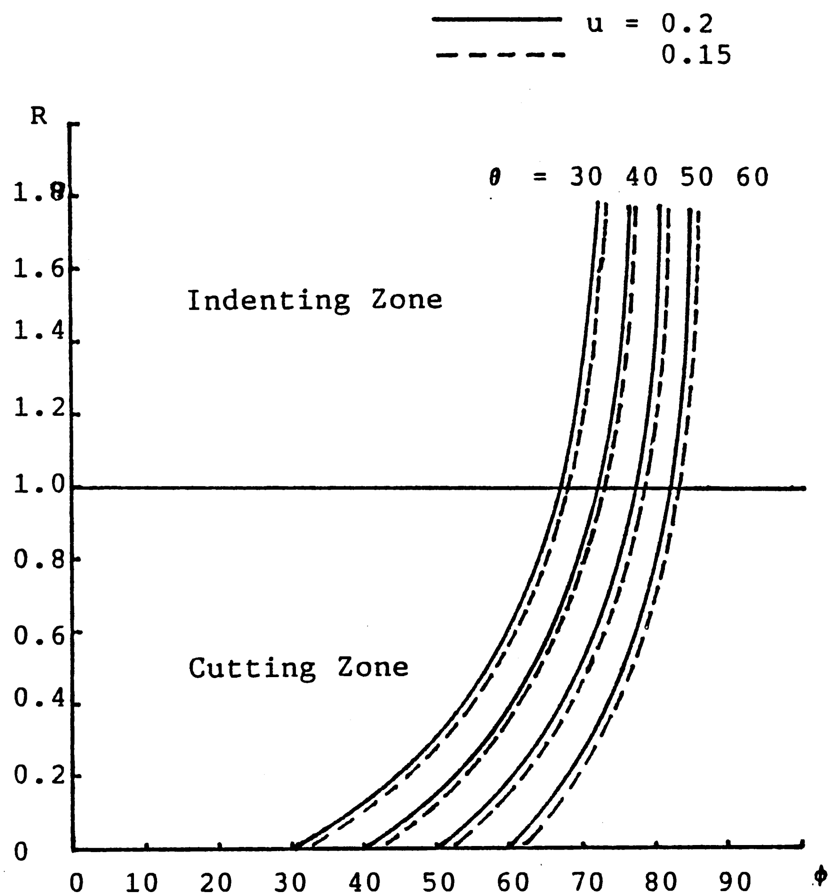

Fig.33 The Characteristic Curves of Cutting-Indenting Force Ratio (69) (1985)

$$\overline{H} = H_m / H_a \tag{3.32}$$

From the calculated cutting depth, the location where the particle contacts with both surfaces, and thus the cutting length, are also obtained by Eqs.(3.33) and (3.34):

$$h = D\cdot\sin\phi - (1 + (H_m/H_f)\cdot F_1)\cdot t_m \tag{3.33}$$

$$X = X_0 \frac{h - h_{min}}{h_{max} - h_{min}} \tag{3.34}$$

where X_0 = the length of clearance from h_{max} to h_{min}

In regard to the toughness effect of a given type abrasive, a destruction function is introduced here:

$$F_3 = \begin{cases} 1 & , \quad 0 < t \leqslant \tau \\ k_t & , \quad \tau < t \end{cases} \tag{3.35}$$

where τ = destruction time of a given particle

k_t = destruction coefficient

This function is to reflect the relative life of the abrasive particles based on the destruction time obtained experimentally.

Therefore, the material volume removed from the harder moving surface by one particle can be estimated by assuming the groove width is the same order of the magnitude as the groove depth:

$$V_i = K \cdot t_{mi}^2 \cdot X_i \cdot F_3 \tag{3.36}$$

where k = constant reflecting the ratio of cutting width to depth

It is noted that this per particle wear model is strongly depending upon three dimensionless functions which represent the effects of particle parameters as illustrated in Fig.34. This relation is expressed by Eq.(3.37):

$$V_i = f(\ F_1(\theta),\ F_2(H_a),\ F_3(\tau\ )) \tag{3.37}$$

Finally, the mathematical model of total wear volume in a period t is built up:

$$V = \dot{Q} \cdot t \cdot \sum_{D_{min}}^{D_{max}} V_i \cdot n_i \tag{3.38}$$

where Q = fluid flow rate

t = duration

n_i = number of particles of size D_i per unit volume fluid at upstream

The computational flow chart for total wear volume is shown in Fig.35.

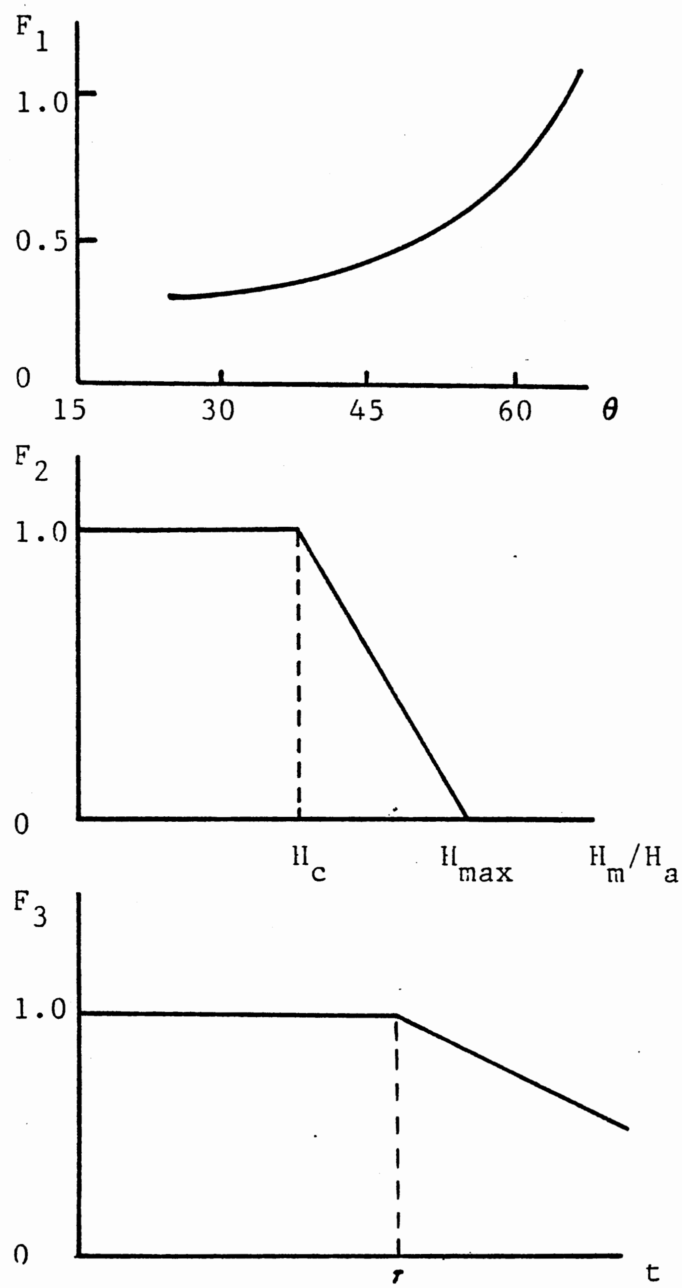

Fig.34 Particle Parameter Functions

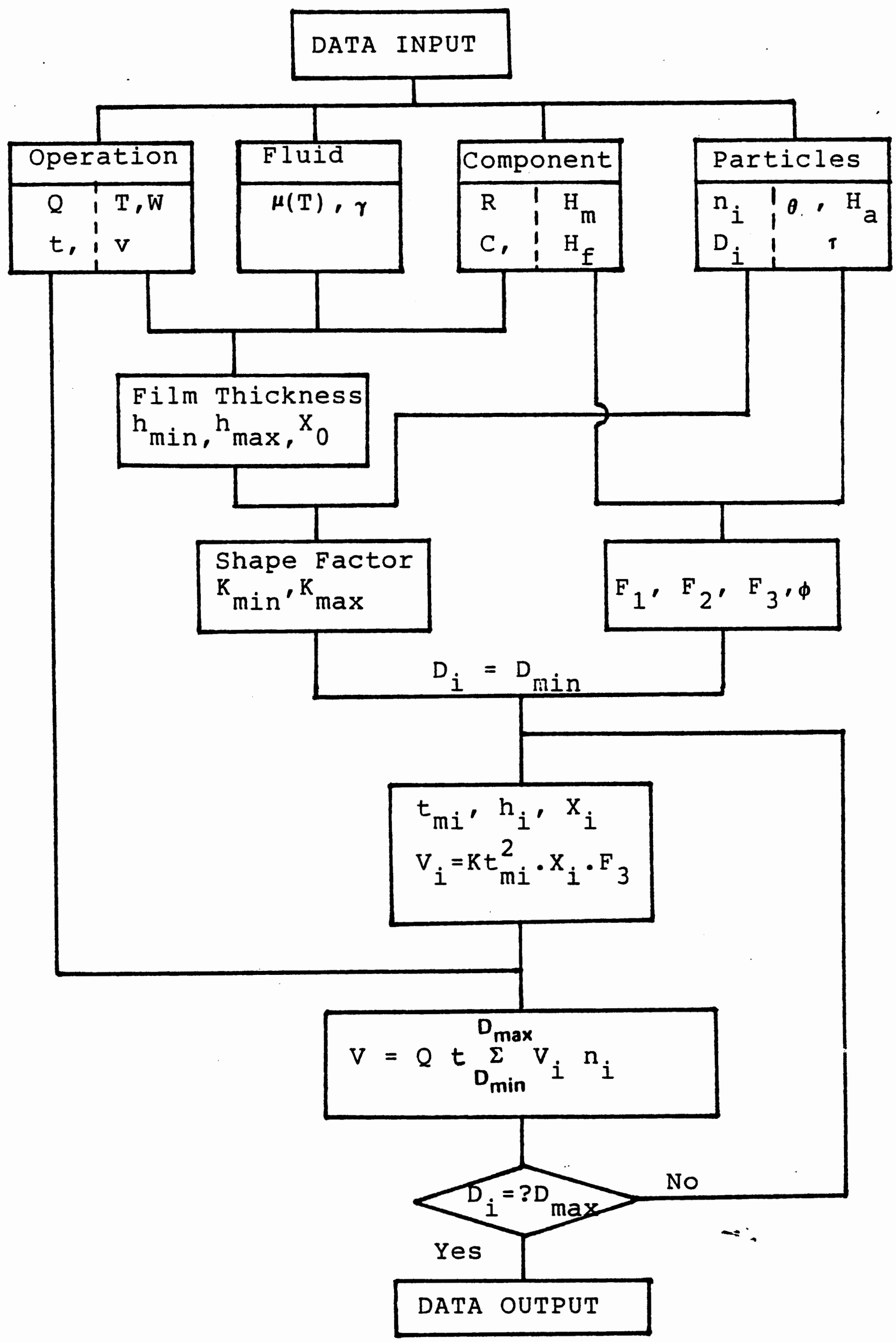

Fig.35 Wear Calculation Flow Chart

Model of Three-body Abrasion Sensitivity

Wear-Leakage-Degradation Analysis

Under abrasive wear conditions, the increasing wear volume will result in an increasing leakage flow path. It is logical to assume that this increase in flow path is equivalent to an increase in clearance based on material volume:

$$C = \frac{\text{Wear Volume}}{\text{Area of Wear Surface}} = \frac{V}{A} \tag{3.39}$$

Certainly, such a change of flow path will result in several forms of degradation in the performance of a fluid tribo-mechanical element, such as the flow degradation in a pump, speed degradation in a hydraulic motor, or pressure degradation in a spool valve. In general, the performance defined by a parameter P is tightly related to three-body abrasive wear, while the degradation rate is related to the development of leakage flow path caused by wear:

$$\frac{dP(t)}{dt} = f(\ C(V)\ ) \tag{3.40}$$

For many cases, when the pressure is kept constant, the performance parameter will be the flow rate; a typical example is the hydraulic pump. It is noted that in such a fluid component a main flow as well as a leakage flow exists, as depicted in Fig.36-a. Let Q_T represent the constant upstream flow, Q_m the main flow, and Q_l the leakage

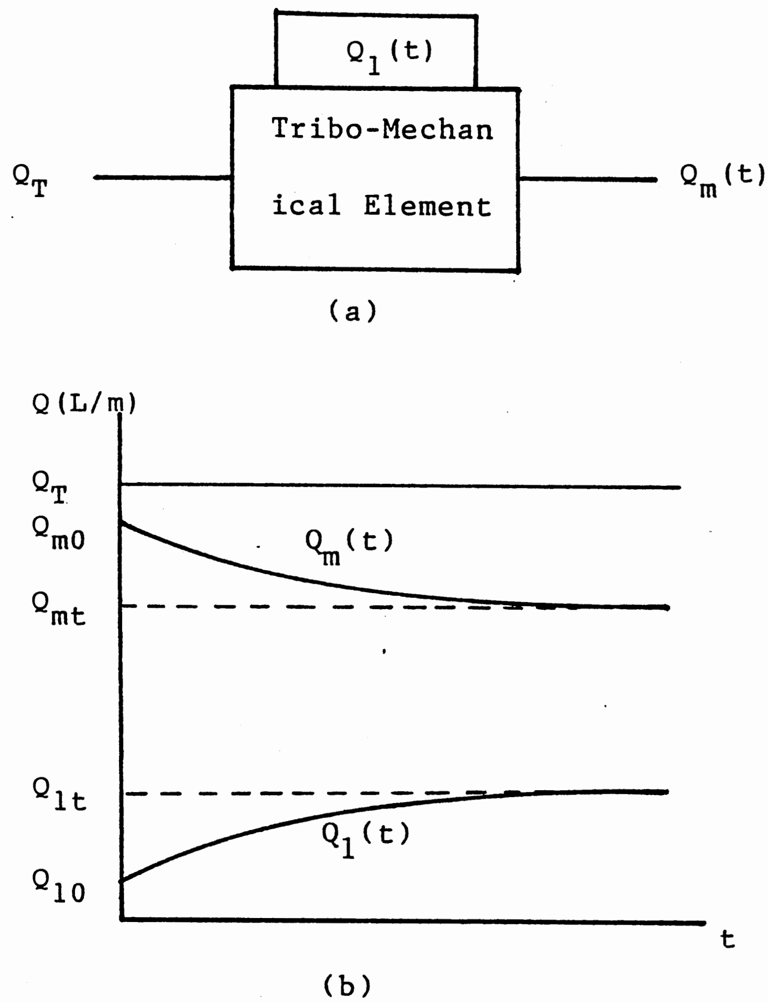

Fig.36 Flow Degradation in a Tribo-Mechanical Component

flow. It is seen from Fig.36-b that both the Q_m and the Q_l are functions of time. Usually for a component operating in a contaminanted environment, the main flow degrades with time and, simultaneously, the leakage flow increases with time since the total upstream flow is a constant. Thus the flow degradation can be described in terms of either one of the two flows.

Most often in previous studies on contaminant sensitivity, the main flow degradation has been considered (94,97,104-110). According to the present contaminant sensitivity theory, the degree of performance degradation in any fluid tribo-mechanical element can be represented by a lumped parameter -- the contaminant sensitivity coefficient, S_i, as expressed in Eq.(2.2). Since the S_i implicitly reflects the abrasive-caused wear damage, the contaminant sensitivity of a component cannot be predicted but must be determined on an experimental base. Now with the rationale of wear-leakage-degradation, the model of lubricated three-body abrasion sensitivity can be developed to theoretically evaluate the contaminant tolerance and life for a component.

Component Sensitivity Model

All fluid components are sensitive in some degree to particulate contaminants entrained in the system fluid, mainly due to the fact that the critical surfaces inside a component are subjected to three-body abrasive wear which results in increased leakage. The flow degradation of a component can be mathematically expressed in terms of leakage flow:

$$Q_l(t+dt) = Q_l(t) + Q_w(t) \tag{3.41}$$

where $Q_w(t)$ = flow caused by three-body abrasive wear in time interval dt

Let A be the area of flow passage, and B the passage width. The wear-induced flow is described by Eq.(3.42):

$$Q_w(t) = \frac{B}{A} v \cdot V \tag{3.42}$$

where v = relative velocity between two surfaces

V = three-body abrasive wear volume in time interval dt

Substituting the wear equation (3.38) into Eq.(3.41):

$$Q_l(t+dt) = Q_l(t) + \frac{B}{A} v \cdot Q_l(t) \cdot dt \sum_{D_{min}}^{D_{max}} V_i \cdot n_i \tag{3.43}$$

Rearranging Eq.(3.43) into a differential form and integrating it from the initial leakage flow to the flow at time t

$$\int_{Q_{l0}}^{Q_{lt}} \frac{dQ_l(t)}{Q_l(t)} = \int_0^t \left(\frac{B}{A} v \sum_{D_{min}}^{D_{max}} V_i \cdot n_i\right) \cdot dt \tag{3.44}$$

Thus the flow degradation represented dy leakage flow is derived:

$$\ln\left(\frac{Q_{1t}}{Q_{10}}\right) = \left(\frac{B}{A}v\sum_{D_{min}}^{D_{max}} V_i \cdot n_i\right)\cdot t \tag{3.45}$$

Also the flow degradation can be expressed using the main flow:

$$\ln\left(\frac{Q_T - Q_{mt}}{Q_T - Q_{m0}}\right) = \left(\frac{B}{A}v\sum_{D_{min}}^{D_{max}} V_i \cdot n_i\right)\cdot t \tag{3.46}$$

where Q_T = theoretical upstream flow

Q_{mt} = main flow at time t

Q_{m0} = main flow at initial

On the other hand, the contaminant-tolerant life of the component is determined by Eq.(3.47):

$$t = \frac{\ln\left(\frac{Q_T - Q_{mt}}{Q_T - Q_{m0}}\right)}{\left(\frac{B}{A}v\sum_{D_{min}}^{D_{max}} V_i \cdot n_i\right)} \tag{3.47}$$

By introducing a three-body abrasion sensitivity coefficient Z_i, Eq.(3.47) can be simplified:

$$t = \frac{\ln\left(\frac{Q_T - Q_{mt}}{Q_T - Q_{m0}}\right)}{\sum_{D_{min}}^{D_{max}} Z_i \cdot n_i} \tag{3.48}$$

where

$$Z_i = \frac{B}{A} v \cdot V_i \tag{3.49}$$

The set of coefficients Z_i represent the sensitivity of a fluid component to three-body abrasive wear since they are derived from wear calculations. Equation (3.48) states that the service life of a fluid component is a function of these coefficients and it is theoretically predictable now since the calculation of Z_i is available.

A detailed examination of these coefficients is conducted by combining Eqs.(3.30), (3.36), and (3.49). It shows that the sensitivity coefficient Z_i depends mainly on the component design (material and clearance) and particle properties. For many cases, the hardness ratio between two surfaces is above three. Thus the resultant form of Z_i can be derived as

$$Z_i = \frac{B}{A} \cdot v \cdot K \cdot (H_f/H_m)^2 \cdot X_i \cdot \zeta \cdot D_i^2 \tag{3.50}$$

where ζ = theoretical particle abrasivity

$$\zeta = (\sin\phi \cdot F_2/F_1^2)^2 \cdot F_3 \tag{3.51}$$

After comparing Eq.(2.4) with (3.48), it is found that the coefficient of contaminant sensitivity S_i is related to the coefficient of three-body abrasion Z_i by a flow rate transfer coefficient k_q:

$$Z_i = K_q \cdot S_i \tag{3.52}$$

where

$$K_q = \ln\left(\frac{Q_T - Q_{mt}}{Q_T - Q_{m0}}\right) / \ln\left(\frac{Q_{m0}}{Q_{mt}}\right) \tag{3.53}$$

CHAPTER IV

EXPERIMENTAL EVALUATION OF WEAR MODEL

In order to validate the feasibility of the wear model and component contaminant sensitivity theory developed in Chapter III, a large number of experimental tests have been conducted. The experimental program consists of two sub-programs : the lubricated three-body abrasive wear tests and the hydraulic pump contaminant sensitivity tests. The experimental details of wear tests is presented in this chapter, while the pump test results will be reported in next chapter.

Experimental Considerations

The wear model, Eq.(3.38), states that the total wear volume in a lubricated three-body abrasion process depends on several parameters : the operating time, t; the rate of flow passing through the clearance, Q; the particle size-concentration distribution in the fluid, D_i - N_i; and the per particle wear volume, V_i. To evaluate the wear model, these parameters need to be measured from tests and specified in calculation. Then the validation of Eq.(3.38) can be estimated by comparing the experimental result with the computational result under the same wear condition.

However, one problem here is that it is almost impossible to directly observe the wear caused by individual particles during a wear test. The per particle wear volume V_i has to be determined by three dimensionless particle property functions as shown by Eq.(3.37). In addition, a qualified wear test system associated with a verified test method is required. Therefore, the wear test subprogram includes the following three test groups :

1. Tests to verify the repeatability and accuracy of the developed test system and to qualify the required wear measuring method and test procedures.
2. Tests to determine the three particle property parameters.
3. Tests to evaluate the feasibility of the wear model for specified operating conditions.

Test System and Wear Measurement

According to the literature survey, few investigations with test system capable of providing a desired and stable fluid film lubrication condition were conducted before Hong (66) developed the Gamma tester at the FPRC in 1983. Commonly used abrasive wear testers in previous studies were pin-on-disc testers, journal-V block (Falex) testers, ball-on-ball (Four Ball) testers, cup-on-block (Timken) testers, etc. Most of these testers were originally designed for testing anti-wear properties of lubricants under boundary or extreme pressure conditions, but not for simulating thick film lubricated three-body abrasive wear condition because

1. The fluid film thickness cannot be controlled due to the design of the contact geometry, loading mechanism, and driving system.
2. The material of the test specimen are usually fixed and not easily be changed.
3. The fluid circulation system is usually not available.
4. The fluid temperature is difficult to control. This leads to an unstable fluid film condition.

Due to the lack of effective test methods for assessing contaminant-induced wear in a lubrication system, an increasing demand for such techniques is being voiced by industry. Hong (66) developed the Gamma Test System on the basis of a previous FPRC Gamma Falex System. Major improvements for establishing a hydrodynamic lubrication condition include changing the specimen geometry from V shape block to 120 degree bearing, increasing rotating speed to 2400 rpm, and reducing the spring loading to 0.5 lbs. Under these conditions, this test system can provide a minimum film thickness of 13.2 micrometers.

The non-linearity of the spring loading mechanism in the Gamma test system is significant under the very low loading conditions that are needed for a wider range simulation of three-body abrasion process; consequently, a test system with lighter and more stable loading capacity is necessary. This need led to the development of the Thick

Film Gamma Machine (70). Fig.37 shows a schematic diagram of the wear test system. The original loading spring was replaced by a simple dead-weight loading mechanism, as shown in Fig.38. In this way, the load is guaranteed to be kept constant even at a very light loading level. Another major modification from the Gamma test system is the compact-sized electrical motor used instead of the hydraulic motor driving system, because only a small driving torque with a rather higher rotating speed is needed in this wear condition. The speed of the electrical motor can be adjusted by using a speed control system. The maximum rotating speed is 3300 rpm. The test specimen has the same geometrical dimensions as that used in Gamma Test System. Fig.39 illustrates the configuration of the journal-bearing assembly. The detailed test procedures are listed in Appendix A.

In last two years (61, 67), the validation of the developed Thick Film Wear Tester and the test method has been evaluated by performing a large number of experiments. These tests are arranged as two major parts for testing the repeatability and sensitivity of the tester and for choosing an accurate wear measuring method.

ACFTD particles of three different size ranges -- 0 - 20, 0 - 50, and 0 - 80 micrometer -- were used to examine the repeatability of the developed test system. For each particle size, fifteen wear tests were run under identical operating conditions: ACFTD concentration level of 100

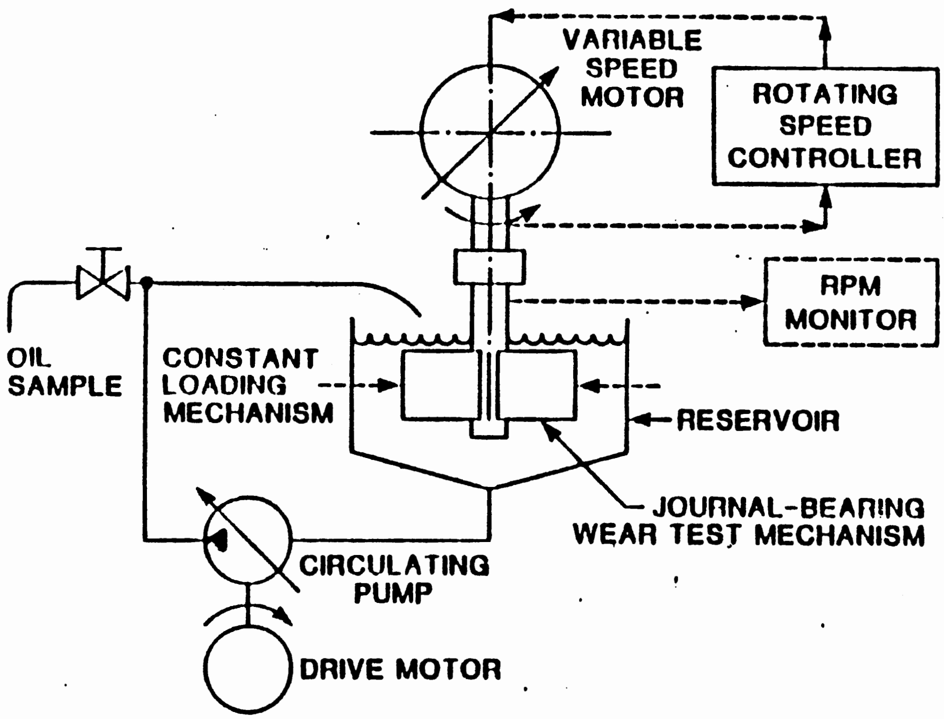

Fig.37 Thick Film Wear Test System

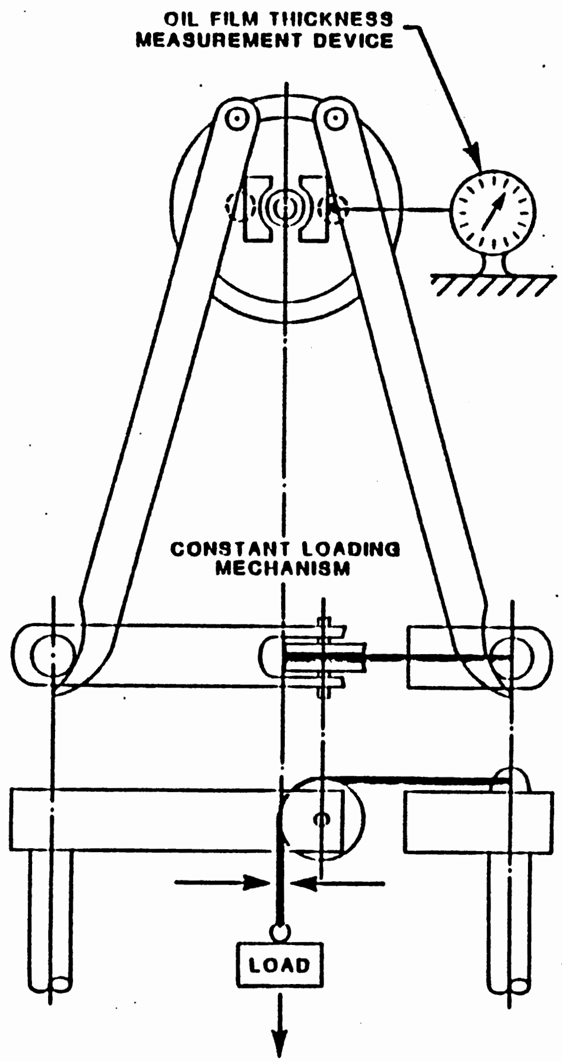

Fig.38 Constant Loading Mechanism

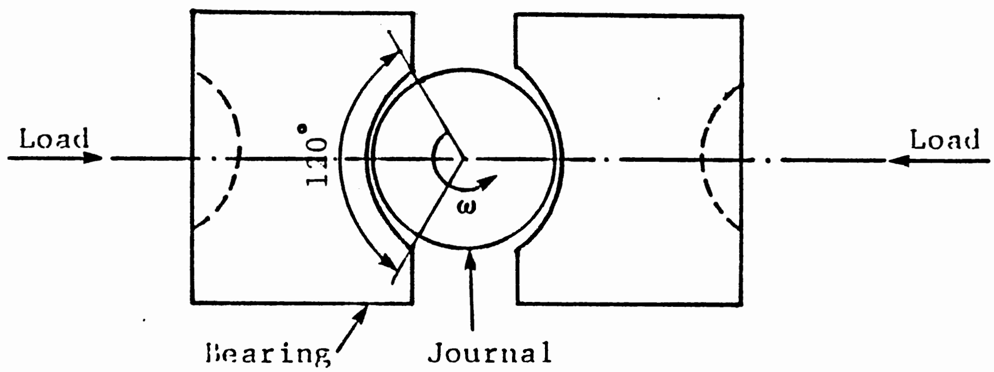

Fig.39 120° Bearing-Journal Assembly used in Thick Film Wear Test System (mg/L), 2104 hydraulic fluid at 25^{o} C temperature, 3000 rpm rotating speed, and a 300 gram applied load. The test specimen is composed of 3135 steel journal and a pair of free cut brass bearings. Test results are listed in Table III and plotted in Fig.40, where the wear is measured by weighting the test journal before and after a 30 - minutes test period. Statistical analysis on test data were performed. The average value of weight loss, the standard deviation, and the 95 percent confidence level intervals for the weight loss and standard deviation are also given in Table III. The accuracy of the test system can be analyzed by the maximum possible error, which is three times the standard deviation. Another important parameter in the repeatability analysis is the coefficient of variation, which is the ratio of the standard deviation to the mean value and is expressed by Eq.(4.1):

$$w = S / X \tag{4.1}$$

where S = standard deviation

X = mean value

Since the variation coefficient w for all three cases is within a five percent range, the repeatability of the tester is satisfied.

A second set of qualifying tests were conducted to examine the sensitivity of the tester as well as the weight loss wear measuring method. The weight loss method was chosen as the wear measure because the weight loss of a

TABLE III

THICK FILM WEAR TESTER REPEATABILITY TEST DATA

Test No.	0-20 um	0-50 um	0-80 um
1	0.7 (mg)	0.49 (mg)	0.42 (mg)
2	0.68	0.475	0.385
3	0.66	0.43	0.41
4	0.73	0.47	0.418
5	0.76	0.42	0.40
6	0.675	0.44	0.388
7	0.68	0.445	0.39
8	0.66	0.478	0.40
9	0.655	0.435	0.415
10	0.69	0.43	0.425
11	0.683	0.46	0.387
12	0.662	0.465	0.395
13	0.705	0.455	0.413
14	0.647	0.44	0.405
15	0.658	0.48	0.395
Mean X	0.683(mg)	0.454(mg)	0.403(mg)
95% Confidence Interval of X	[0.66,0.7]	[0.44,0.47]	[0.39,0.41]
Standard Deviation S	0.0307	0.0216	0.0131
95% Confidence Interval of S	[0.023,0.048]	[0.016,0.034]	[0.0096,0.0206]
Max.Possible Error 3S	0.0921	0.0648	0.0393
Variation Coefficient w	4.5 %	4.7 %	3.2 %

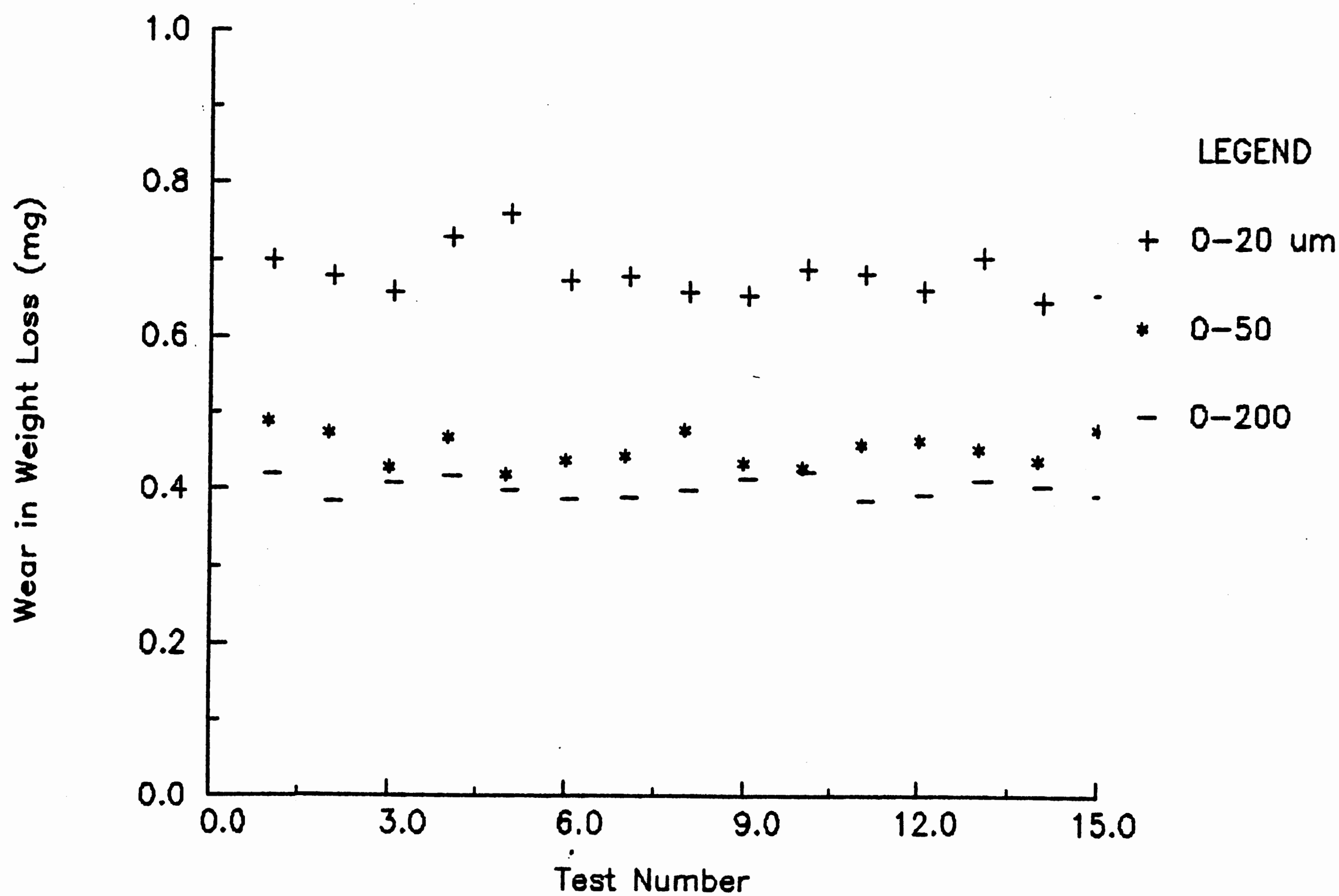

Fig.40 Thick Film Wear Tester Repeatability Test Results

specimen directly reflects the amount of material removed from the surface. This value was precisely measured in this study by using a precision balance, which provides a 10 ug resolution. Considering that the surface roughness of a standard journal should vary with the wear process, the journal surface roughness was also measured using a stylus profilometer. The roughness change can be used to compare the sensitivity and accuracy of the weight loss measuring method.

First, four tests were run with the same size (0 - 50 um) ACFTD particles but at one of four different concentration levels : 0 (mg/L), 50 (mg/L), 100 (mg/L), and 200 (mg/L). All other operating parameters remained the same as those in previous tests. Fig.41 (a) shows the wear data in terms of weight loss, while Fig.41 (b) depicts the wear measured by the roughness change on the journal surface. The relationship between wear in 30 minutes and concentration levels is summarized in Fig.42 (a) for the weight loss method and in Fig.42 (b) for the roughness measure. These figures show that when using this system, 0.20 mg material was removed from the journal surface in a 30 minute period even under clean fluid conditions because of the unexpected surface contact at the start and end of test. If this value is taken as a base wear level, a relative wear measurement can be made. By comparing Fig.41 (a) and 41 (b), it is found that the wear reading is consistent up to 100 (mg/L) concentration level, measured by

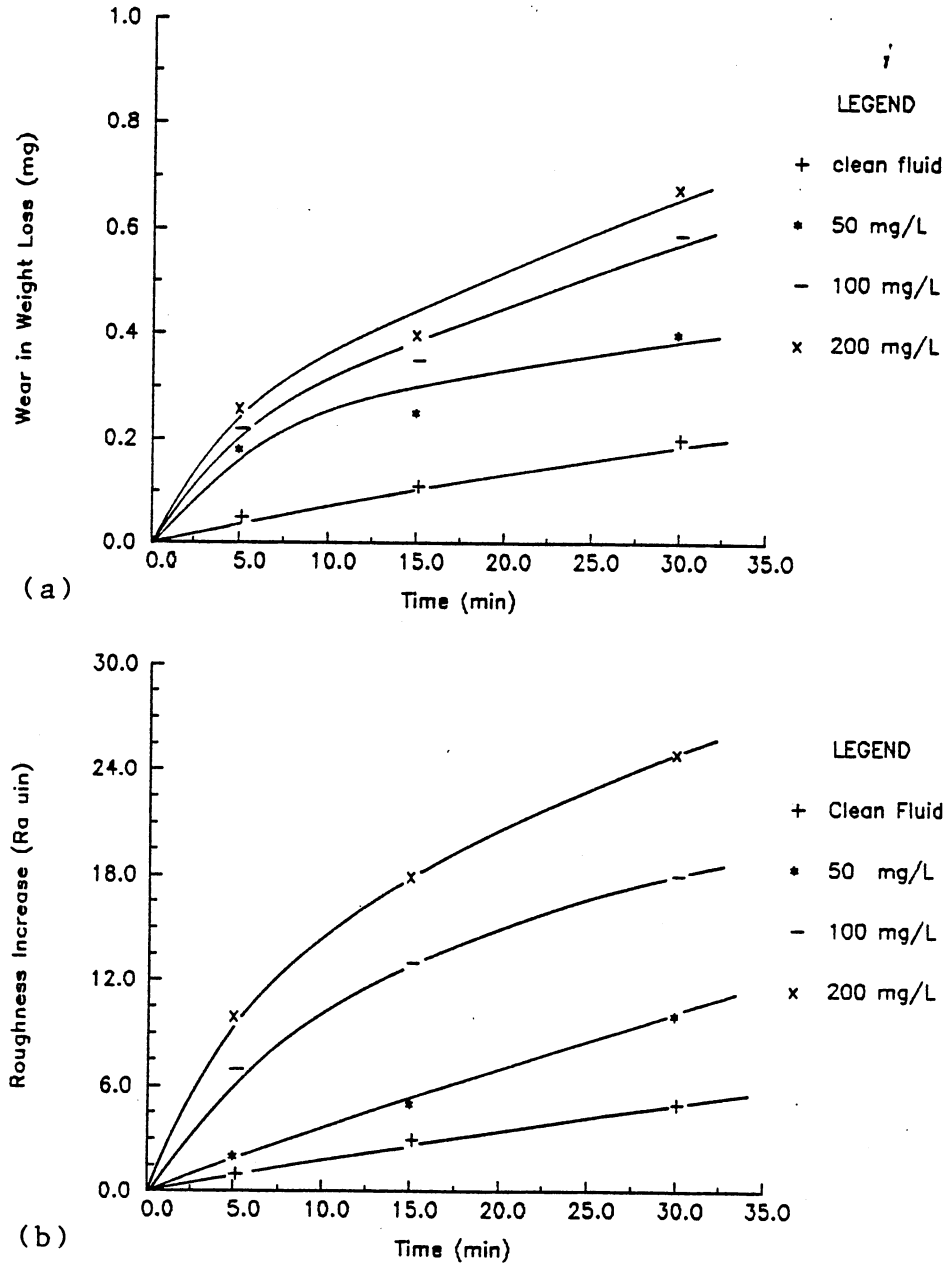

Fig.41 Abrasive Wear vs. Concentration (ACFTD, 0-50 um)

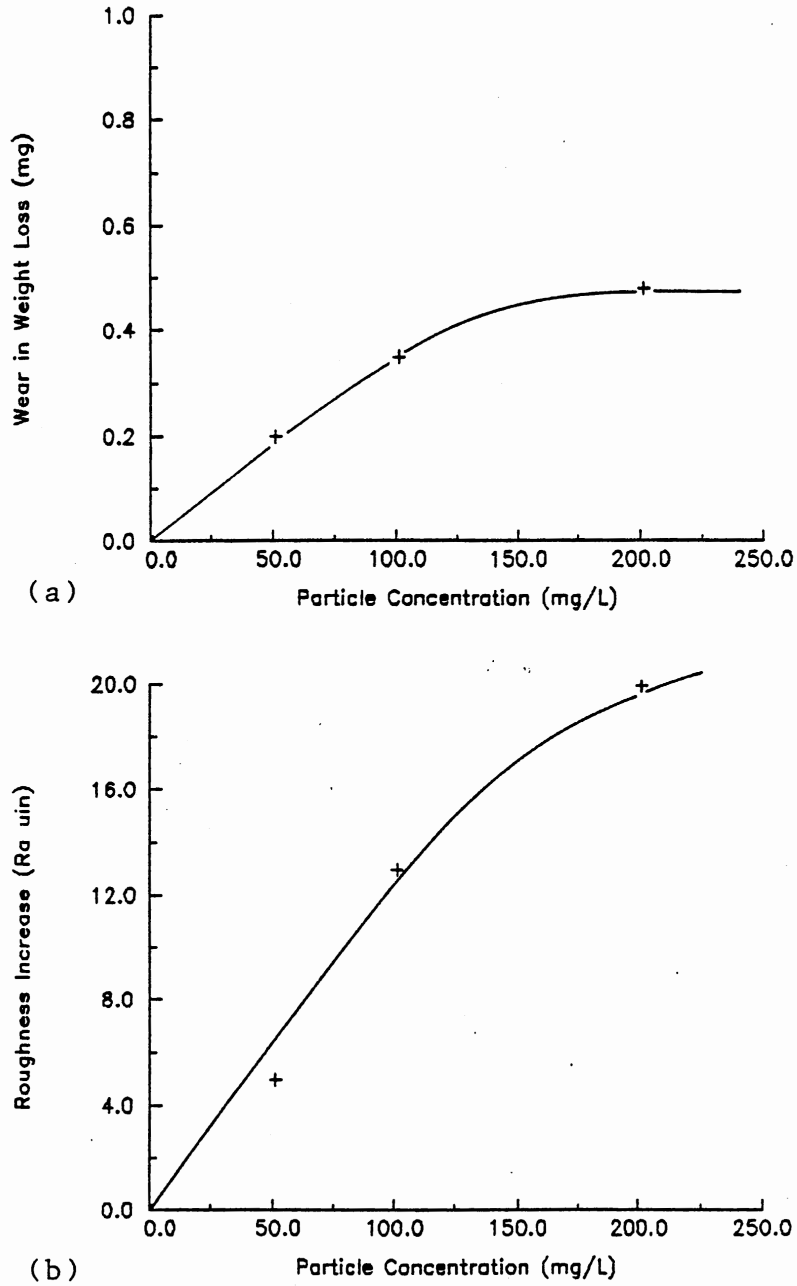

Fig.42 Abrasive Wear vs. Concentration of ACFTD Particles

either the weight loss method or the roughness change method. Above this level, the wear value becomes unstable. Therefore, the 100 (mg/L) concentration level was considered as an optimal operating level. The significance of this selection was double checked by carrying out another set of wear tests. Particles obtained from five types of rocks classified as A, B, C, D, and E were used in five tests. The particle concentration was 100 (mg/L) and the size range was 0-50 um. In each test, the journal specimen was weighed at 0, 5, 15, and 30 minutes and its surface roughness was also measured and recorded. These results are shown in Fig.43 and illustrate that the developed wear test system associated with the weight measuring method is sensitive enough to distinguish various wear situations caused by particles of different properties, even for very similar particles as C and D.

As a summary, the repeatability model of the Thick Film Wear Tester is constructed based on the analysis of three wear data sets, with a total of 54 tests. According to this model, when a multiple number of lubricated three-body abrasive wear tests are conducted under identical test conditions, at least 83 percent will fall within a normal distribution with a variation coefficient of 3.2 to 4.7 percent, or with a standard deviation of 0.01313 to 0.03 for a mean value of 0.4 to 0.68. In addition, the developed test system is able to distinguish different wear situations

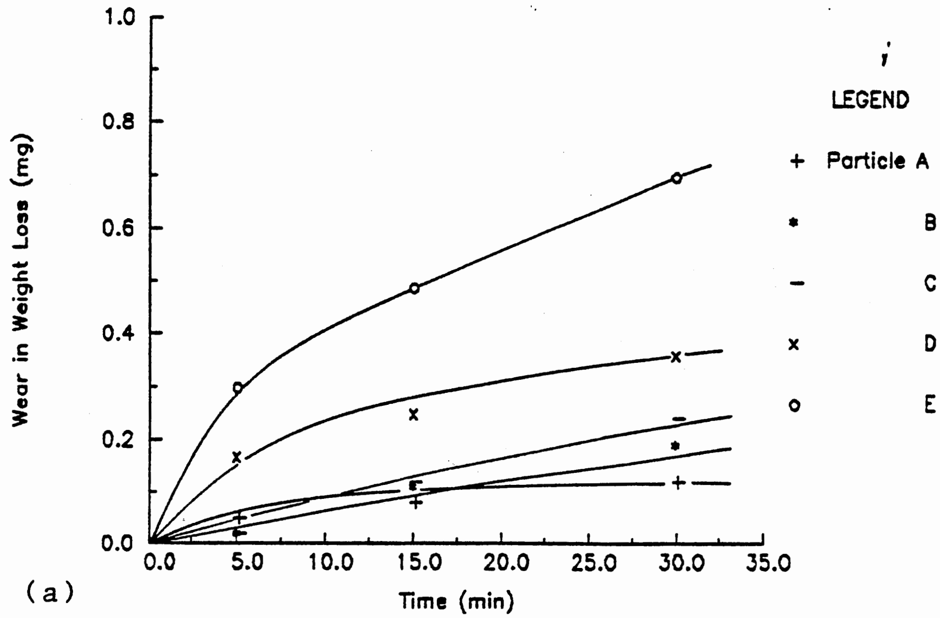

(a)

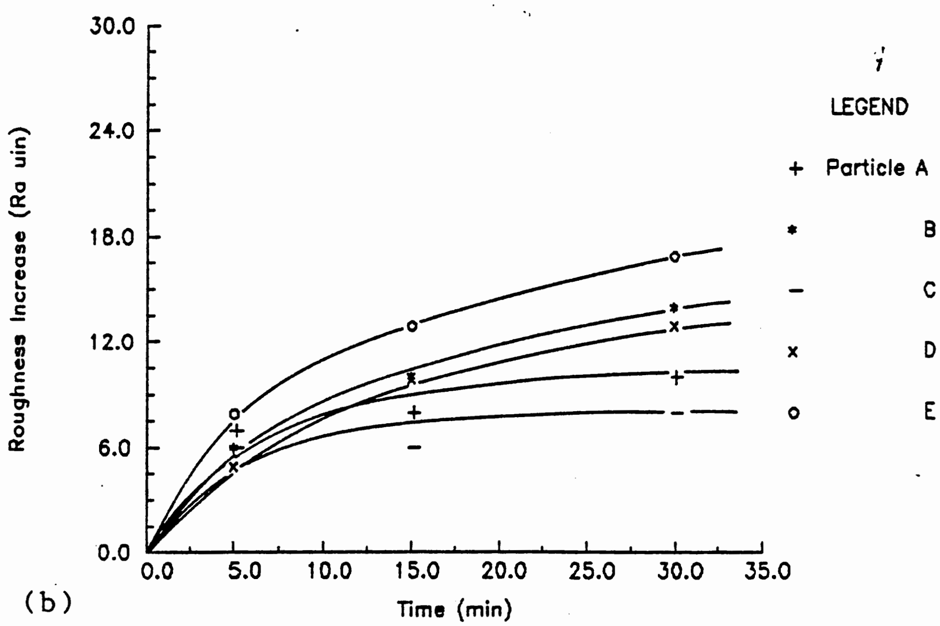

(b)

Fig.43 Wear Caused by Different Abrasives.
(100mg/L, 0-50 um)

caused by different particle sizes or different types of particles, at the test concentration level of 100 mg/L.

Evaluation of Particle Property Effect

As stated in Chapter III, the particle properties play an important role in the process of three-body abrasive wear. In the theoretical model, the wear volume is accumulated by the N_i wear volumes V_i at each particle size D_i from the smallest harmful particle size D_{min} to the largest size D_{max}, while the individual wear volume V_i depends upon three particle-related functions. In order to verify the wear model developed, some critical parameters involved in these three functions -- the shape, the hardness, and the toughness -- need to be determined experimentally. The parameter involved in the particle shape function F_1, Eq.(3.27), is the average wedge angle . Actually, most types of contaminants have a variety of shapes. Therefore, the parameter is sometimes hardly obtainable. Each inorganic particle, however, does have features that depict their origin, generating mode, and subsequent exposure prior to being captured (1). Many people tried to characterize particle shapes as precisely as possible in order to calibrate the automatic particle counters or to improve the filtration technology (126, 133, 134). Usually, the shape of a particle is observed under a microscope. Dimensions that can always be measured with respect to any irregular particles are the maximum cord length (L) and the minimum cord length or width (W). Walker (1, 134) studied the average length and width of common particles except the microbeads of glass. In the present research, the shape of glass beads of sizes from 10 - 40 um were examined under a Trans-Sonics microscope with one thousand magnification. It was found that these glass beads belong to the well rounded group. For simplifying the analysis, the average length-to-width ratio is estimated to be about 1.1. Thus four kinds of particles, ACFTD, Al_2O_3, Iron Powder, and Glass beads, are selected in the abrasion research for their distinctive properties in hardness, brittleness (toughness), and shape. By adding Walker's average length and width data for the first three particles, Table IV is constructed to show the major shape parameters for these four particles, where the half wedge angle θ is calculated by Eq.(4.2)

$$\theta = \tan^{-1}(W / L) \tag{4.2}$$

where W = Average particle width.

L = Average particle length.

The hardness function F_2, Eq.(3.31), is more difficult to determine since it should represent the complex relationships among hardnesses of the journal, bearing, and particles involved in three-body abrasion process. Four journal metals, three bearing metals and four kinds of abrasives were selected to simulate a variety of practical

TABLE IV

SHAPE PARAMETERS OF FOUR TYPICAL PARTICLES

Particle Type	Particle Shape Parameters		
	Average Width W	Average Length L	Average Wedge Angle $\theta°$
ACFTD	1	1.49	33.86
Al_2O_3	1	1.48	34.0
Iron Powder	1	1.64	31.37
Glass Beads	1	1.1	42.27

situations. These materials and their hardnesses in Rockwell, Knoop, and Moh's scales are listed in Table V. By using the Knoop hardness values, the bearing-to-journal hardness ratio (H_f/H_m) and the journal-to-abrasive hardness ratio (H_m/H_a) are calculated and listed in Tables VI and VII, respectively. Eight tests were arranged to examine the wear dependence on abrasive hardness with two bearing-to-journal combinations (H_f/H_m = 0.3 and 0.6), since it is known from Fig.24 that both of these hardness ratios (H_f/H_m and H_m/H_a) affect the wear severity. The wear was measured by journal weight loss in each test. Also, the actual particle numbers were counted. Major test results are illustrated in Table VIII, which shows the total wear in 30 minutes, the initial particle concentration of the size 20 - 40 um in the fluid, and the per particle wear on this size base. The data of total wear are plotted in Fig.44. It is clearly seen from this figure that the effects of bearing-to-journal hardness ratio and journal-to-abrasive hardness ratio are significant. However, these data show that the wear is not linearly dependent upon the H_m/H_a ratio as analyzed based on earlier research, but varies geometrically with the H_m/H_a ratio at either H_f/H_m level tested. In fact, by plotting these data on a log-log diagram, quite good straightline relations are revealed between the wear and the journal-to-abrasive hardness ratio, for both the total wear case and the per particle wear case, as shown in Figs.45 and

TABLE V

HARDNESS OF JOURNAL, BEARING, AND PARTICLES

Materials		Rockwell Hardness	Knoop Hardness kg/mm^2
Journal (Steel)	3135	Rb 89	200
	1020	Rc 20-24	290
	4130	Rc 41-45	480
	1095	Rc 56	660
Bearing	Brass	Rb 74	150
	Al	Rb 80	170
	Steel	Rb 89	200
Particles	Iron Powder	MOH's 3.5	240
	Glass Beads	MOH's 5.2	590
	ACFTD	MOH's 6.9	1100
	Al_2O_3	MOH's 8.5	2100

TABLE VI

BEARING-TO-JOURNAL HARDNESS RATIO

H_m \ H_f	Brass	Al	Steel
3135 Steel	0.75	0.85	1.00
1020 Steel	0.52	0.59	0.69
4130 Steel	0.31	0.35	0.42
1095 Steel	0.23	0.26	0.30

TABLE VII

JOURNAL-TO-ABRASIVE HARDNESS RATIO

H_m \ H_a	Iron	Glass	ACFTD	Al_2O_3
3135 Steel	0.83	0.34	0.18	0.10
1020 Steel	1.20	0.50	0.26	0.14
4130 Steel	2.00	0.82	0.44	0.23
1095 Steel	2.75	1.12	0.60	0.31

TABLE VIII

TEST DATA ILLUSTRATING HARDNESS EFFECT ON WEAR

Test Number	Particle	Journal	Bearing	H_f/H_m	H_m/H_a	Total Wear	Number 20-40um	Wear/ Particle
H1	Iron	1095	Steel	0.3	2.75	0 mg	292	0 ug
H2	Glass	1095	Steel	0.3	1.12	0.12	237	0.5
H3	ACFTD	1095	Steel	0.3	0.60	0.43	200	2.2
H4	Al_2O_3	1095	Steel	0.3	0.31	1.21	70	17.2
H5	Iron	1020	Al	0.6	1.20	0.72	292	2.5
H6	Glass	1020	Al	0.6	0.50	2.05	237	8.6
H7	ACFTD	1020	Al	0.6	0.26	2.81	200	14.1
H8	Al_2O_3	1020	Al	0.6	0.14	5.09	70	72.7

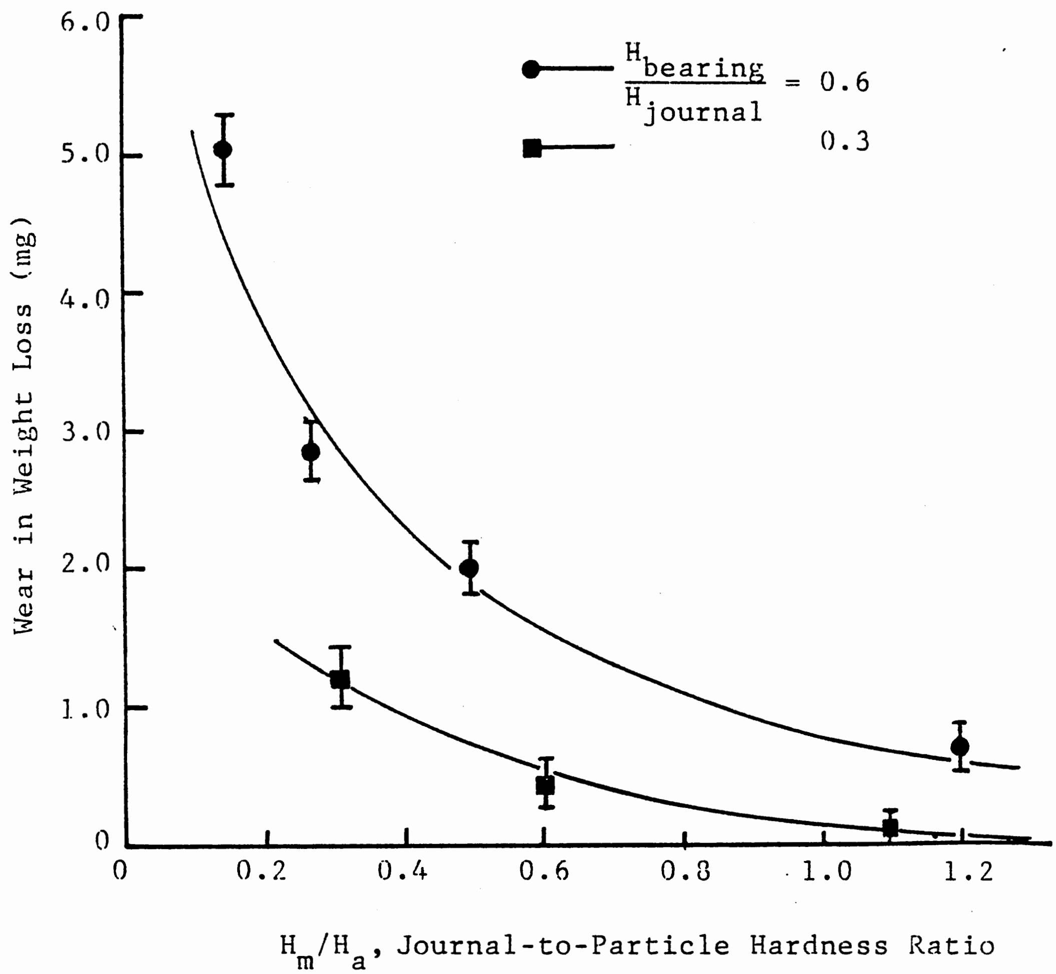

Fig.44 Wear Results Showing the Hardness Effect

46, respectively. Therefore, the hardness function F_2, Eq.(3.31) must be modified as

$$F_2 = \begin{cases} 1 & , 0 < \overline{H} \leqslant \overline{H}_c \\ a \cdot \overline{H}^b / \overline{H}_c & , \overline{H}_c < \overline{H} \leqslant \overline{H}_{max} \\ 0 & , \overline{H}_{max} < \overline{H} \end{cases} \qquad (4.3)$$

where a, b = constants.

In Eq.(4.3), constants a and b can be obtained by using the least square curve fitting method for each data set, as shown in Table IX. The critical hardness ratio and maximum ratio for 0.3 H_f/H_m level are estimated as 0.3 and 1.2, respectively; and 0.15 and 3 for 0.6 H_f/H_m level.

The parameter involved in the particle toughness function F_3 is the destruction time constant . Previously, this value was estimated based on the flow degradation rate in a pump test. Using the Thick Film Wear Tester, the abrasive destruction time can be determined by using inexpensive specimens. Four tests were run for this purpose. In each test, the journal wear was measured every three minutes for a total of 15 minutes; at the same time, a fluid sample was collected and the number of particles in the fluid was counted. 1020 steel journal and aluminum bearings were used. The particle counting results are illustrated in Appendix B. The wear data is shown in both Table X and Fig.47. Various criteria can be applied here to determine

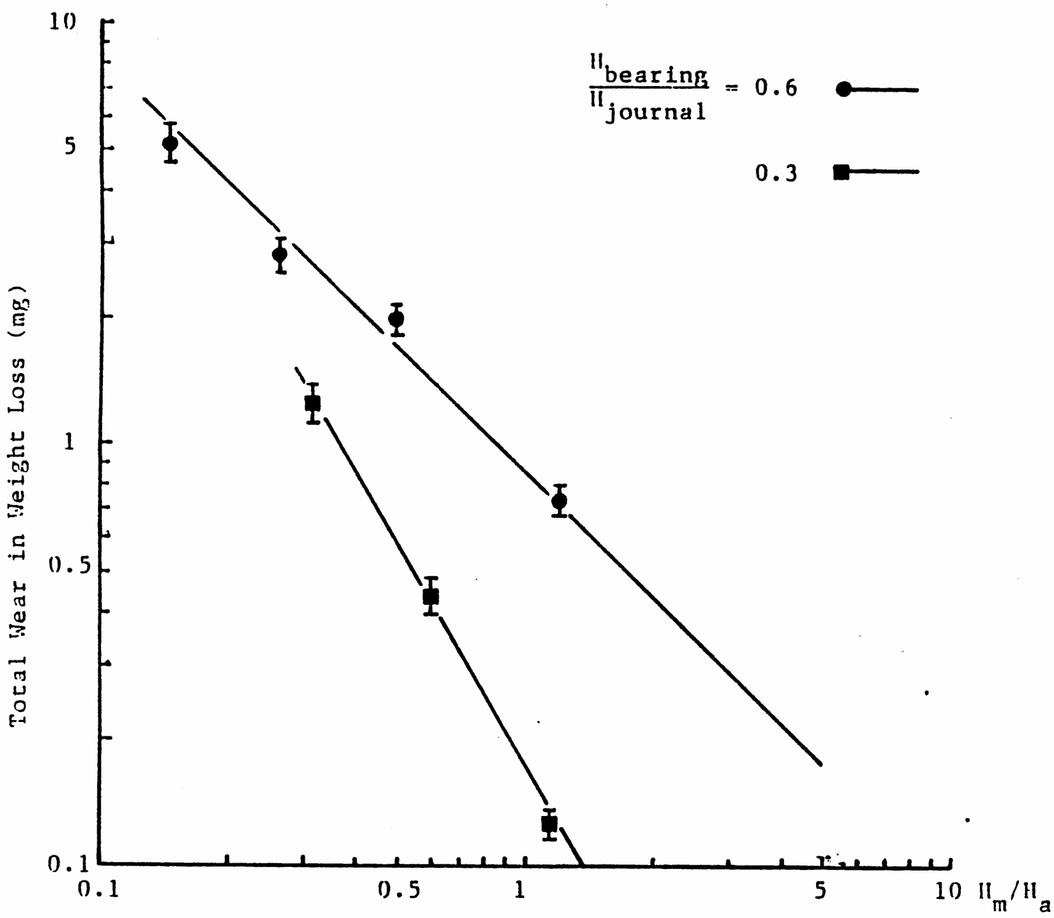

Journal-to-Abrasive Hardness Ratio

Fig.45 Total Wear vs. Hardness Ratio H_m/H_a

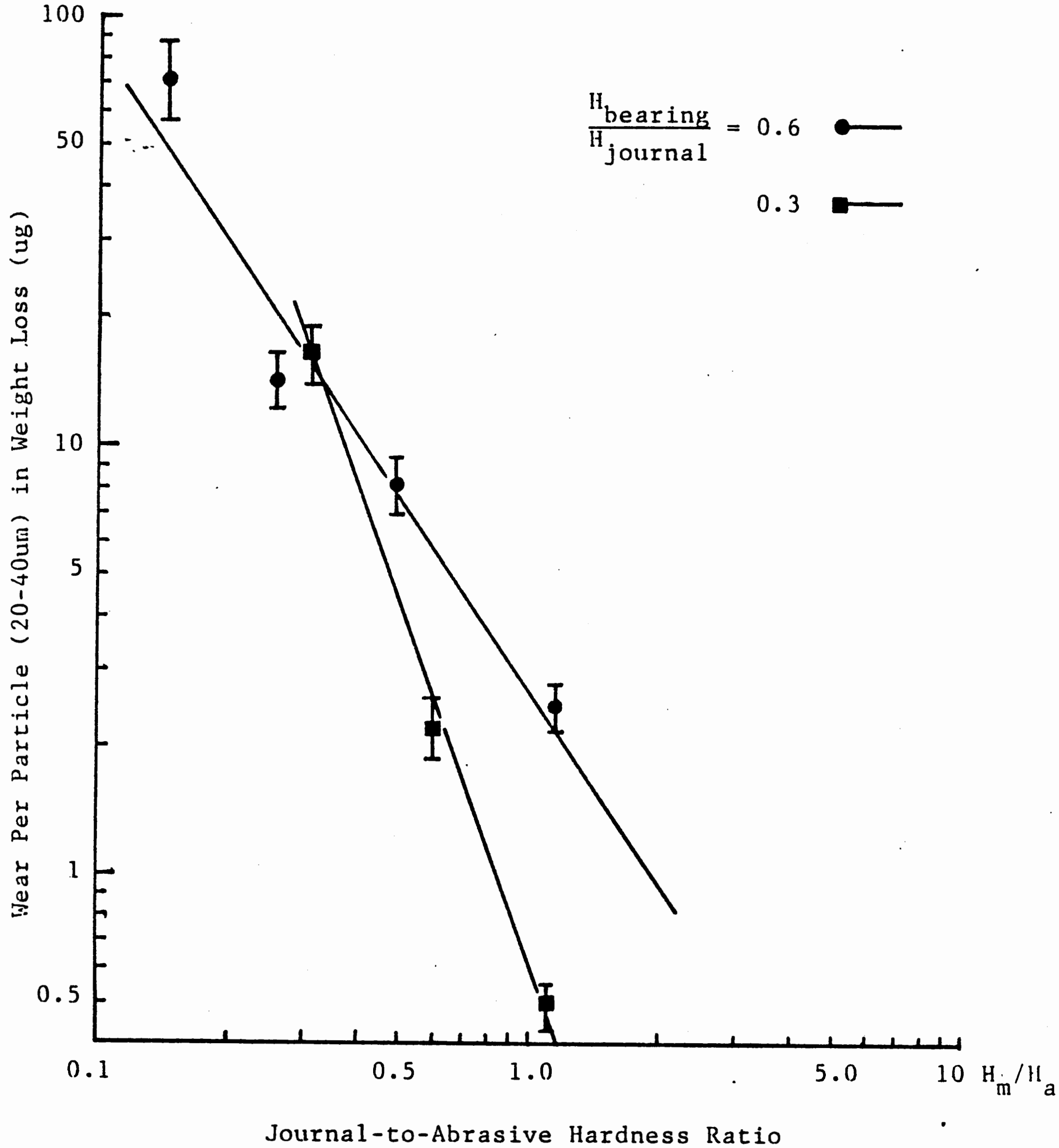

Fig.46 Per Particle Wear vs. Hardness Ratio H_m/H_a

TABLE IX

DETERMINATION OF CONSTANTS A AND B

Wear	H_f/H_m	a	b
Total	0.3	0.182	-1.686
	0.6	0.85	-0.91
Per Particle (20 - 40 um)	0.3	2.687	-1.62
	0.6	0.4484	-3.11

the destruction time constants depending on each application (as shown in bottom of Table X). However, it can be seen that the nine minutes destruction time for ACFTD particles used previously equals the value in the wear test on the 64 % base. It takes the time when the total wear increased up to 64 percent of the maximum wear as the destruction time of the abrasives tested. Nevertheless, the destruction time constant of ACFTD will extend to 17 to 19 minutes if based on the time at 90 percent maximum wear. From these data, it has been shown that the glass beads have the longest destruction constant; while both the aluminum oxide particles, which is extremely hard and brittle, and the iron powder, which is rather soft but tougher, have almost the same short destruction time. The correctness of these time constants are supported by the particle counting data for each test. The variation of numbers for particles larger than 20 um is shown in Fig.48, and larger than 5 um shown in Fig.49. The number of larger (> 20 um) Al_2O_3 particles decreased rapidly within 6 to 9 minutes; simultaneously, the smaller (> 5 um) Al_2O_3 particles increased rapidly due to the generated wear chips and breakdown of larger particles. After 12 minutes, the particle number became stable. For iron powder, a similar rapid decrease in number of larger particles was found, which corresponds to a short destruction time constant. But the number of particles was

TABLE X

DETERMINATION OF PARTICLE DESTRUCTION TIME

Particle / Test Time (min)	Iron	Glass	ACFTD	Al_2O_3
0	0	0	0	0
3	0.35	0.45	0.54	1.51
6	0.50	0.51	1.25	3.12
9	0.63	0.78	1.51	4.23
12	0.65	1.25	1.82	4.61
15	0.68	1.35	2.10	4.73
30	0.72	2.05	2.81	5.09
τ_1 (min) on 64% Base	4-5	13-15	10-11	6-7
τ_2 (min) on 90% Base	9-12	21-24	17-19	10-12

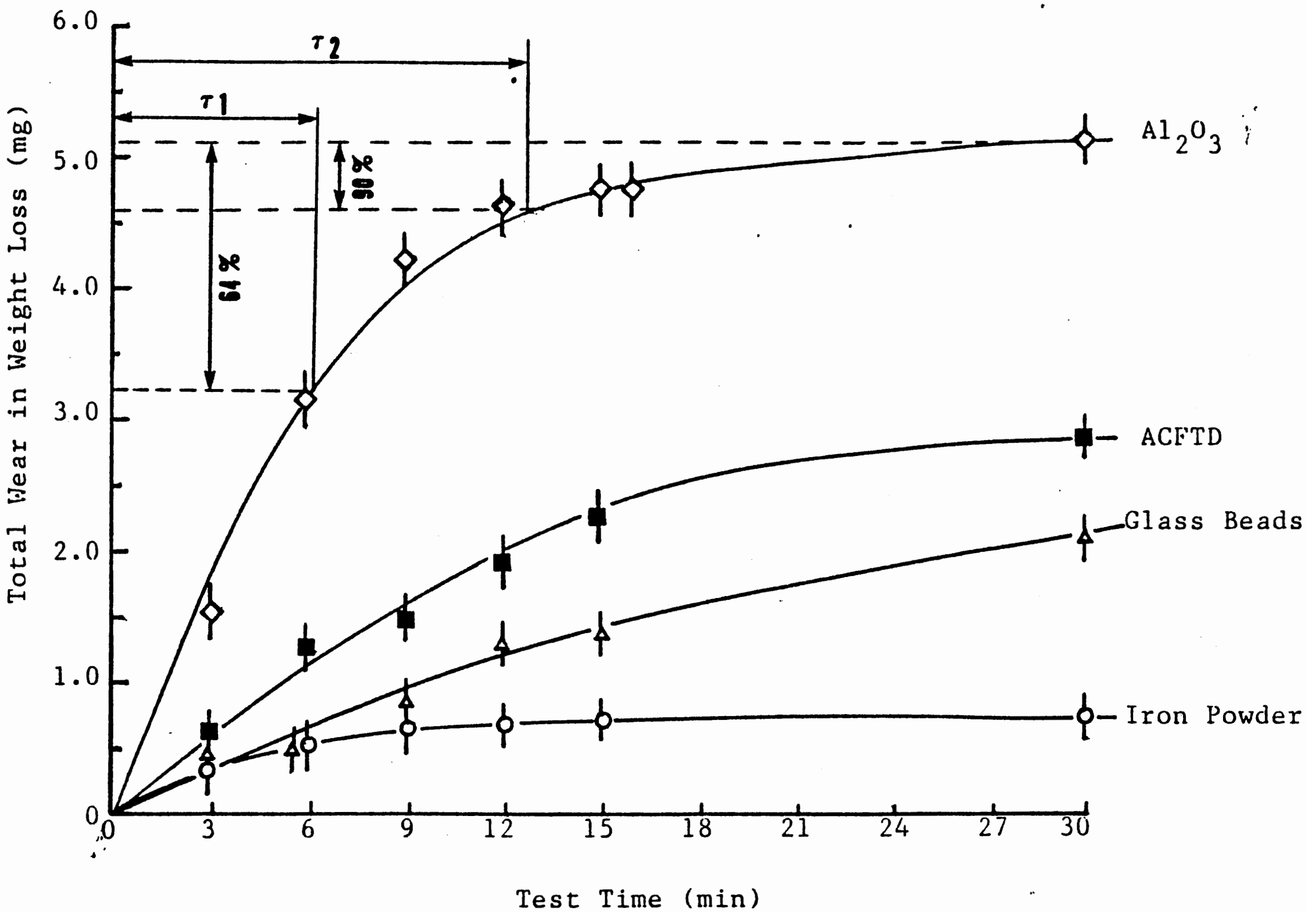

Fig.47 Determination of Particle Destruction Time

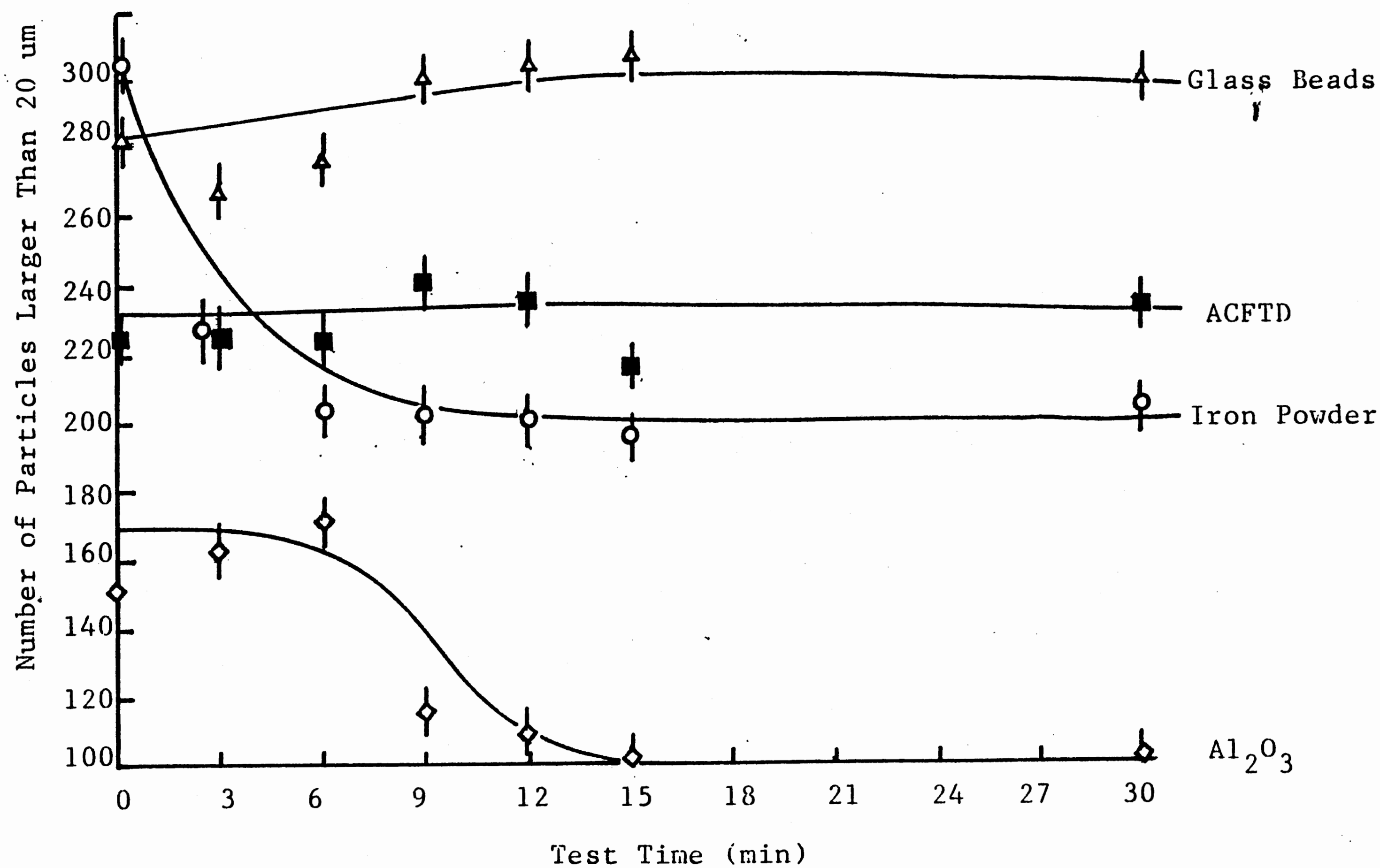

Fig.48 Variation of Number of Particles Larger than 20 um

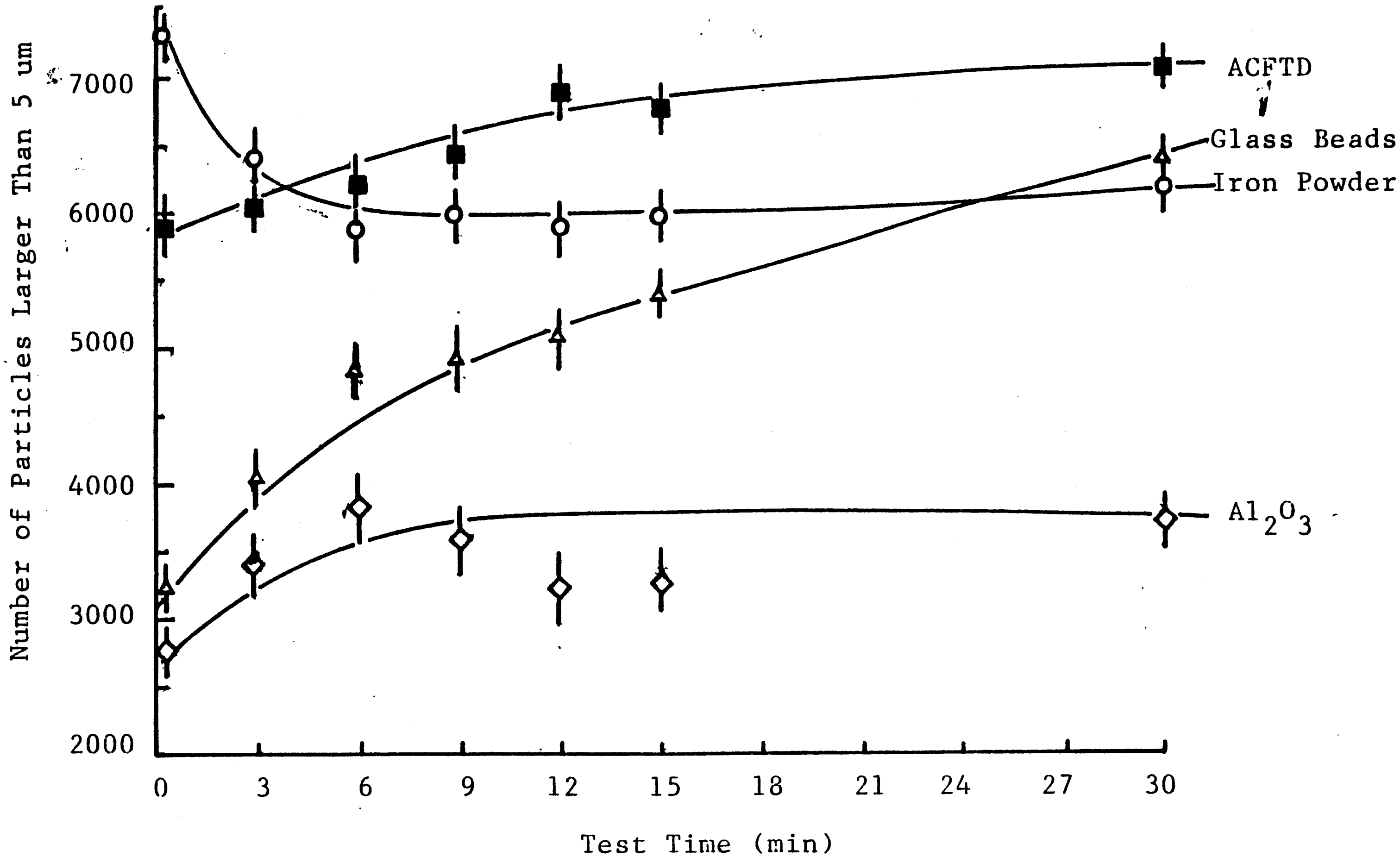

Figure 49 Variation of Number of Particles Larger than 5 um

also found to decrease. This is probably because more particles smaller than 5 um were generated or because of the fast deposit of iron powder in fluid and the sampling error.

For the other two abrasives with longer destruction time, no significant changes in the number of larger particles were observed.

Basically, the method applied here to obtain the destruction time constants of the four test abrasives has been shown correct. The time constants were determined and can be used to predict the wear behavior for a given condition.

Evaluation of Wear Model

Upon the three particle-related variables obtained, the wear for a given condition can be estimated and the wear model, thus, can be evaluated. According to the wear calculation flow chart, Fig.35, the required computational parameters are listed in Table XI, where they are arranged into four basic parameter groups as the operating parameters, fluid parameters, design parameters, and particle parameters. During the tests, most of these parameters were kept the same as described in Table XI, except the journal-bearing assembly and the abrasives, which were specified in each computation and comparison test.

From the analysis of particle shape effect, the size

TABLE XI

COMPUTATIONAL PARAMETER DESCRIPTION

Operating Parameters	applied load	W	300	[gram]
	relative velocity	v	100	[cm/sec]
	fluid flow rate	Q	0.255	[cm^3/sec]
	fluid tempersture	T	25	[C]
	operation time	t	30	[min.]
	min.film thickness	h_{min}	15	[um]
	max.film thickness	h_{max}	35	[um]
Fluid Parameter	viscosity	μ	0.8E-7	[kg-s/cm^2]
Design Parameters	journal radius	R	0.3167	[cm]
	clearance	C	2.54E-4	[cm]
	journal hardness	H_m	(TABLE V)	
	bearing hardness	H_f	(TABLE V)	
Particle Parameters	abrasive hardness	H_a	(TABLE V)	
	wedge angle	θ	(TABLE IV)	
	destruction time	τ	(TABLE X)	
	number at size D_i	n_i	(TABLE XIII,XIV) (Figures 50,51)	
	maximum size	D_{max}	(TABLE XII)	
	minimum size	D_{min}	(same as h_{min})	

range of harmful particles can be determined by Eq.(4.4) and (4.5),

$$D_{min} = h_{min} \tag{4.4}$$

$$D_{max} = \frac{h_{max} \cdot k_{lw}}{\text{Sin } (90 - \theta)} \tag{4.5}$$

where h_{min} = minimum fluid film thickness

h_{max} = maximum fluid film thickness

k_{lw} = ratio of particle length to width (Table IV)

θ = particle half wedge angle (Table IV)

The maximum harmful sizes of the four test abrasives are listed in Table XII, where the D_{max} is expressed either in terms of h_{max} or in terms of actual size if the h_{max} is known. For the case of the thick film tester, the h_{max} is estimated to be 35 um.

Two sets of wear tests were conducted for the purpose of wear model evaluation. The first set comprises three tests, all using the 3135 steel journal with the brass bearings. Iron powder was tested in test T1, glass beads in test T2, and ACFTD particles in test T3. The second test set consisted of four tests with the 1020 steel journal-bearing combination, and iron powder in test H5, glass beads in H6, ACFTD in H7, and Al_2O_3 particles in H8. The actual

TABLE XII

EASTIMATION OF MAXIMUM HARMFUL PARTICLE SIZE

	Iron	Glass	ACFTD	Al_2O_3
W_{max}/h_{max}	1.16	1.35	1.19	1.21
D_{max}/h_{max}	1.90	1.48	1.77	1.79
D_{max} (um) (h_{max}=35)	66	52	62	63

concentration level in each test was carefully examined by counting the number of particles in the test fluid. The particle number larger than each size interval is shown in Table XIII for test set one and in Table XIV for set two. These particle numbers can be expressed as a linear function of size when plotted on a log-log^2 diagram, as illustrated in Fig.50 and 51. Thus, the particle number at a size interval D_{i-1} to D_i is calculated by Eqs.(4.6) and (4.7),

$$N_i = 10^{k_1 \cdot \log^2 D_i + k_2} \tag{4.6}$$

$$n_i = N_{i-1} - N_i \tag{4.7}$$

where N_{i-1} = number of particles larger than size D_{i-1}

N_i = number of particles larger than size D_i

n_i = number of particles of size D_{i-1} to D_i

k_1, k_2 = concentration coefficients

The k_1 and k_2 were calculated in each computer simulation based on two input data, the numbers of particles of size larger than 5 um and 20 um, respectively. By knowing the actual number of particles in the test fluid, the wear volume generated by individual particles and the total wear by all the particles can be calculated for each case. Table XV and Fig.52 present the calculation of wear

TABLE XIII

PARTICLE COUNTING DATA IN WEAR TEST SET ONE

Size (um)	Test Number T1	T2	T3
3	---	---	15,087
5	17,873	789	8,295
10	8,210	545	792
15	---	---	354
20	1,849	435	162
30	374	298	33
40	120	168	--
50	49	90	--

(unit : particle number per milliliter fluid)

TABLE XIV

PARTICLE COUNTER DATA SET 2 IN WEAR TESTS

Size (um)	Test Number H5	H6	H7	H8
5	7,331	3,210	5,940	2,728
10	2,385	938	1,414	628
20	310	283	224	148
30	65	119	82	96
40	18	46	25	80
50	7	17	9	58

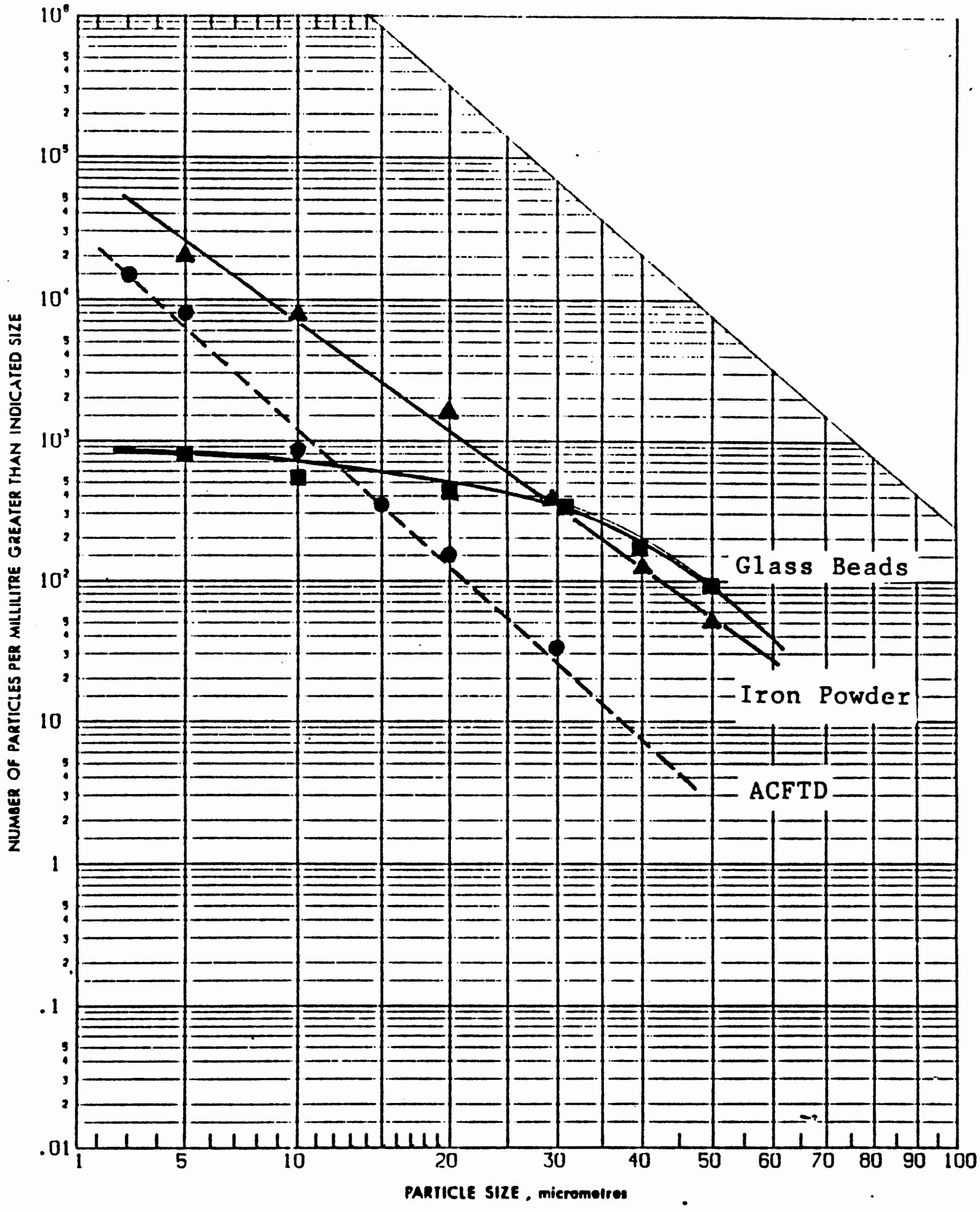

Fig.50 Concentration Levels in Wear Test Set One

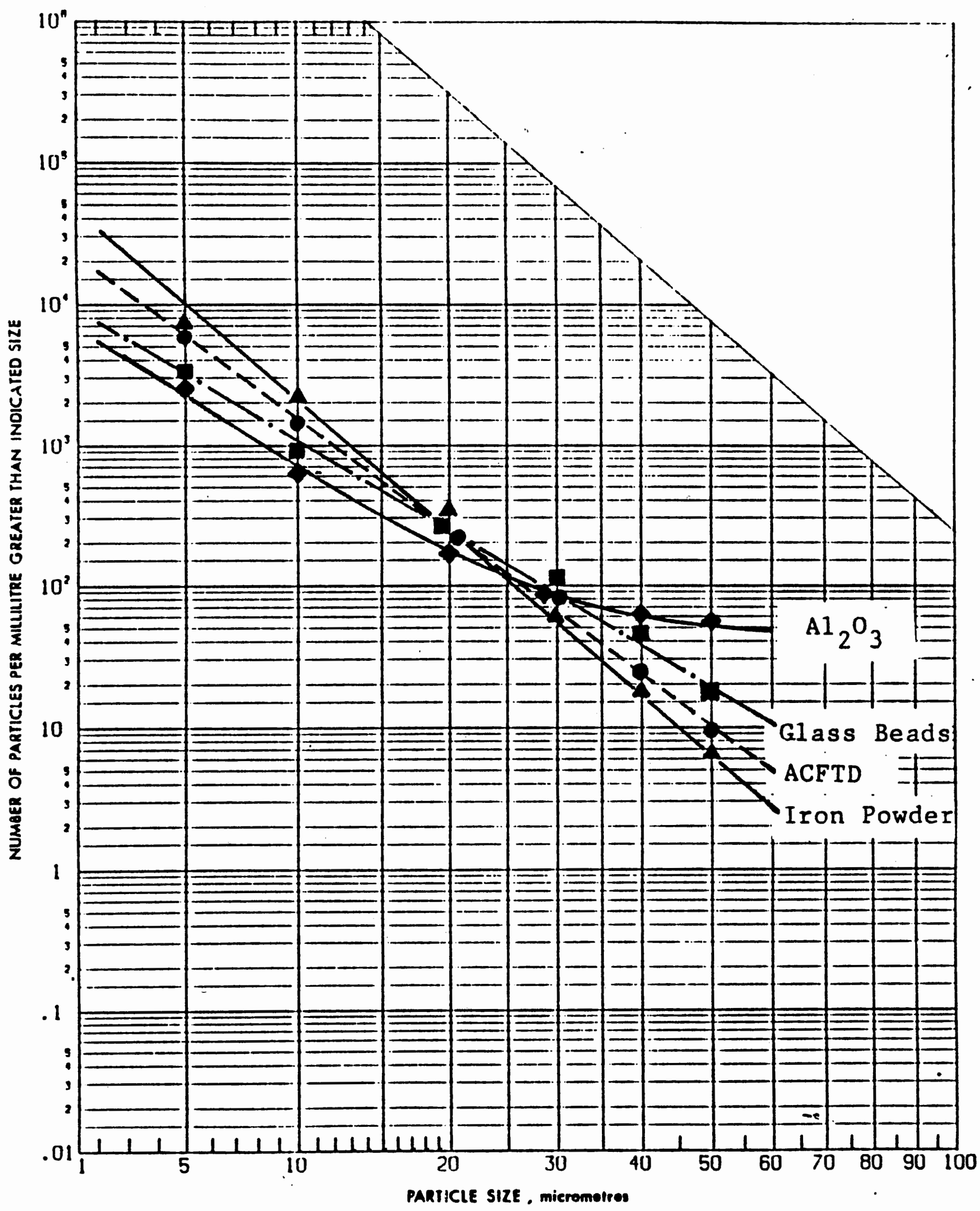

Fig.51 Concentration Levels in Wear Test Set Two

per second by iron powder (test T1). The wear is calculated for particles of sizes from 15 um to 66 um. The per particle wear is shown to be a square function of particle size, as analyzed in the wear model. The total wear, on the other hand, shows a steady linear increase with increasing size until a critical size of about 52 um; above this size, wear decreases due to fewer particles. Finally, no wear is generated if the particles are larger than D_{max} since it is assumed that these particles cannot get into the clearance between surfaces. This prediction agrees with previous test results shown in Fig.21.

According to the wear model, the total wear in a test period t is the summation of the wear in each time interval dt. Experimental data of the seven tests are compared with theoretical predictions and shown in Table XVI. By plotting the data on Fig.53 for the first test set and on Fig.54 for the second set, it can be clearly seen that the destruction time constants obtained in earlier tests are basically correct and these values have a significant effect on wear prediction. The maximum relative error of the wear model is 18 to 36 percent for iron powder, 14 to 28 percent for glass beads, 16 to 21 percent for ACFTD, and 16 percent for Al_2O_3 particles. However, the wear model is shown to be effective and applicable for performance degradation analysis of general tribo-mechanical components, if all the computational

TABLE XV

WEAR CALCULATION FOR IRON POWDER (TEST T1)

Particle Size D_i (um)	Wear Per Particle of Size D_i (E-8 mg)	Total Wear of Size D_i (E-3 mg)
15	0.0	0.00
30	1.4	3.54
32	3.8	8.05
34	7.4	12.50
36	11.9	16.75
38	17.5	20.52
40	24.1	23.73
42	31.7	26.37
44	40.2	28.46
46	49.5	30.02
48	59.7	31.08
50	70.5	31.73
52	81.9	32.01
54	93.8	31.97
56	106.0	31.67
58	118.7	31.14
60	131.6	30.44
62	144.5	29.60
64	157.6	28.65
66	170.7	27.61

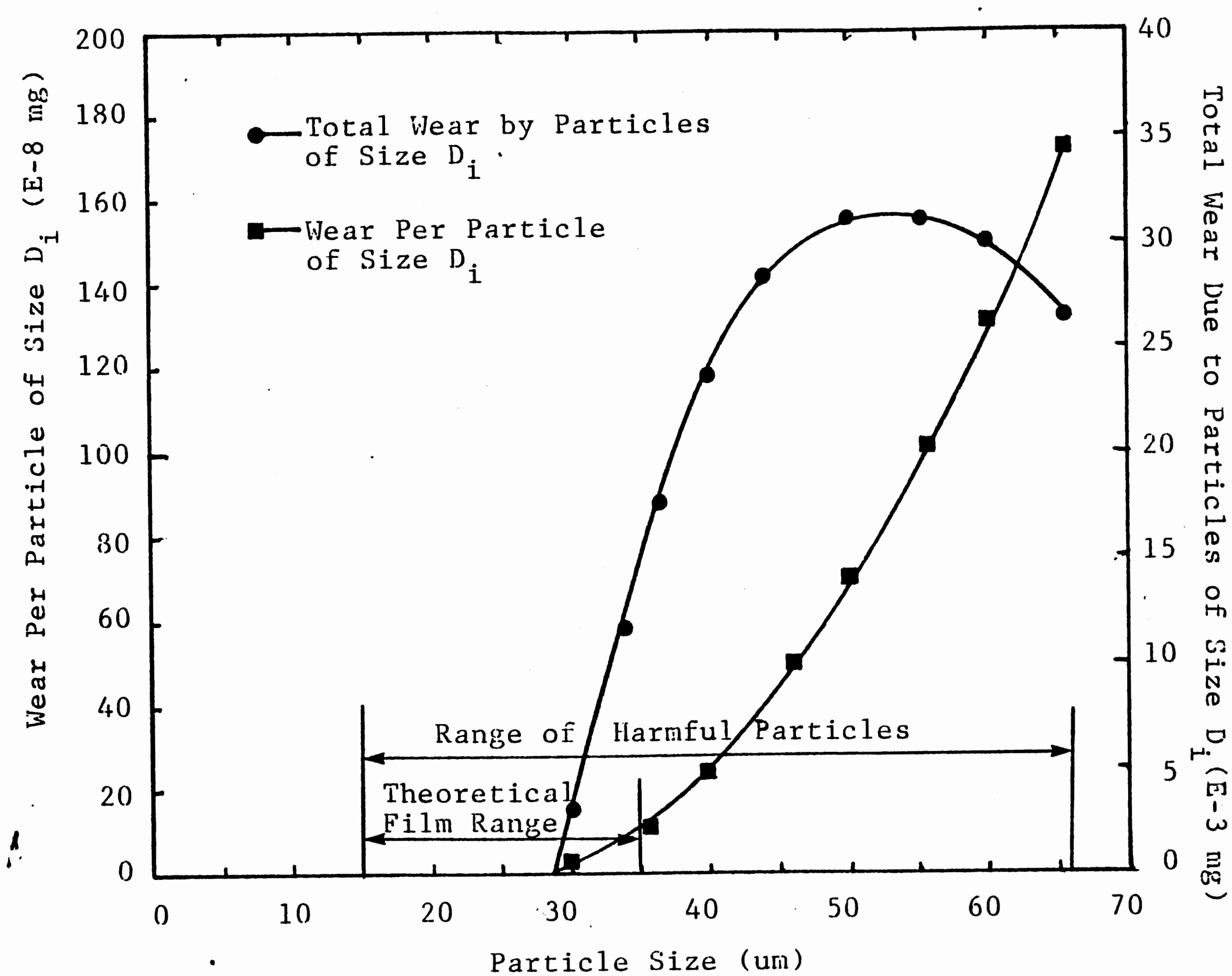

Fig.52 Wear Calculation for Iron Powder (Test T1)

TABLE XVI

COMPARISON BETWEEN EXPERIMENTAL DATA AND THEORETICAL PREDICTION

Test No.	Particle in Test	Test Data (mg)	Wear Model (mg)	Error (%)
T1	Iron	2.51	2.06 - 2.56	-18 - +2
T2	Glass	4.50	4.48 - 5.14	-0.5 - +14
T3	ACFTD	1.50	1.59 - 1.82	+6.0 - +21
H5	Iron	0.72	0.80 - 0.98	+11 - +36
H6	Glass	2.05	2.11 - 2.62	+3.0 - +28
H7	ACFTD	2.81	2.79 - 3.25	-0.7 - +16
H8	Al_2O_3	5.09	5.33 - 5.92	+5.0 - +16

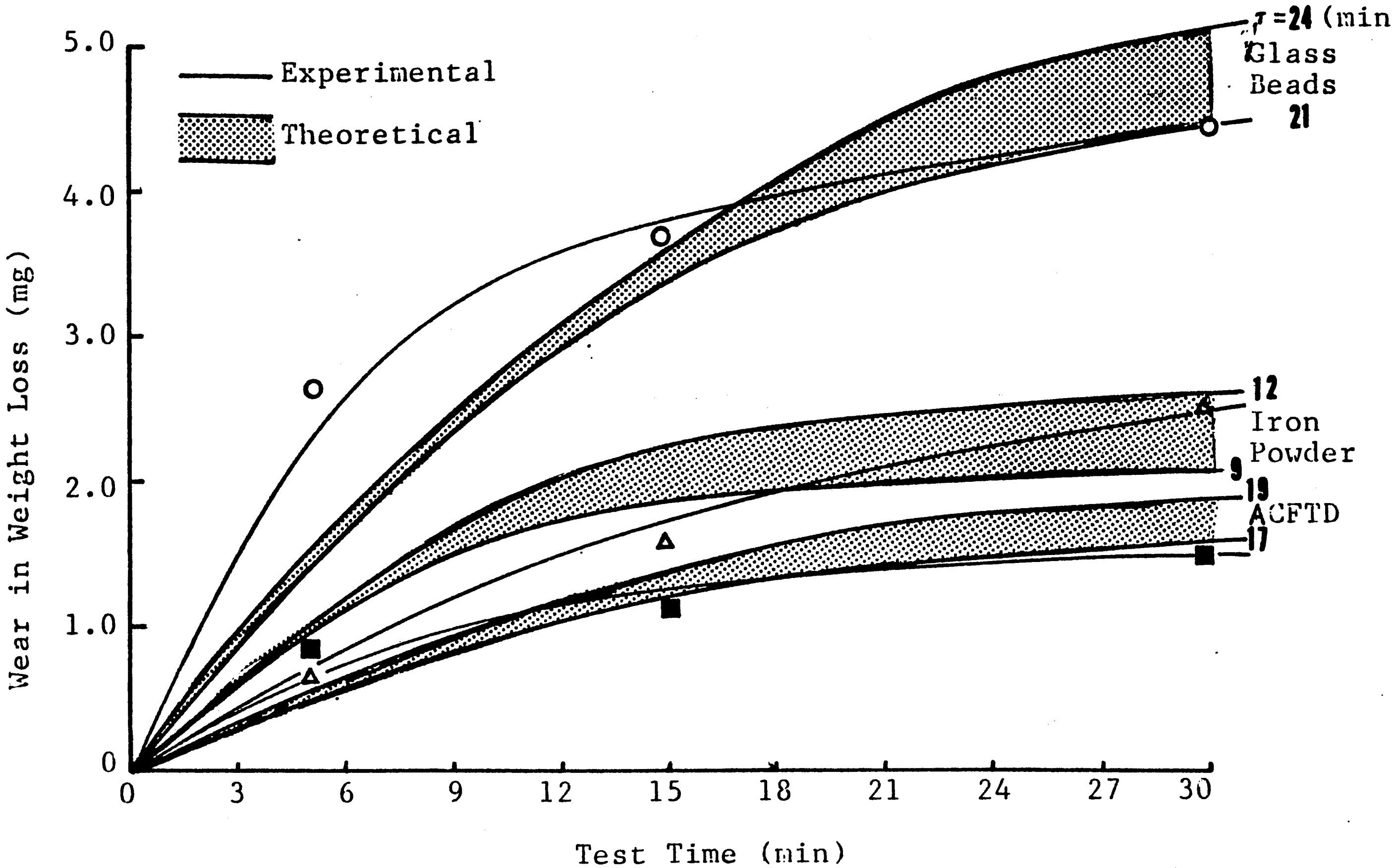

Fig.53 Evaluation of Wear Model by Wear Test Set One

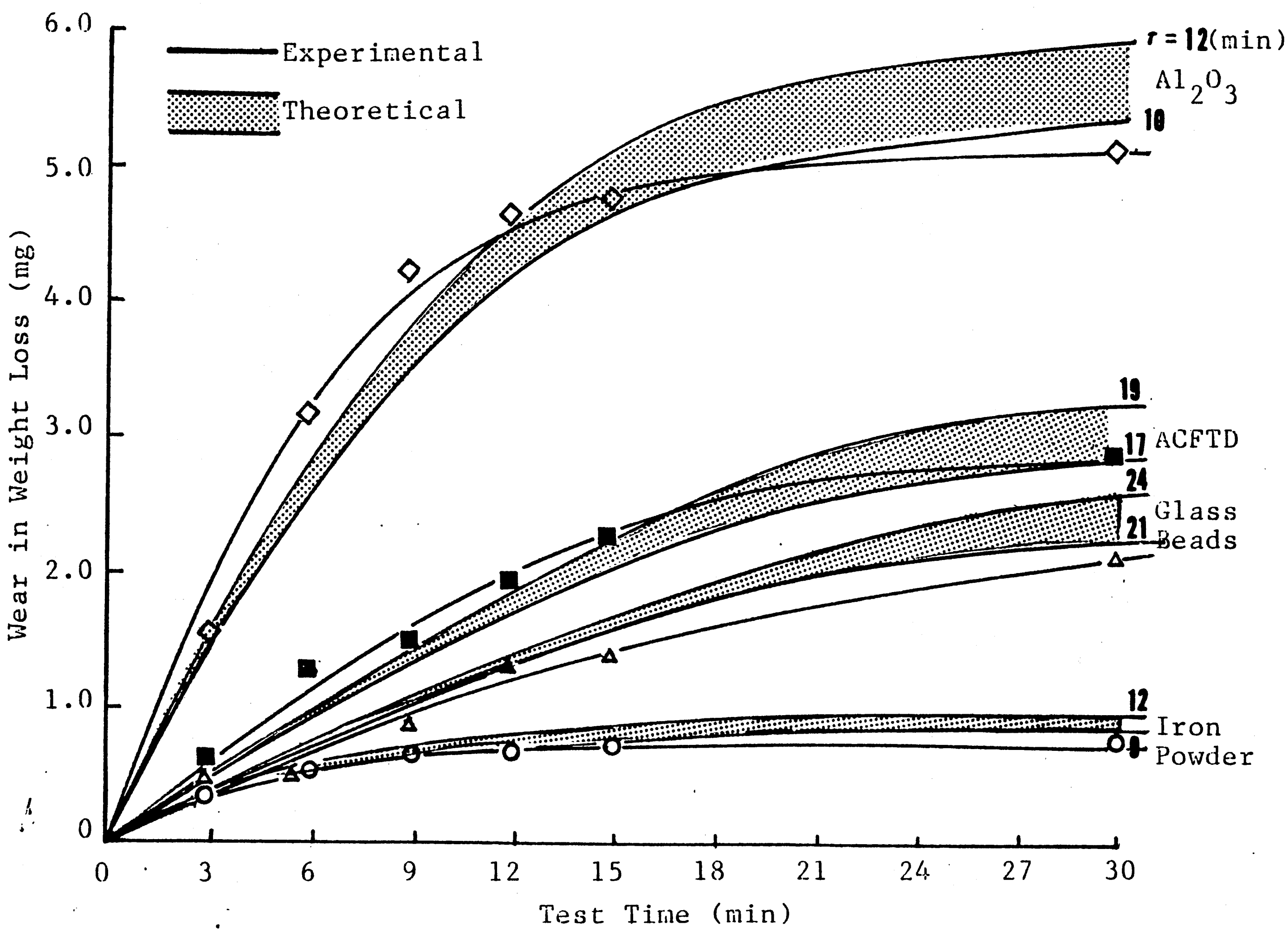

Fig.54 Evaluation of Wear Model by Wear Test Set Two

parameters can be specified in the same way as described in this chapter.

CHAPTER V

EXPERIMENTAL EVALUATION OF THREE-BODY ABRASION SENSITIVITY THEORY

General Consideration

The time-dependent performance degradation processes that occur in many mechanical components are mainly caused by the working fluids containing abrasives. These particulate contaminants make the situation of fluid film lubricated three-body abrasive wear possible, which results in deterioration on internal critical surfaces, increase of clearances, and degradation of major performance parameters. These components are called tribo-mechanical components because they are usually lubricated in operation in order to reduce friction and avoid wear damage. However,the tolerance of most of these components is limited. The sensitivity of a tribo-mechanical component varies widely but basically depends on both the component design and the working environment, which both affect the internal wear process. Therefore, if the verified wear model is correctly incorporated with the analysis of performance degradation, the sensitivity, or the tolerance life, of a component will be predictable. In order to evaluate the sensitivity prediction, the contaminant sensitivity tests on hydraulic pumps, which are typical tribo-mechanical components, were performed for comparison.

The pump contaminant sensitivity test procedure is a NFPA (National Fluid Power Association) recommended standard and ISO proposed standard. The required test system is schematically illustrated in Fig.55. Three identical piston pumps were tested according to the standard procedure; each was exposed to one of the three test abrasives, Iron powder, ACFTD, and Al_2O_3 particles. Then the flow degradation and sensitivity of the pump to each kind of abrasive were experimentally determined.

Wear and Degradation Analysis

The time-dependent wear process inside the pump should be estimated in order to predict the pump flow degradation and pump contaminant sensitivity under each condition. As stated in the previous chapter, a set of computational parameters are required for wear analysis. In the case of a piston pump, two parameters are important : the clearances between critical surfaces and the hardness ratio of the surfaces.

The axial piston pump tested in this research has many parts which move relative to one another. These parts are separated by a small oil-filled clearance through which the working fluid leaks, forced by fluid pressure. Fig.56 shows the five major pump parts : the valve plate, cylinder block,

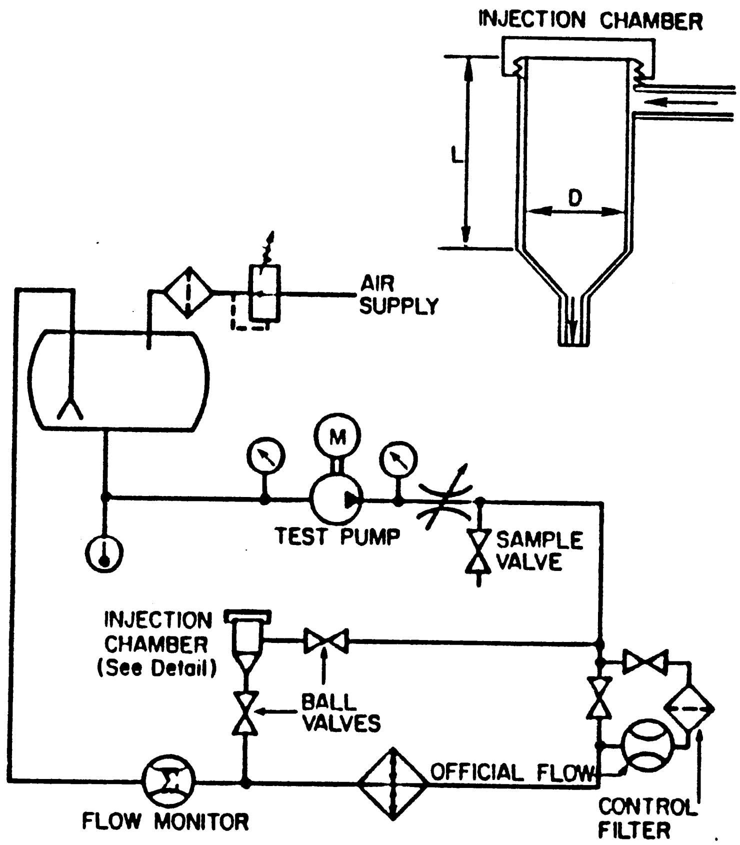

Fig.55 Test System for Evaluating Pump Contaminant Sensitivity

piston, piston shoes, and swashplate; and the associated four critical clearances between these parts.

The hardness of each part was tested and shown in Fig.56. The surface hardness ratio and the surface-to-abrasive ratio, therefore, can be obtained and listed in Table XVII.

The exact clearances are more difficult to determine since it is impossible to measure them directly. It is generally found in practice that the areas particularly subject to clearance problems are cylinder-to-valveplate and shoe-to-swashplate (Fig.56). These clearances are relatively bigger than others and they are the main paths for internal leakage flow. From Silva's (112) experiments, it is known that the test pump has a 96.3 percent volumetric efficiency under conditions of 2500 (psi) pressure, 2600 (rpm) speed, and 150 (^{o}F) temperature with 2104 hydraulic fluid. This means that there is an internal leakage flow of 60 milliliters per second corresponding to a total flow rate of 26.4 gallon per minute. By measuring the dimensions of each part, the average clearance in the pump is between 5 um to 40 um, estimated from Eq.(5.1),

$$h = \left(\frac{12 \cdot \mu \cdot l \cdot Q}{b \cdot \Delta p}\right)^{1/3} \tag{5.1}$$

where μ = fluid viscosity [kgf-sec/cm^2]

l = average leakage length [cm]

b = average leakage width [cm]

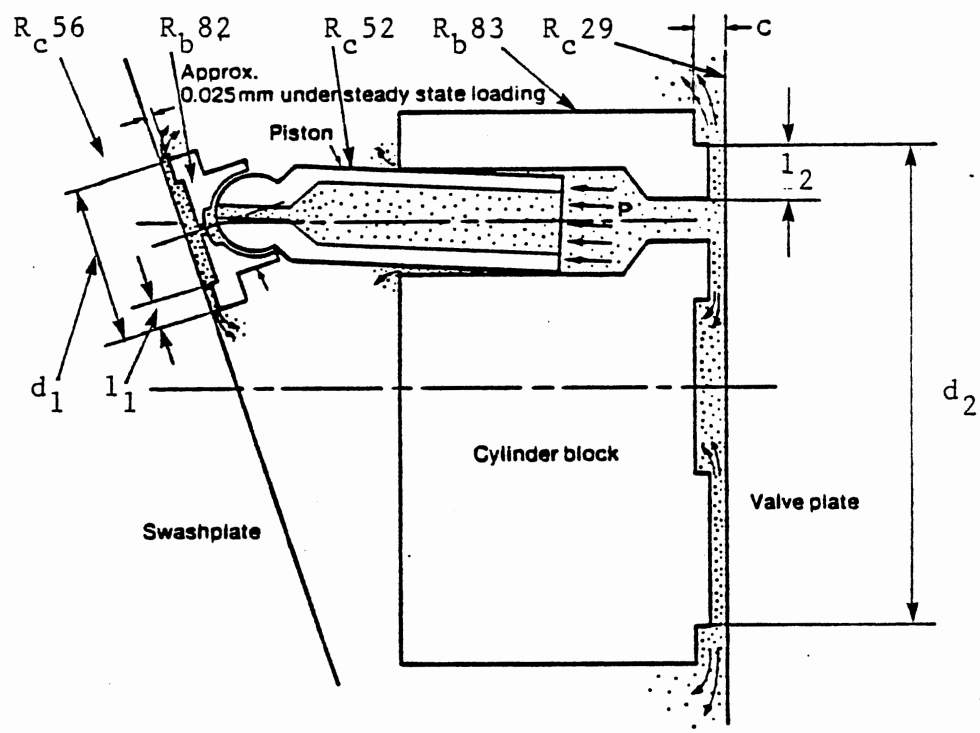

Fig.56 Parts Hardness and Clearances in a Axial Piston Pump

TABLE XVII

HARDNESS DATA OF MAJOR PISTON PUMP PARTS

H_f/H_m	$\frac{\text{Swashplate}}{\text{Shoe}}$	$\frac{\text{Shoe}}{\text{Piston}}$	$\frac{\text{Piston}}{\text{Block}}$	$\frac{\text{Block}}{\text{Valveplate}}$
	0.28	0.3	0.3	0.6
H_m/H_a				
Iron	2.75	2.45	2.45	1.375
ACFTD	0.6	0.54	0.54	0.30
Al_2O_3	0.314	0.28	0.28	0.157

TABLE XVIII

COMPUTATIONAL PARAMETERS IN PUMP WEAR ANALYSIS

Operating Parameters	operating pressure	p	172	[kgf/cm^2]
	rotating speed	v	2600	[rev/min]
	fluid flow rate	Q	60	[cm^3/sec]
	fluid tempersture	T	65	[C]
	max.operation time	t	30	[min.]
	min.film thickness	h_{min}	5	[um]
	max.film thickness	h_{max}	40	[um]
Fluid Parameter	viscosity	μ	0.13E-7	[$kg\text{-}s/cm^2$]
Design Parameter	average width	b	63	[cm]
	average length	l	0.25	[cm]
	surface hardness	H	(Fig.56)	
Particle Parameters	abrasive hardness	H_a	(TABLE XVII)	
	wedge angle	θ	(TABLE IV)	
	destruction time	τ	(TABLE X)	
	number at size D_i	n_i	(TABLE XIX) (Fig.57,58,59)	
	maximum size	D_{max}	Iron 76 [um] ACFTD 70 [um] Al_2O_3 72 [um]	

TABLE XIX

ABRASIVE CONCENTRATION IN PUMP TESTS

SIZE (UM)	ABRASIVE TYPE Iron Powder		ACFTD		Al_2O_3	
	0-20	0-40	0-20	0-40	0-20	0-40
5	386,137	202,794	292,014	236,415	891,093	41,060
10	83,299	80,946	71,154	61,429	477,693	17,618
20	7,193	9,525	5,443	8,554	23,556	5,835
30	1,071	1,540	963	2,376	589	5,557
40	261	372	71	826	36	4,475
50	38	111	27	294	17	3,641

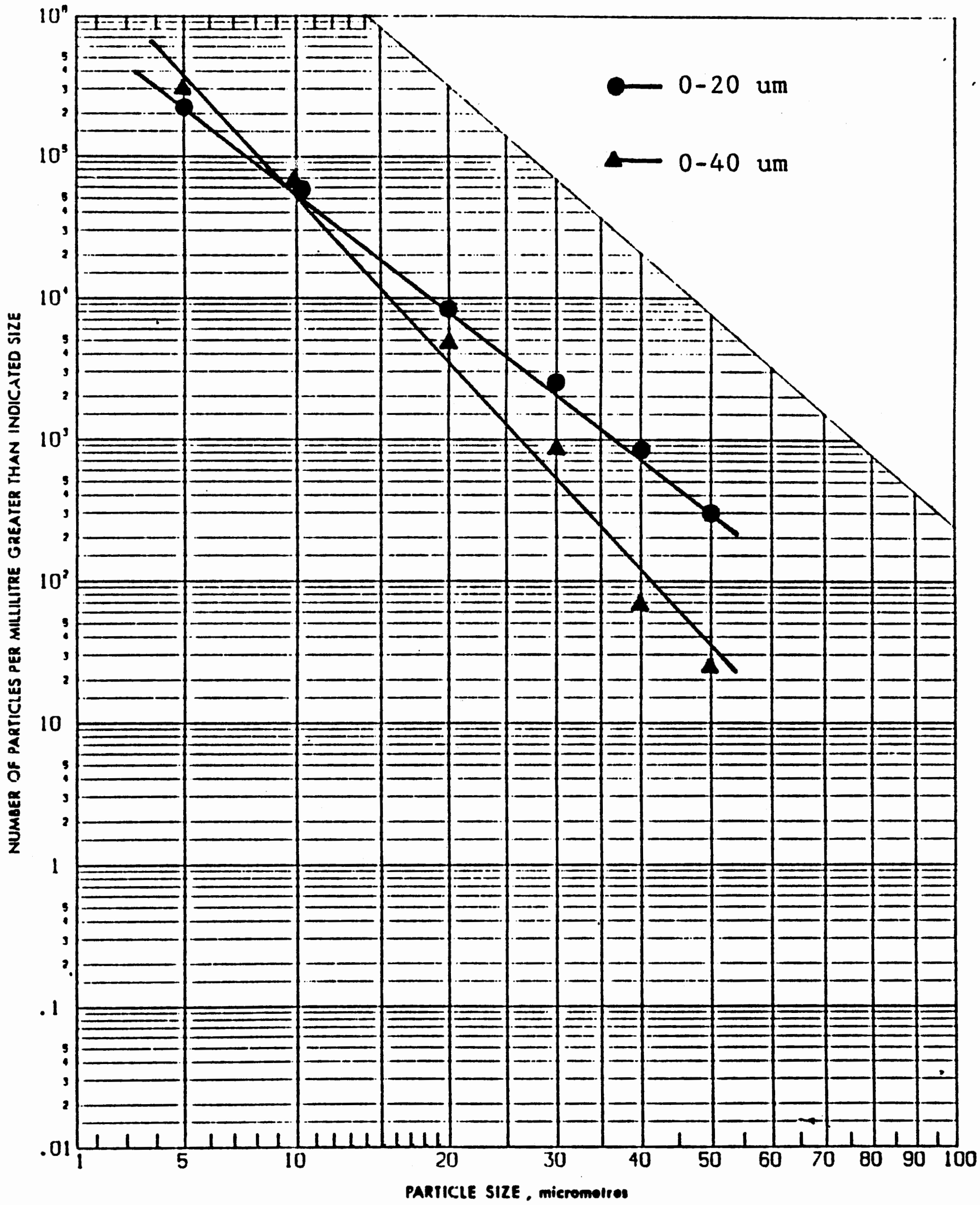

Fig.57 Two Concentration Levels of ACFTD Particles Used in Pump Test

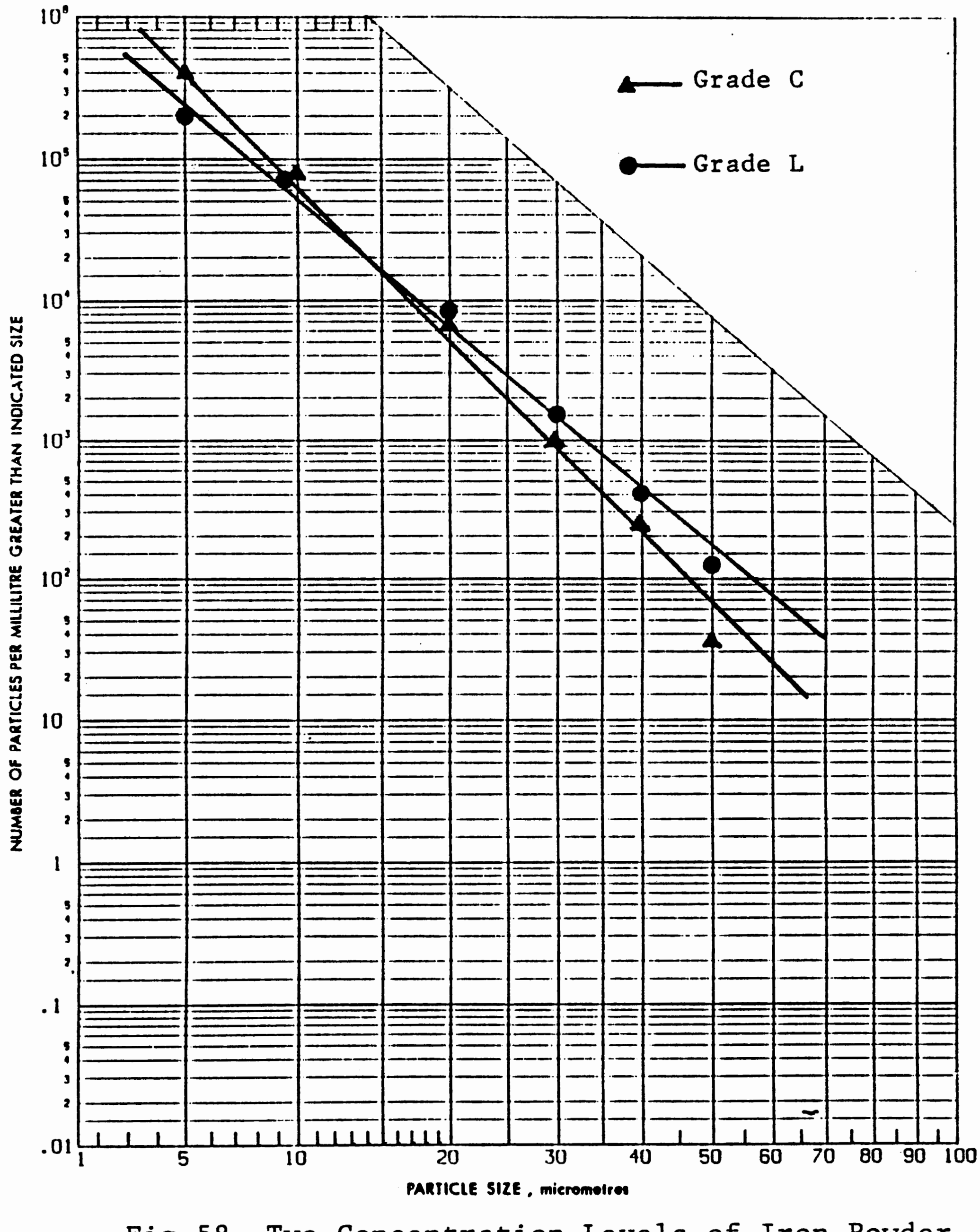

Fig.58 Two Concentration Levels of Iron Powder Used in Pump Test

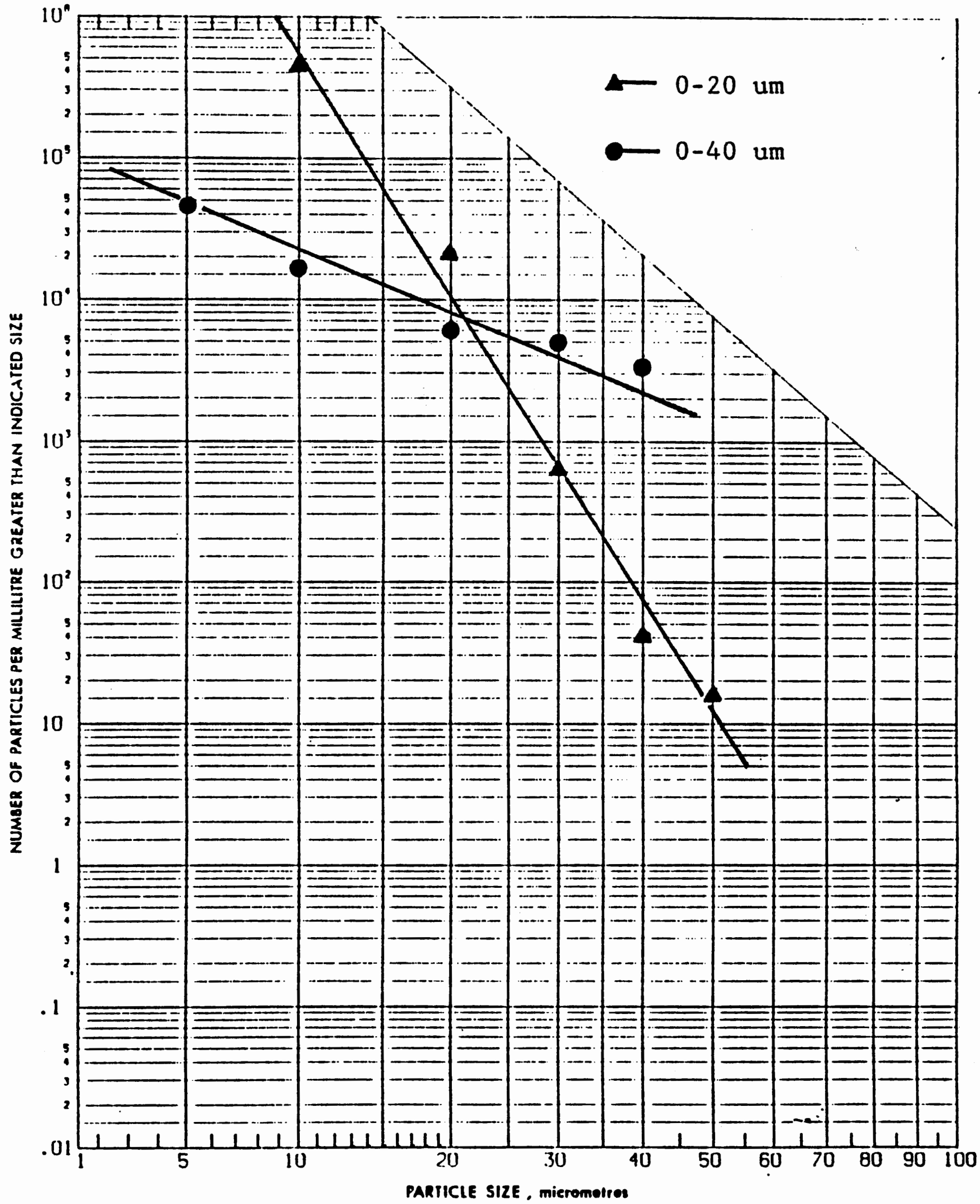

Fig.59 Two Concentration Levels of Al_2O_3 Particles Used in Pump Test

Q = leakage flow rate [cm^3/sec]

Δp = fluid pressure [kgf/cm^2]

The parameters required for pump wear analysis are listed in Table XVIII, the width b($b=\pi d$) and length l of main leakage paths are indicated in Fig.56, and the particle number-size distributions are shown in Table XIX and Figs.57, 58, and 59. With this information, the pump wear in a test period can be calculated. The total wear volume is used to calculate the increase of clearance by Eq.(3.39). Consequently, the leakage flow and the degradation of main flow are also obtained.

Wear Measuring Method

One difficulty in evaluating pump wear and performance degradation is that the weight loss method previously used in wear tests is not practicable in pump tests. Therefore, a newly developed instrument called the "wear debris analyzer" was applied in pump wear analysis. This instrument was designed to detect the wear condition by measuring the magnetic particle concentration in fluid samples. To qualify this method, first, fluids containing mixtures of Iron powder and ACFTD particles were tested. The results shown in Fig.60 reveals that this instrument is insensitive to the presence of ACFTD particles and that the amount of magnetic powder can be linearly correlated with the concentration reading (ppm). Thus, this method is suitable

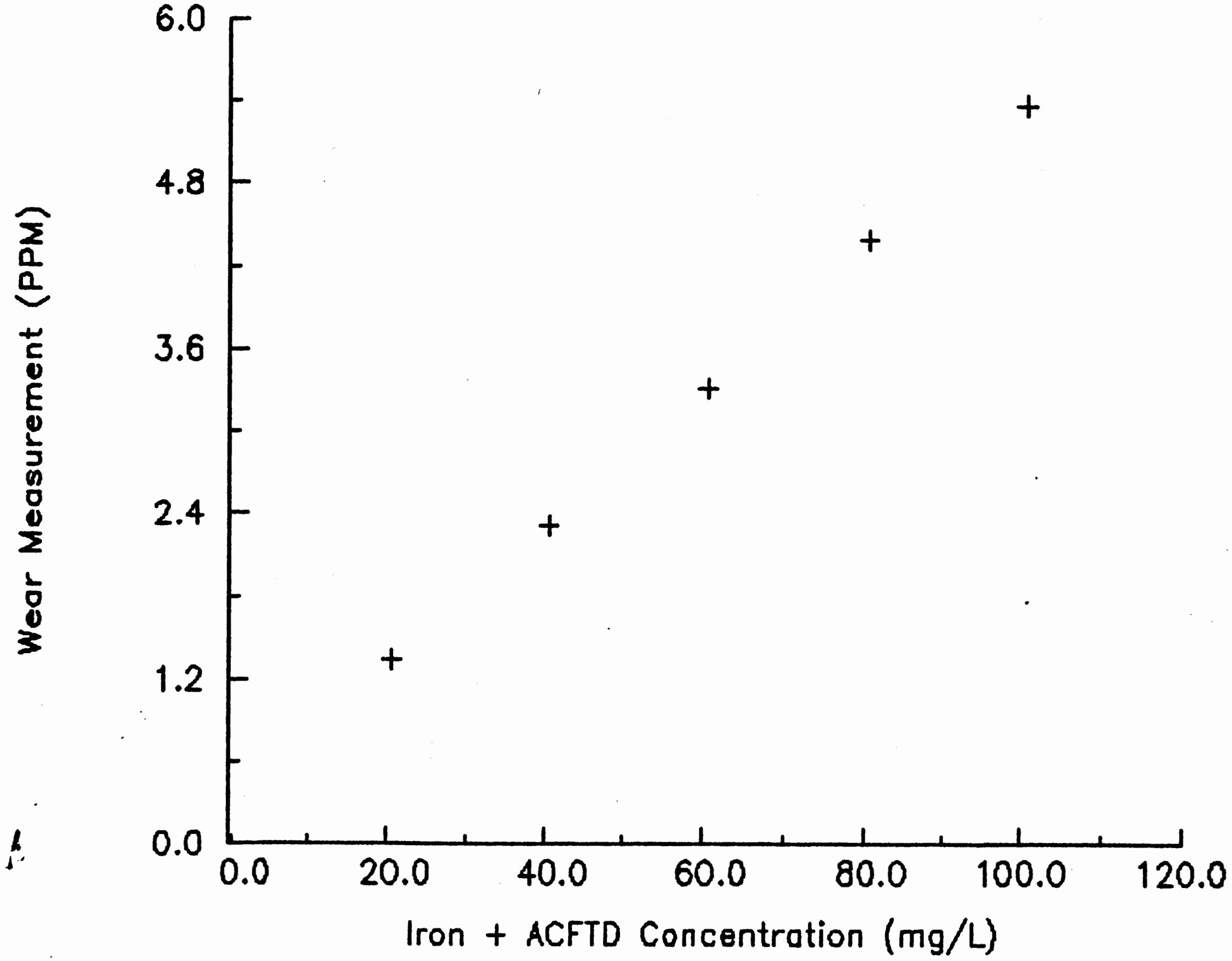

Fig.60 Wear Debris Measurement vs. Iron Concentration

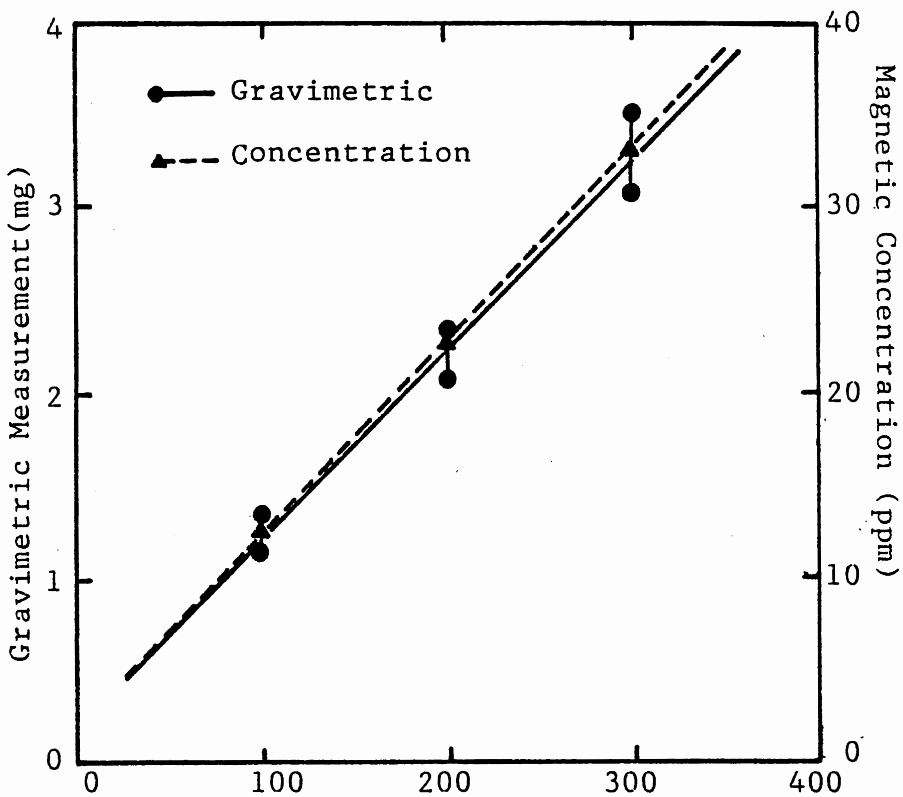

Fig.61 Wear Debris Concentration Method Qualification Data

to sense the pump wear. Also, fluids containing different amounts of pure Iron powder were tested using both the gravimetric method and the debris analysis method. The results are shown in Fig.61. A good correlation is found between the gravimetric level (mg) and the concentration reading (ppm). It helps to evaluate the pump wear analysis.

Evaluation of Abrasion Sensitivity Theory

The results of pump contaminant sensitivity tests are listed in Table XX, where the theoretical flow degradation and wear volume are compared with the test data. These data are also plotted in Fig.62 for ACFTD, in Fig.63 for iron powder, and in Fig.64 for Al_2O_3 particles. In the case of the ACFTD particles, the calculated flow data agrees with that from experiment very well until the 0-20 um size interval. But above this size, the actual flow rate drops more rapidly. In the second test, since the iron powder is much softer than both the valve plate and the swash plate, the wear predicted is very low; therefore, little degradation in flow rate was expected. In this test, both the wear data and the flow data are compatible with test results. The maximum relative error in flow degradation prediction is within ten percent, while for the Al_2O_3 particles, the wear and flow degradation were predicted to increase quickly up to particle size 0-30 um. Actually, the pump was worn out, as revealed by the fast reduction in flow rate and fast increase of magnetic particles found in the

TABLE XX

COMPARISON OF WEAR AND FLOW DEGRADATION

Abrasive	Size(um)	Wear (mg)		Flow Rate (gpm)	
		Test	Model	Test	Model
ACFTD	0-5	0.72	0.07	26.71	26.51
	0-10	0.83	0.116	26.67	26.40
	0-20	0.93	0.19	26.35	26.20
	0-30	1.27	0.588	24.32	25.18
	0-40	1.45	1.16	21.10	23.70
Iron	0-5	0.21	0.004	26.28	26.27
	0-10	0.25	0.008	26.27	26.26
	0-20	0.236	0.024	26.26	26.22
	0-30	0.241	0.072	26.25	26.10
	0-40	0.26	0.20	26.24	25.78
Al_2O_3	0-5	1.91	0.096	25.30	26.10
	0-10	2.48	0.346	24.80	25.45
	0-20	4.62	1.34	18.50	22.85
	0-30	----	3.36	-----	17.60
	0-40	----	6.00	-----	10.32

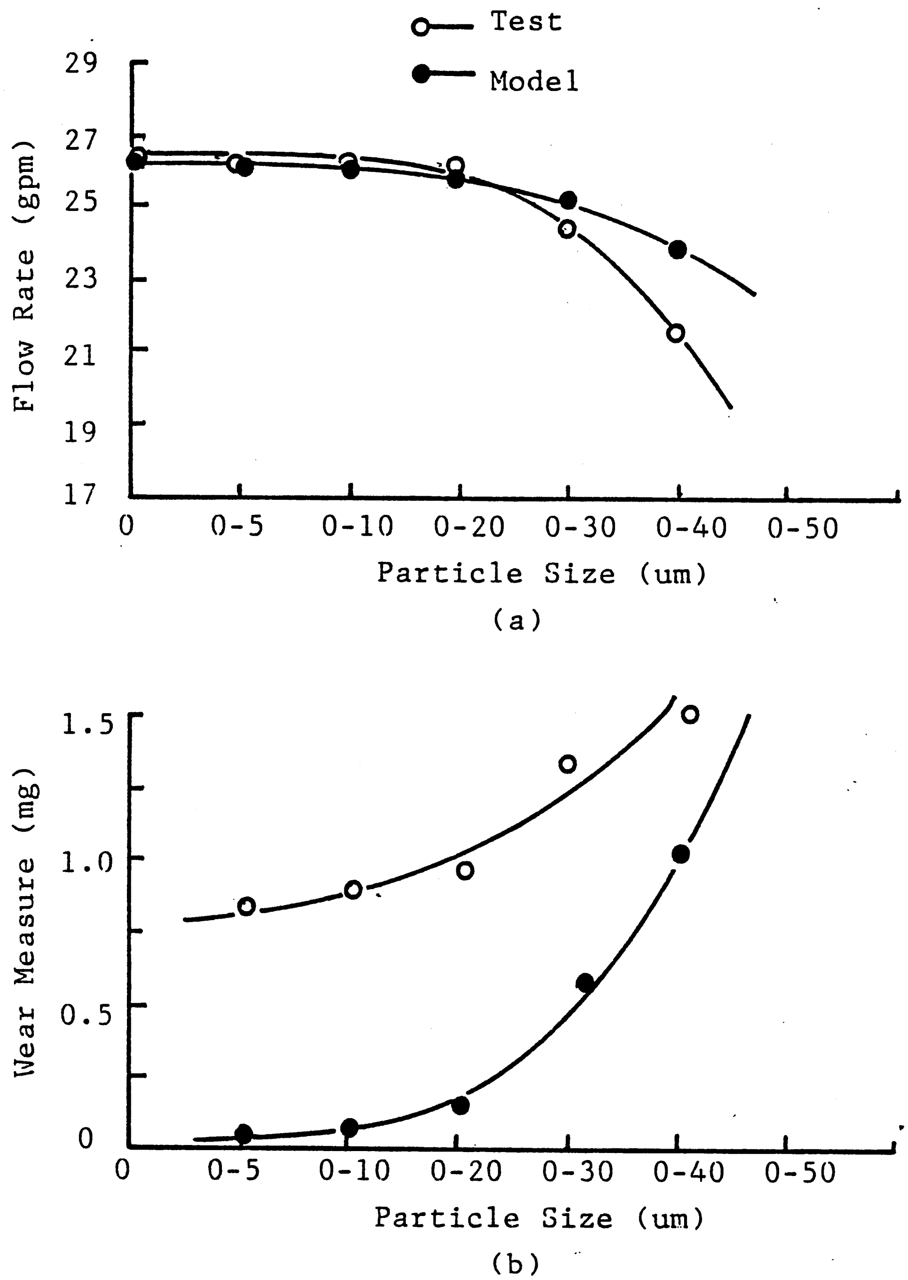

Fig.62 Comparison between Test Data and Model Prediction When Using ACFTD Particle

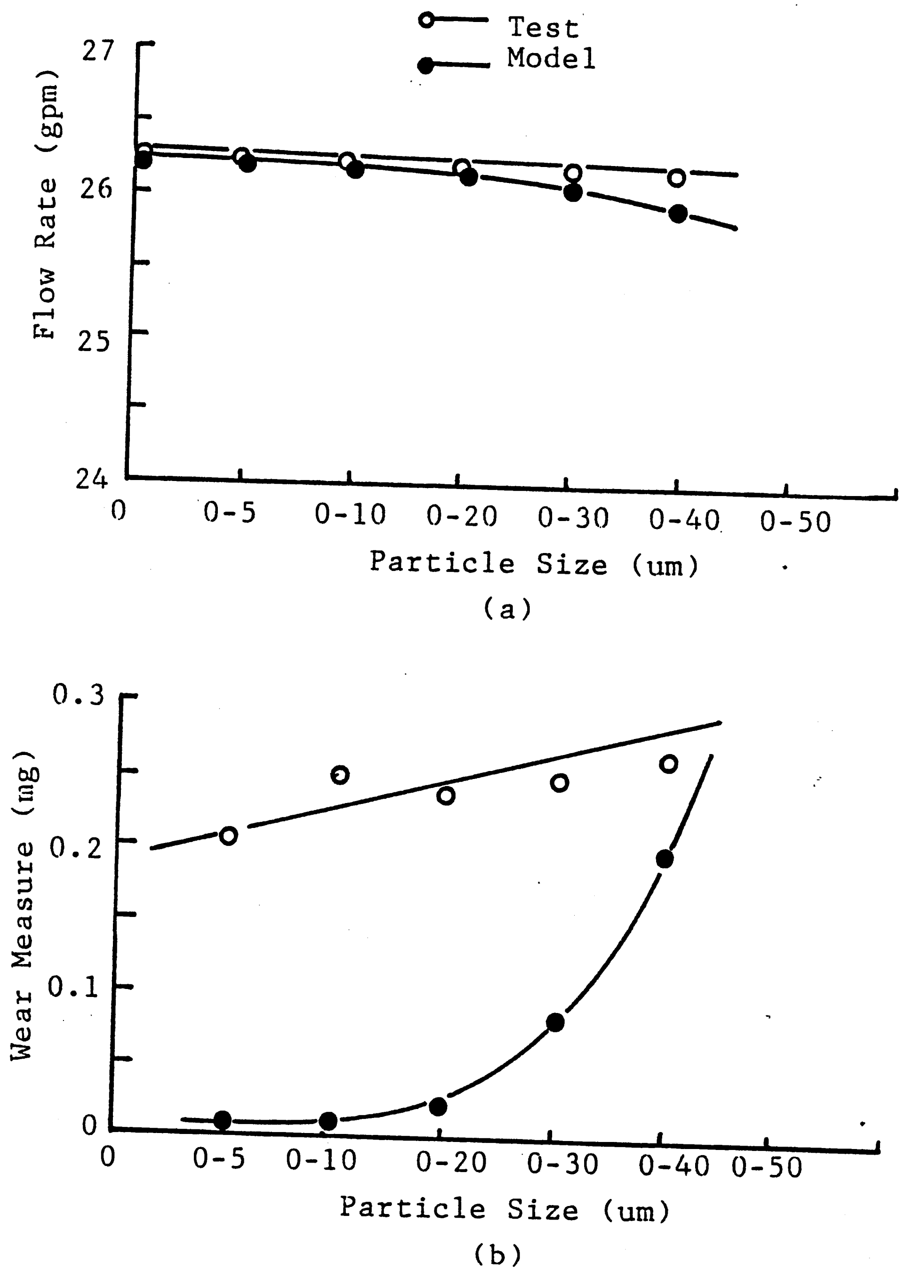

Fig.63 Comparison between Test Data and Model Prediction When Using Iron Powder

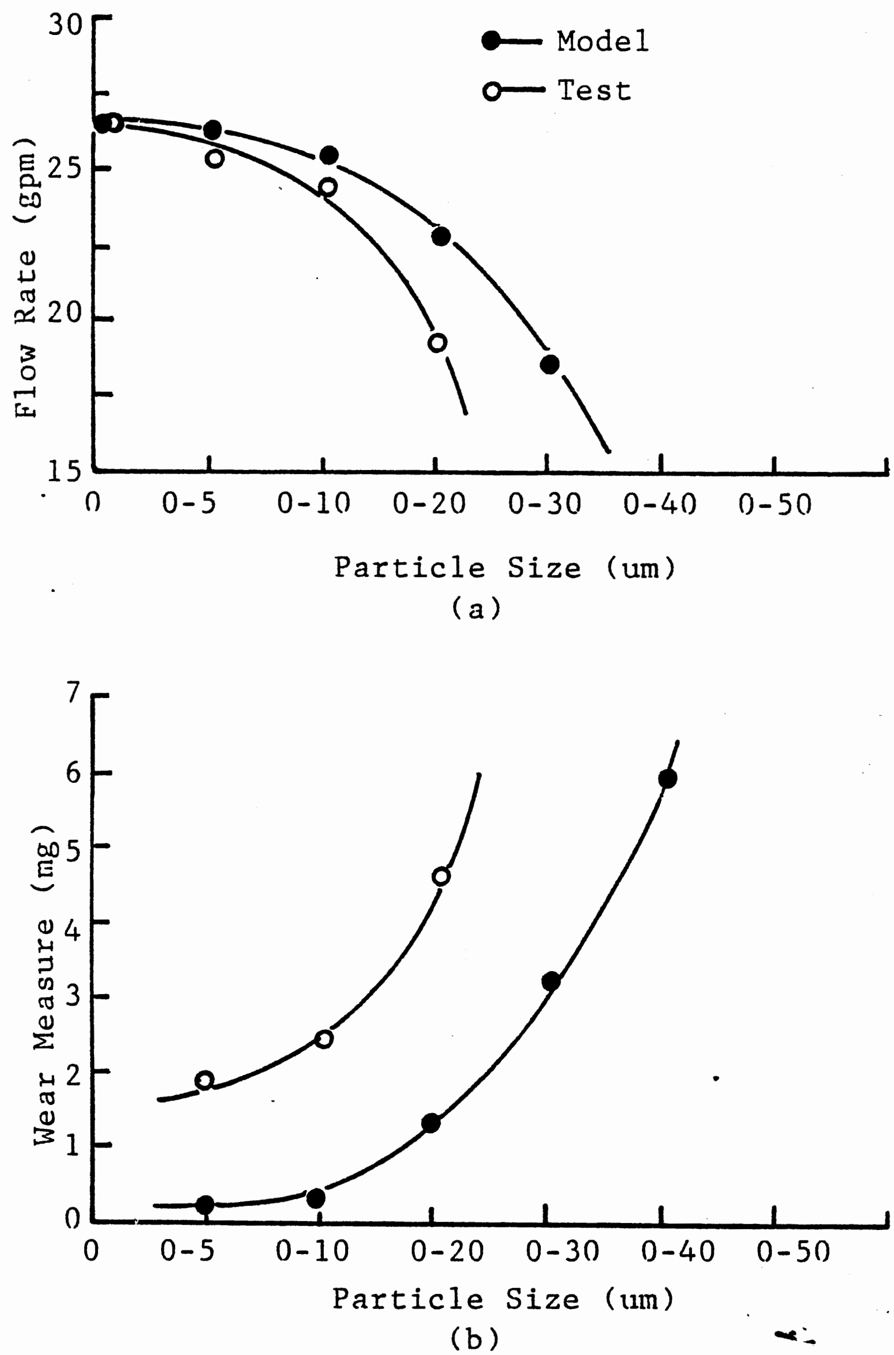

Fig.64 Comparison between Test Data and Model Prediction with Al_2O_3

fluid just eight minutes after the injection of 0-20 um particles.

From these comparisons, the following four points related to the lubricated three-body abrasion sensitivity theory are clarified:

1. The method of incorporating the wear calculation with the performance analysis is correct. The pump flow degradation has a good correlation with the internal three-body abrasive wear severity.
2. The prediction of wear and degradation is close enough to the experimental data if the test specimen has a higher metal-to-abrasive hardness ratio, such as in tests using the Iron powder. In cases of using harder abrasives, the pump degrades faster than predicted for two possible reasons : One is the effect of wear debris generated. In tests with harder particles, more material is removed from the harder surfaces and these debris in turn accelerate the process of wear and performance degradation. Another reason is the effect of particle size, which is more important in pump wear analysis. Since the internal geometry of a piston pump is much more complex than the wear test specimen, the harmful particle size range is wider than expected, therefore, flow degrades even when smaller particles are injected.
3. The effect of hardness ratios and destruction time are shown to be correct since in all three pump tests the wear predictions agree with the experiments. This leads

to correct prediction of the trends of performance degradation.

4. Based on the flow degradation analysis with ACFTD particles, the contaminant sensitivity of the piston pump can be determined.

From the flow data obtained by calculation and by tests for ACFTD abrasives, two sets of coefficients representing pump contaminant sensitivity were calculated using the method described in (106) and shown in Table XXI. Based on the coefficients, two tolerance profiles, each representing an one-thousand hour service life for the pump tested, were also constructed and plotted in Fig.65. By superimposing these curves on the standard filter profile, as shown by the broken line in Fig.65, it is found that the developed sensitivity theory does provide a close estimate of the pump sensitivity to ACFTD abrasives. The predicted sensitivity rating (Omega value)is about 1.02 while the experimental Omega value is 1.04. The pump tolerance profiles for conditions of Iron powder (predicted Omega 1.00444, test Omega 1.005) and Al_2O_3 particles (predicted Omega 1.1, test Omega 1.3) are plotted in Figs.66 and 67, respectively. By examining these three cases, it is clear that the present model for sensitivity analysis is feasible although some errors exist in prediction. Basically, the theory predicts an upper tolerance bound, or less sensitivity, for harder abrasives; whereas a lower tolerance bound will be given by

TABLE XXI

COMPARISON OF PUMP CONTAMINANT SENSITIVITY

Size (um)	Test	Model
5	0	5.09E-16
10	0	1.52E-14
20	6.38E-13	1.17E-12
30	2.71E-10	1.39E-10
40	8.19E-09	3.84E-09
50	1.11E-07	5.01E-08
60	9.21E-07	4.09E-07
70	5.57E-06	2.44E-06
80	2.71E-05	1.17E-05
90	1.11E-04	4.76E-05
100	3.98E-04	1.68E-04

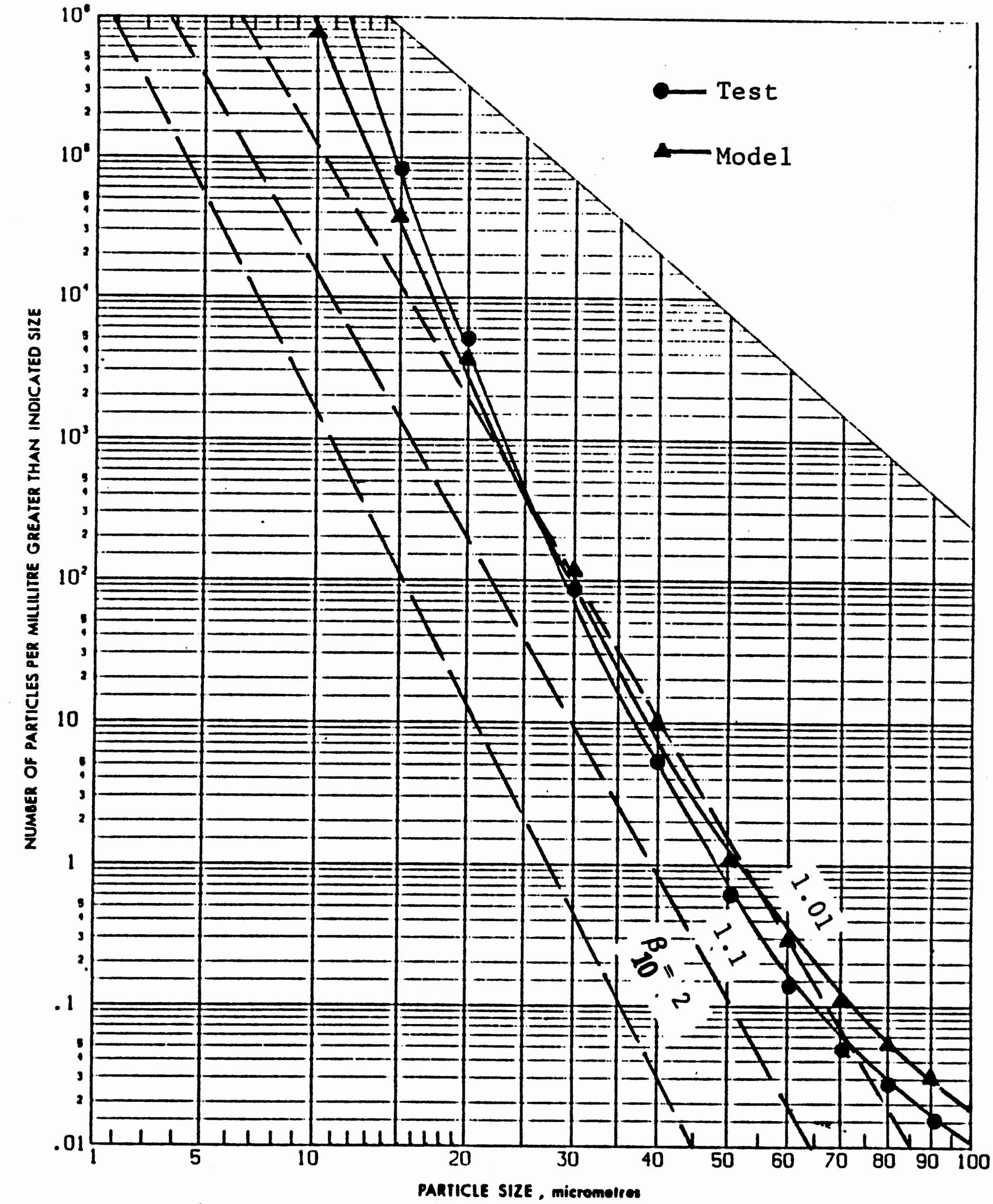

Fig.65 Pump Contaminant Sensitivity Analysis
(ACFTD Particles)

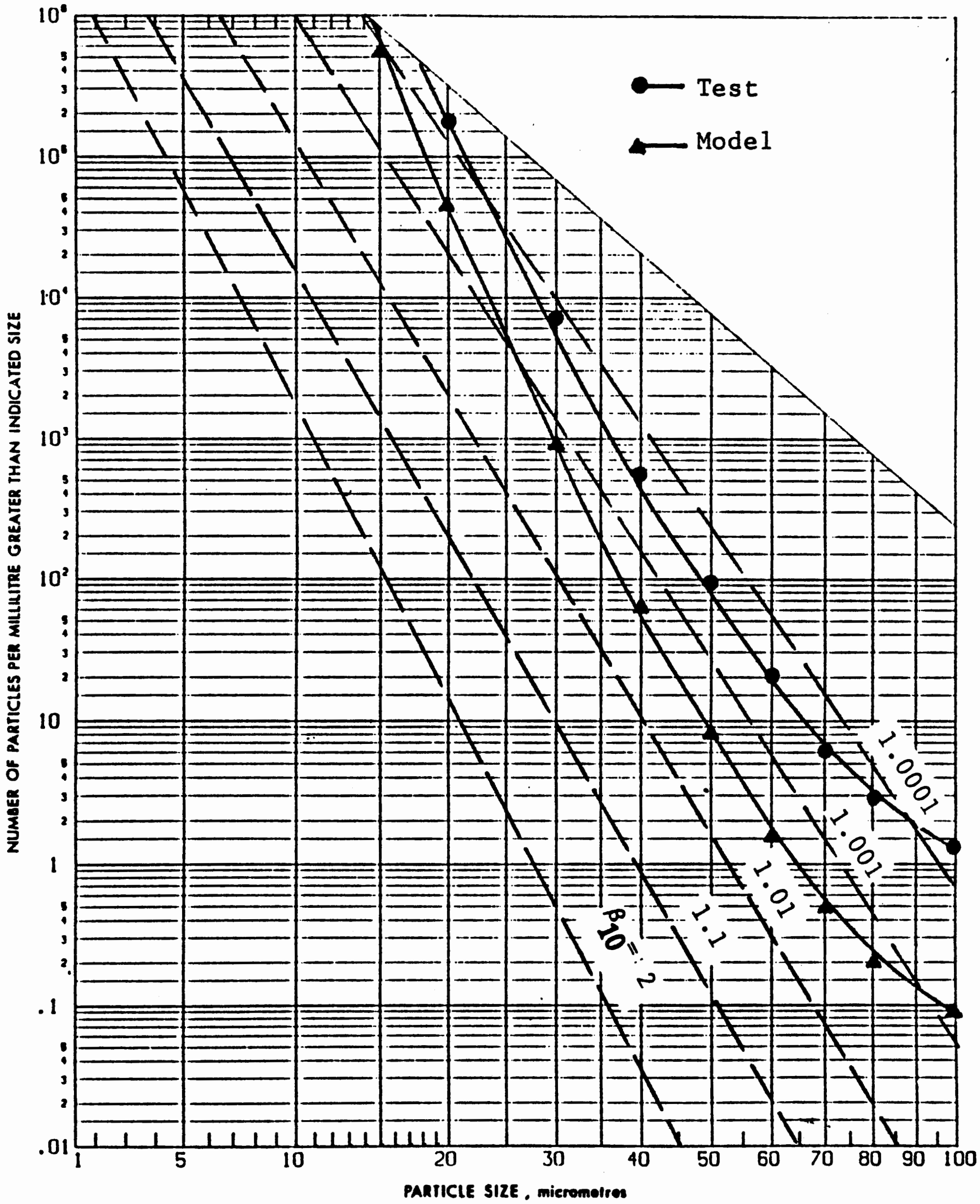

Fig.66 Pump Contaminant Sensitivity Analysis
(Iron Powder)

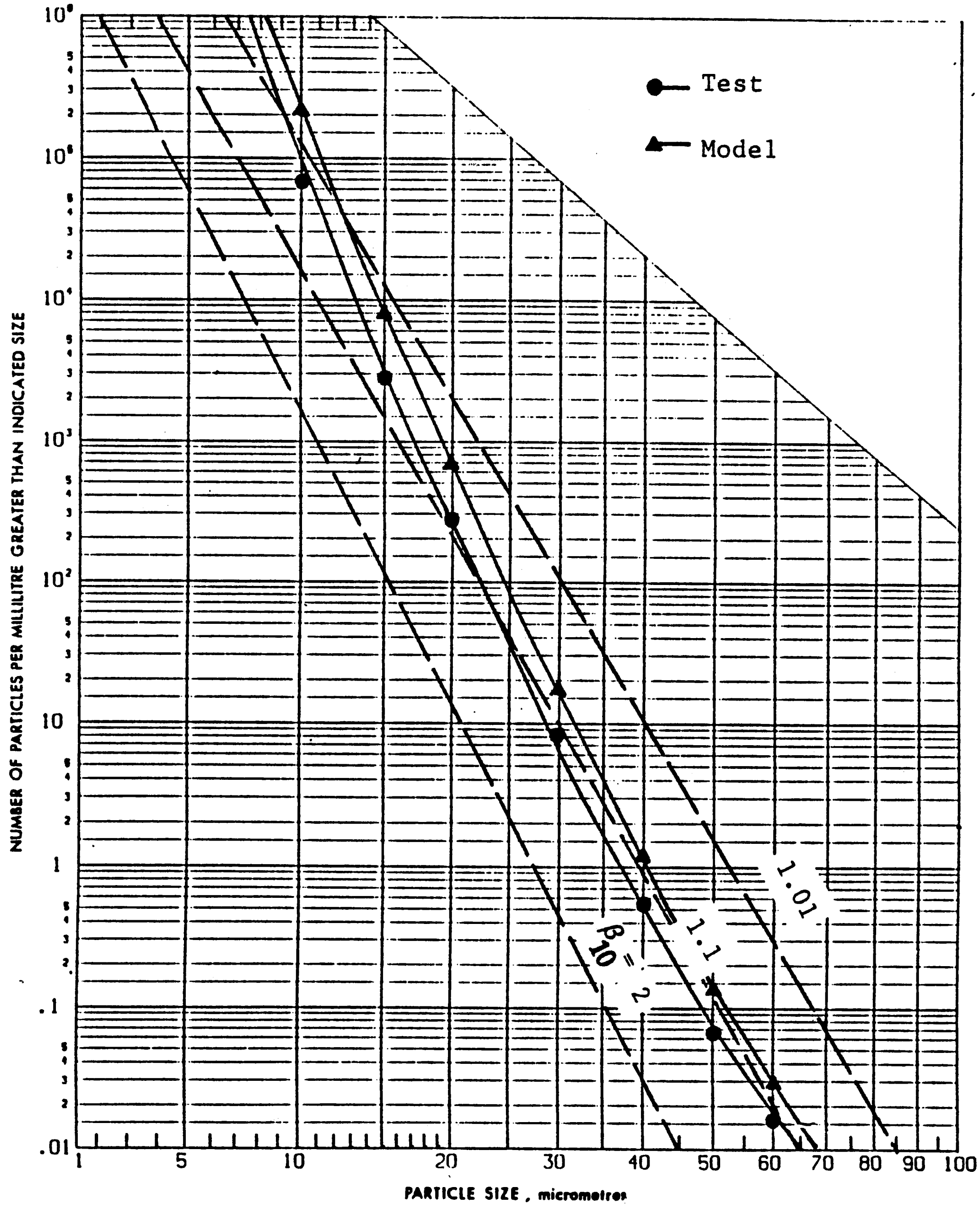

Fig.67 Pump Contaminant Sensitivity Analysis (Al_2O_3 Particles)

the model for cases with softer particles. That is, specifically when ACFTD particles are presented in the system fluid, a tribo-mechanical component would have a longer predicted service life. In order to avoid unexpected wear damage, the lower tolerance bound always needs to be specified. In practice, this value can be estimated from the upper bound analyzed under the similar operating conditions. For the present example, the standard sensitivity (to the ACFTD abrasives) of the pump can be estimated from about Omega 1.04 (lower bound) to Omega 1.02 (upper bound). This difference is also an evaluation for the abrasion sensitivity theory.

CHAPTER VI

APPLICATIONS AND EXTENSIONS OF THE RESEARCH

Most tribo-mechanical components which work under fluid flow lubrication conditions are sensitive to particulate contaminants in the fluid because the three-body abrasive wear process occurs on internal critical surfaces and can jeopardize the service life of the component and even the system. Preventing this problem requires fundamental knowledge as well as effective analysis methods, which are partly provided in the present research.

One direct application of this research is the reliability analysis for a given component and its working environment. From this analysis, the tolerance of the component within that environment can be predicted. In addition, in order to maintain the required service life at this specified sensitivity level, the necessary sealing devices and filtration techniques can be selected based on the predicted critical contaminant level. Furthermore, with the fundamental knowledge of various parameters that affect the wear and performance degradation, the selection of material combination and clearance of a component may be modified in the design stage to improve the performance and to extend the safe operating period.

The analysis of component reliability can be described as follows: For a tribo-mechanical component with all the design parameters specified, it is desirable to find out how fast its major performance parameter will degrade. Or for a component with an unknown design but with a known standard contaminant sensitivity rating (the Omega value subject to ACFTD particle test), it is interesting to find out how tolerant this component will be if it is under the attack of a different abrasive contaminant. The first problem is demonstrated by the analysis of the hydraulic pump. By knowing those computational parameters shown in Table XI in Chapter IV, the time-dependent wear volume can be computed; then the rate of performance degradation is able to be predicted. For components abraded by abrasives other than the ACFTD particles, the three particle property functions should be analyzed. Comparing the ACFTD and Al_2O_3 particles, the Al_2O_3 particles are almost twice as hard as that of ACFTD (Table V and Fig.45) but have a shorter destruction time (Table X and Fig.47). The average shape parameters (Table IV) are similar for both particles. Therefore, for the same concentration level in the system fluid, the pump will be less tolerant to the Al_2O_3 particle. The sensitivity ranting increases from Omega 1.02 for ACFTD to about 1.08 for Al_2O_3 particles, as shown in Fig.68. This analysis indicates that the hydraulic pump will not keep operating

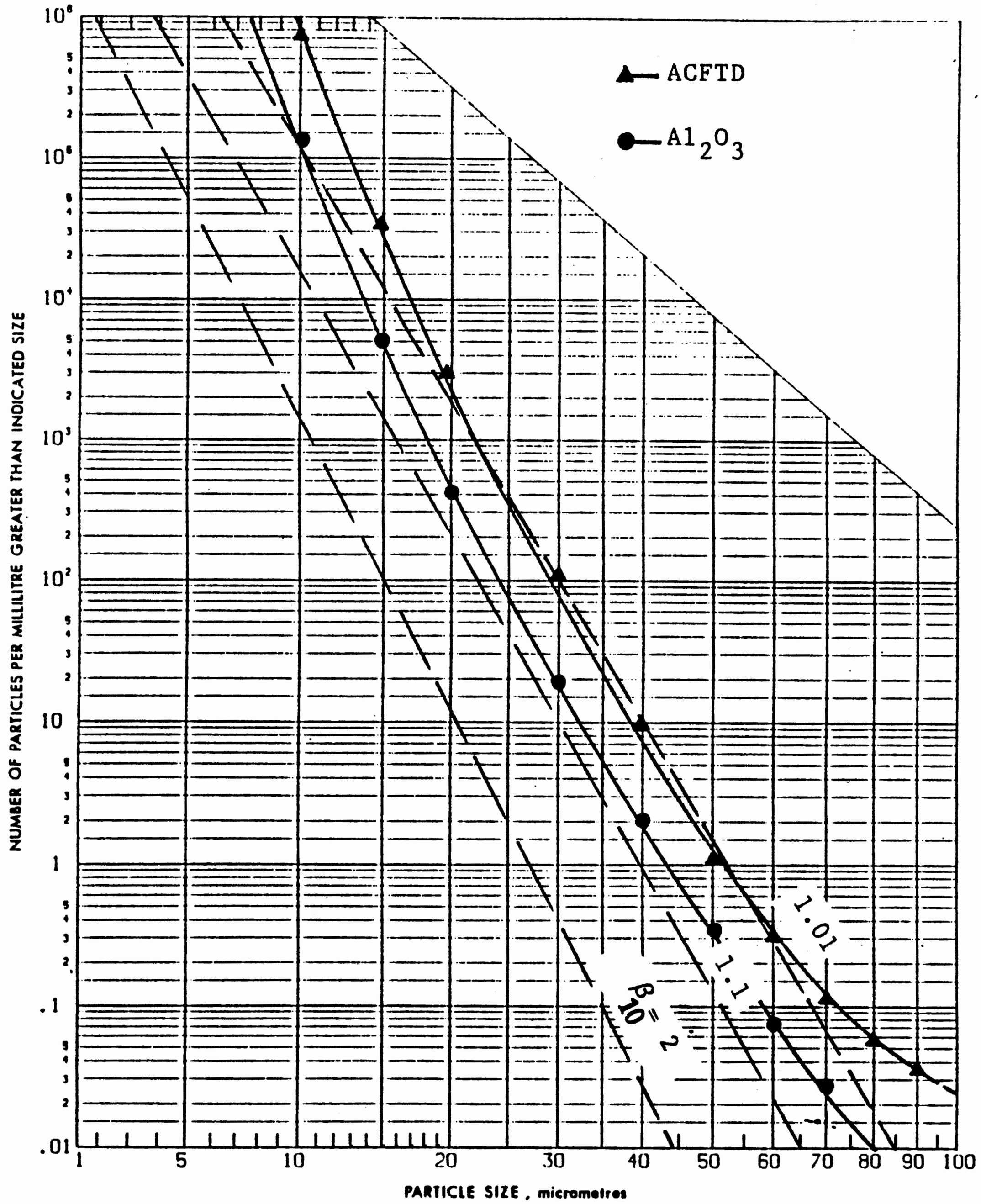

Fig.68 Effect of Abrasives on Pump Contaminant Sensitivity

for one-thousand hours under the attack of Al_2O_3 abrasives although, theoretically, it is reliable when subject to ACFTD particles. Consequently, in order to protect this pump to operate for one-thousand hours, a better filter of at least BETATEN 1.08 will be necessary.

The pump performance also can be improved by modifying the design. When comparing the pump tested with a pump designed by another manufacturer, which is supposed to have the identical design except for softer metals for the swashplate and the valve plate, the metal-to-abrasive hardness ratio is reduced and a shorter service life is expected because of the higher wear damage, see Figs.45 and 46.

Recommendation for Further Study

The research provides valuable technical knowledge as well as a generic analysis method for tribological wear research and the contamination control theory. In order to continue the advancement of this field, the following related investigations are recommended for future study:

1. Further experimentation should be conducted to determine the three particle property parameters for other abrasives. These experiments should help finalize the abrasivity rating for major particles.
2. The effect of two hardness ratios is significant to abrasive wear and this information is directly related to the material selection in component design. Therefore,

more experimental tests should be carried out to test a wider range of material combinations under different abrasive conditions.

3. Based on these experimental data, more accurate coefficients involved in the shape function, hardness function, and destruction time function can be obtained and then a tribological wear database should be established to help the wear analysis.
4. Tribo-Mechanical components of various design structures should be tested and analyzed to be able to specify the relationship between wear and performance parameters other than flow degradation.
5. A contamination control database should be established based on the particle abrasivity ranting and performance analysis methods suitable for different component structures.

CHAPTER VII

SUMMARY AND CONCLUSIONS

Summary

This thesis is concerned with a fundamental topic in both the areas of tribology and contamination control: the investigation of the time-dependent performance degradation process caused by abrasive particles in most fluid tribo-mechanical components. The overall objective of this research is to develop a theoretical model for simulating the contaminant-induced three-body abrasive wear process and to establish a three-body abrasion sensitivity theory for analysis of system reliability, contaminant control, and component design.

Tribo-mechanical components include many modern mechanical elements which are designed to work under fluid film lubricated condition to reduce friction and to avoid wear on internal critical surfaces. However, in many cases, the performance of a component degrades much earlier than the expected design life because of the deterioration of critical surfaces and the change of clearances. This damage is often caused by particulate contaminants present in the fluid, which can bridge the surfaces originally separated by a fluid film and thus make the three-body abrasive wear possible. In order to solve this problem, i.e. to be able to predict, prevent, and diagnose the degradation process, the wear process should be analyzed and the correlation between wear and performance degradation should be established.

The severity of the lubricated three-body abrasion basically depends on four types of parameters: the operating parameters, the fluid parameters, the design parameters, and the particle parameters. For a tribo-mechanical component with known internal surface geometry and under constant operating conditions, the thickness of the fluid film is determined. This value limits the maximum size of a specified abrasive particles which may enter the surface clearance. The wear is caused by part of these entrained particles. Fundamentally, the wear volume produced by an individual particle is proportional to the square of the cutting depth, which is a function of many variables including the particle size, particle shape, metal surface hardness ratio, and metal-to-abrasive hardness ratio. These parameters directly affect the per particle wear volume, while the total wear damage within a specified time interval is the summation of all the individual wear volume. The particle toughness and brittleness affect the total wear amount by reducing the particle number after a specified destruction time of the particles.

Under abrasive wear conditions, the increasing wear volume will result in an enlarged leakage flow path. The increase in leakage flow causes the degradation of major performance parameter of a component. Different tribo-mechanical components have different performance measures. In the case of a hydraulic piston pump, the degradation of main flow directly results from the increasing leakage flow. By expressing the leakage flow in terms of the wear volume due to three-body abrasion occurred at pump critical clearances, the main flow degradation in a specified environment is analyzed. This prediction leads to the theoretical estimation of pump contaminant sensitivity. The tolerance of the pump in a contaminanted environment other than the standard ACFTD abrasives can also be determined.

The theoretical wear model was validated by conducting wear tests on the Thick Film Wear Tester, which is modified from the Gamma machine. The contaminant sensitivity model was verified through three pump tests subject to three different abrasive conditions.

Conclusions

The accomplishments of this research effort have contributed significantly to the areas of abrasive wear and contaminant control. Prior to this work, the theoretical analysis on three-body abrasive wear under fluid film lubrication had not been successfully achieved. Also, only experimental technique was available in determining the contaminant sensitivity of general tribo-mechanical components. From the research work described in the preceding

Chapters, several noteworthy contributions can be outlined as follows:

1. The model which simulates the three-body abrasive wear process was developed. This model includes four types of parameters involved in a metal-fluid-particle-metal tribo-system. The cutting wear occurs under force and moment balance conditions. The per particle wear volume varies with the square of cutting depth. The total wear is a sum of the individual wear volume.
2. Three particle property functions were developed to reflect the effects of particle shape, hardness ratio, and particle destruction time on three-body abrasion.
3. A generic concept of performance degradation was presented based on the wear-leakage-degradation analysis.
4. The contaminant sensitivity model was developed which incorporates the wear model with the degradation analysis to theoretically analyze the tolerance of a component under a specified environment.
5. Experimental activities were performed to verify the developed particle property functions and the wear model by using a Thick Film Wear Tester which provides stable and light loading.
6. The metal-to-particle hardness ratio was found important in the analysis of abrasive wear. Wear varies geometrically with the H_m/H_a ratio. The coefficients in hardness function F_2 were experimentally determined and used in wear calculation.

7. The destruction time constants of four abrasives, Iron powder, glass beads, ACFTD particles, and Al_2O_3 particles, were experimentally obtained. Thus, the particle toughness function F_3 was constructed.
8. Seven wear tests were conducted. The model prediction was close to the test data in that for a known film thickness the total wear linearly increases with the particle size up to a critical value, then decreases. For different metal combinations tested, the maximum prediction error is between 14 to 36 percent.
9. Piston pump tests were conducted and the wear debris analysis method was qualified and used to measure the pump wear. Test results showed that the contaminant sensitivity model is feasible. The prediction of wear and flow degradation is in agreement with test data. The model provides a lower tolerance bound for cases of higher metal-to-abrasive hardness ratio, and provides an upper bound for harder particle cases due to the effects of generated wear debris and complex internal geometry of the test pump.
10. The applications of this research in reliability analysis, contaminant control, and component design were discussed.

A SELECTED BIBLIOGRAPHY

1. Fitch, E.C., An Encyclopedia of Fluid Contamination Control, 2rd ed., FES, Inc., Stillwater, 1986.

2. Ronen, A., S.Malkin and K.Loewy, "Wear of Dynamically Loaded Hydrodynamic Bearings by Contaminant Particles", Trans.of ASME, 102 (1980), 452-458.

3. Tao, F.F. and J.K.Appeldoorn, "An Experimental Study of the Wear Caused by Loose Abrasive Particles in Oil", Trans.of ASLE, 13 (1969), 169-178.

4. Needelman, W.M., "Survey of Wear Process in Hydraulic, Lubrication, and Pneumatic Systems", Proc. Nat. conf.of Fluid Power, (1977), 106-115.

5. Smith, R.J., "Establishing the Reliability of Orifice Operation as a Function of System Contamination Levels", Proc. Nat.Conf.of Fluid Power, (1979), 41-46.

6. Needelman, W.M., "Fluid Particulate Contamination, Component Wear and Performance", Fundamentals of Tribology, Ed.N.P.Suh and N.Saka, The MIT Press, 1980, 555-566.

7. Watanabe, S., K.Saki, S.Asanabe and M.Fukutomi, "Evaluation for Wear Life of Journal Bearing Lubricated by Contaminanted Oils", Proc.of The JSLE Int.Tribology Conf., Japan, (1985), 85-90.

8. Jahanmir, S., "Future Directions in Tribology Research", J. of Tribology, Trans.of ASME, 109 (1987), 207-214.

9. Seehra, R.S., T.V.Balasubramanian, and J.Lal, "Wear Technology and Its Realisation", Tribology Int., (1978), 43-47.

10. Jost, H.P., Report on Lubrication (Tribology) Education and Research, HMSO, London, 1966.

11. Ko, P.L., "Metallic Wear -- A Review with Special References to Vibration Induced Wear in Power Plant Components", Tribology Int., 20 (1987) 66-78.

12. Burwell, J.T.,"Survey of Possible Wear Mechanisms" Wear, 1 (1958), 119-141.

13. Khrushchov, M.M.,"Resistance of Metals to Wear by Abrasion as Related to Hardness", Proc.Int.Conf.on Lubrication and Wear, I.Mech.E., London, (1957), 655-659.

14. Hirano, F. and S.Yamamoto,"Four-ball Test on Lubricating Oils Containing Solid Particles", Wear, 2 (1958/1959), 349-363.

15. Toporov, G.V.,"The Influence of Structure on the Abrasive Wear of Cast Iron", Friction and Wear in Machinery, ASME, New York, Vol.12, 1960, 39-59.

16. Rabinowicz, E., L.A.Dunn, and P.G.Russell,"A Study of Abrasive Wear under Three-body Conditions", Wear, 4 (1961), 345-355.

17. Rabinowicz, E., Friction and Wear of Materials, J.Wiley, New York, 1965.

18. Wahl, H.,"A Survey of the Field of Wear", Metalen, 9 (1954), 4-6.

19. Khrushchov, M.M. and M.A.Babichev," Experimental Fundamentals of Abrasive Wear Theory", Russian Eng. J., 44, 6 (1964), 43-47.

20. Richardson, R.C.D.,"The Wear of Metallic Materials by Soil-Practical Phenomena", J.Agric.Eng.Res., 12, (1967), 22-29.

21. Richardson, R.C.D.,"The Wear of Metals by Relatively Soft Abrasives", Wear, 11 (1968), 245-275.

22. Nathan, G.K. and D.Jones,"The Influence of the Hardness of Abrasives on the Abrasive Wear of Metals", Proc.Fifth Lubrication and Wear Conv., I.Mech.E., London, (1967), Paper 24.

23. Tabor, D.,"Mohs Hardness Scale -- A Physical Interpretation", Proc. Phys. Soc., B67 (1954), 249-257.

24. Richardson, R.C.D.,"The Wear Of Metals by Hard Abrasives", Wear, 10 (1967), 291-309.

25. Richardson, R.C.D.,"The Maximum Hardness of Strained Surfaces and the Abrasive Wear of Metals and Alloys", Wear, 10 (1967), 353-382.

26. Nathan, G.K. and W.J..Jones,"The Empirical Relationship between Abrasive Wear and the Applied Conditions", Wear, 9 (1966), 300-309.

27. Larsen-Badse, J.,"Influence of Grit Diameter and Specimen Size on Wear during Sliding Abrasion", Wear, 12 (1968), 35-53.

28. Broeder, J.J. and J.W.Heijnekamp,"Abrasive Wear of Journal-Bearings by Particles in the Oil (Apparatus, Experiments, and Observations)", Proc.Instn.Mech.Engrs., 180 (1965-66), 21-31.

29. Wright, K.H.R.,"Mechanisms of Wear", Tribilogy Handbook, Ed. M.J.Neale, Halsted Press, New York, 1973.

30. Stroud, M.F. and H.Wilman,"The Proportion of the Groove Volume Removed as Wear in Abrasion of Metals", Brit.J.of Appl.Phys., 13 (1962), 173-178.

31. Mulhearn, T.O. and L.E.Samuels,"The Abrasion of Metals : A Model of the Process", Wear, 5 (1962), 478-498.

32. Scott, W.,"Relationship between Solid Particle Contaminant Size and Thickness of Oil Films in Hydraulic Systems",I.Mech.E., (1976), 93-100.

33. Tessmann, R.K.,"Summary of FPRC Wear Mechanism Study", The BFPR Journal, 11, 2 (1977), 217-222.

34. Tessmann, R.K. and E.C.Fitch,"Contaminant Induced Wear Debris for Fluid Power Components", I.Mech.E., (1978), 127-130.

35. Suh, N.P., H.C.Sin and N.Saka,"Fundamental Aspects of Abrasive Wear", Fundamentals of Tribology, Ed.N.P.Suh and N.Saka, The MIT Press, 1980.

36. Misra, A.,"A Study of Abrasive Wear", (Unpub. Ph.D. Dissertation, University of California, Berkeley, 1979.)

37. Misra, A. and I.Finnie,"A Classification of Three-body Abrasive Wear and Design of a New Tester",Wear, 60 (1980),111-121.

38. Misra, A. and I.Finnie,"An Experimental Study of Three -body Abrasive Wear", Proc.Third Int.Conf.on Wear of Materials, ASME,(1981), 426-431.

39. Misra, A. and I.Finnie,"On the Size Effect in Abrasive and Erosive Wear", Wear, 65 (1981), 359-373.

40. Misra, A. and I.Finnie,"Correlation between Two-body and Three-body Abrasion and Erosive Wear of Metals", Wear, 68 (1981), 33-39.

41. Misra, A. and I.Finnie,"A Review of The Abrasive Wear of Materials", Trans.ASME, 104 (1982),94-101.

42. Peterson, M.B.,"Classification of Wear Process", Wear Control Handbook, Ed.M.B.Peterson and W.O.Winer, ASME, New York, 1980, 9-15.

43. Archard, J.F.,"Wear Theory and Mechanisms", Wear Control Handbook, Ed.M.B.Peterson and W.O.Winer, ASME, New York, 1980, 35-80.

44. Rabinowicz, E.,"Wear Coefficients -- Metal", Wear Control Handbook, Ed.M.B.Peterson and W.O.Winer, ASME, New York, 1980, 475-506.

45. Godet, M.,"Mechanics versus or with Materials in the Understanding of Tribology", Lub. Eng., 40, 7 (1984), 410-414.

46. Zum Gahr, K.H.,"Formation of Wear Debris due to Abrasion", Wear of Materials, ASME, 1981, 396-405.

47. Chen, N.P. and Y.J.Liu,"Shape and Microstructure of Abrasive Wear Debris", Wear of materials, ASME, 1983, 19-25.

48. Burr, B.H.,"An Equation for the Abrasive Wear of Elastomeric O-Ring Materials", Wear, 81 (1982), 347-356.

49. Zum Gahr, K.H. and D.Mewes,"Severity of Material Removal in Abrasive Wear of Ductile Metals", Wear of Materials, ASME, 1983, 130-139.

50. Tong, J.M., Y.Y.Sun, H.Y.Zhang, and X.W.Kong,"Investigation of Abrasive Wear Resistance and Wear Mechanism of Composite Alloys", Tribology Int., 18, 2 (1985), 101-105.

51. Odi-Owei, S. and B.J.Roylance,"Lubricated Three-body Abrasive Wear -- Contaminant Condition versus Bounding Surface Material Hardness", Tribology Int., 20, 1, (1987), 32-40.

52. Sasada, T., N.Emori, and M.Oike,"The Effect of Abrasive Grain Size on the Transition between Abrasive and Adhesive Wear", Wear of Materials, ASME, 1983, 26-31.

53. Kosel, T.H. and C.M.Rao,"The Size Effect in Abrasion of Dual-Phase Alloys", Trans. ASLE, 28, 3 (1984), 343-350.

54. Odi-Owei, S. and B.J.Roylance,"The Effect of Solid Contamination on the Wear and Critical Failure Load in a Sliding Lubricated Contact", Wear, 112 (1986), 239-255.

55. Moore, M.A. and P.A.Swanson,"The Effect of Particle Shape on Abrasive Wear : A Comparison of Theory and Experiment", Wear of Materials, ASME, 1983, 1-11.

56. Swanson, P.A. and A.F.Vetter,"THe Measurement of Abrasive Particle Shape and Its Effect on Wear", Trans. ASLE, 28, 2 (1984), 225-230.

57. Kato, K., K.Hokkirigana, T.Kayaba, and Y.Endo,"Three-Dimensional Shape Effect on Abrasive Wear", Trans. ASME, 108 (1986), 346-351.

58. Larsen, B.J. and B.Premratne,"Effect of Relative Hardness on Transitions in Abrasive Wear Mechanism", Wear of Materials, ASME, 1983, 161 -166.

59. Rabinowicz, E.,"The Wear of Hard Surfaces by Soft Abrasives", Wear of Materials, ASME, 1983, 12-18.

60. Xuan, J.L.,"Attrition Characteristics of Abrasive Particles under Lubricated Conditions", The TSF Journal, 5 (1986), 65-68.

61. Eleftherakis, J.G.,"Effect of Composite Contaminants on the Wear of Ball Type Valves", (Unpub. M.S.Thesis, Oklahoma State University, Dec.1986)

62. Ikramov, U.,"Abrasive Wear Mechanism", Proc. Fourth European Tribology Congress, IV., Section 5-3, (1985)

63. Fitch, E.C., Hydraulic Failure -- Analysis and Prevention, FES,Inc., 1984.

64. Inoue, R.,"Surface Contact Wear And Abrasive Wear in Lubricated Sliding Mechanisms",(Unpub.Ph.D. Dissertation, Oklahoma State University, 1982)

65. Hong, I.T.,"Sliding Contact Wear Caused by Loose Abrasive Particles in Interfacing Lubricant -- Part 1 : Related Literature Survey", The

BFPR Journal, 15, 1 (1982), 43-48.

66. Hong, I.T.,"Effects of System Filtration Characteristics on Tribological Wear of Rotating Elements", (Unpub. Ph.D. Dissertation, Oklahoma State University, 1983)

67. Ito, T., I.Khalil, and I.T.hong,"Abrasive Wear under Hydrodynamic Lubrication : Part 1 -- Theoretical Development", The FRH Journal, 5, (1984) 125-130.

68. Khalil, I., T.Ito, and I.T.Hong,"Abrasive Wear under Hydrodynamic Lubrication : Part 2 -- Procedure and Experimental Verification", The FRH Journal, 5, 2 (1984) 131-136.

69. Luo, C.W.,"The Effects of Wedge Angles of Abrasive Particles on Three-body Abrasive Wear -- An Analysis on Three-body Abrasive Wear", The BFPR Journal, 18, 1 (1984), 201-208.

70. Xuan, J.L.,"Zeta Rating -- An Investigation of Contaminant Abrasivity -- Part 1 and 2 : Theoretical and Experimental Fundamentals", The TSF Journal, 7 (1986), 19-35.

71. Xuan, J.L.,"Characterization of Three-body Abrasion Mechanisms", The TSF Journal, 8 (1987),69-76.

72. Fitch, E.C.,"The Developing Science of Contamination Control",Fluid and Lubricant Iders, July/August, (1981), 23-27.

73. Cantrell, D.N.,"Effective Contamination Control from Piece Part to Complete Unit", Proc.Nat.Conf.of Fluid Power, (1977), 102-105.

74. Gram, M.D.,"Contamination Control -- A Hydraulic Design Parameter", Proc.Nat.Conf.of Fluid Power, (1979), 37-40.

75. Peterson, M.B. and A.J.Koury,"Tribological Failures and Mechanical Design", Tribilogical Technology, II., Ed.P.B.Senhdzi, Martinus Nijhoff Publisher, 1982, 499-534.

76. Fitch, E.C., The FPRC Approach to Condition Monitoring, Report No.61182, Fluid Power Research Center, Oklahoma State University, Stillwater, OK, 1982.

77. Spencer, J.B.,"Effective Contamination Control in Fluid Power Systems", Industrial Tribology, Ed.M.H.Jones and D.Scott, Elsevier Scientific Publishing

Company, 1983, 291-329.

78. Ronen, A., S.Malkin, and K.Loewy,"Wear of Dynamically Loaded Hydrodynamic Bearings by Contaminant Particles", Trans.ASME, 102 (1980) 452-458.

79. Eyre, T.S., N.Dent, and P.Dale,"Wear Characteristics of Piston Rings and Cylinder Liners", Lub. Eng., April, (1983), 216-221.

80. Sudarshan, T.S. and S.B.Bhaduri,"Wear in Cylinder liners", Wear, 91 (1983), 269-279.

81. Steele, F.M.,"Contamination Control in Turbomachinery Oil Systems", Lub. Eng., August, (1984), 487-496.

82. Quintas, A.C.,"Monitoring Equipment Wear in a Paper and Pult Plant", Lub.Eng., Nov. (1984), 648-658.

83. Stecki, J.S.,"Condition Monitoring of Jet Engines", Lub.Eng., August (1985), 485-493.

84. South, C.T.,"Aircraft Hydraulic Supply Circuit Health Monitoring", Proc.7th Int.Fluid Power Symposium, Bath, England, (1986), 295-302.

85. Scott, D.,"Particle Tribology", Proc.Instn.Mech.Engrs., Vol.189 (1976), 623-629.

86. Hunt, T.M.,"A Review of Condition Monitoring Techniques Applicable to Fluid Power Systems", Proc.7th Int. Fluid Power Symposium, Bath, Engiand, (1986), 285-294.

87. Tessmann, R.K. and L.E.Bensch,"What's Ahead in Fluid Power Contamination Control", Proc.Nat.Conf.on Fluid Power, (1976), 341-353.

88. Fitch, E.C. and I.T.Hong, Pump Contaminant Sensitivity --An FPRC Position Report", Unpub.Report to ISO /TC-131/SC-8/WG-8, Fluid Power Research Center, Oklahoma State University, Stillwater, OK.,1984.

89. Fitch, E.C.,"Filter Selection Based on Component Sensitivity Analysis", Fluid Power Research Conf., Paper No.P75-7, (1975), 7.1-7.8.

90. Fitch, E.C. and R.K.Tessmann,"Controlling Contaminant Wear through Filtration", Fluid Power Research Conf., Paper No.P75-9, (1975), 9.1-9.8.

91. Wolf, M.L., Contaminant Particle Effects as A Function of Size, Type, and Concentration, Report R 65-9,

Fluid Power Research Center, Oklahoma State University, 1965.

92. McBurnett, J.R., Contaminant Sensitivity of Fluid Power Pumps, Basic Fluid Power Research Program Annual Report No.5, Sec.71-2, Oklahoma State University, Stillwater, OK, 1971.

93. Bensch, L.E. and E.C.Fitch,"A New Theory for the Contaminant Sensitivity of Fluid Power Pumps", Basic Fluid Power Research Program Conf., Paper No.72-CC-6, Oklahoma State University, Stillwater, (1972).

94. Bensch, L.E.,"Pump Contaminant Sensitivity Analysis", Basic Fluid Power Research Program Conf., Paper No.72-CD-1, Oklahoma State University, Stillwater, (1972).

95. Fitch, E.C.,"The Tolerance of Fluid Machinery to Contaminant Wear", Proc.2rd.Int.JSME Symp.on Fluid Machinery and Fluidics, Tokyo, Japan, (1972).

96. Fitch, E.C.,"Fluid Contamination Control -- Its Tech-Nological Status", Proc.Int.Congress on Fluids Contamination, 4th Italian Exhibition of Oleo-Hydraulic Pneumatic Equipments and Lubrication, Milano, Italy, (1974).

97. Fitch, E.C.,"Component Contaminant Sensitivity -- A Status Report on Pump", Proc.Nat.Conf.on Fluid Power, also Presented at ISO/TC-131/SC-6 Meeting, London, (1974).

98. Tessmann, R.K.,"Non-Intrusive Analysis of Contaminant Wear in Gear Pumps through Ferrography", (Unpub. Ph.D. Dissertation, Oklahoma State University, Stillwater, OK, 1977)

99. Inoue, R. and E.C.Fitch,"The Omega Pump Rating System", The BFPR Journal, 12 (1979), 141-144.

100. Inoue, R.,"The Pump Omega Distribution", The BFPR Journal, 12, 2 (1980), 99-101.

101. Lawrence, M.D.,"A Brief Report about the Pump Contaminant Sensitivity Test at CETIM", CETOP Communal Research, 7/8, June , 1983.

102. Winner, D.,"Wear Sensitivity of Various Pump Units", Olhydraulik und Pneumatik, 28, 4 (1984).

103. Xia, Z.X.,"A Review on the Theory and Test of Pump

Contaminant Wear", The BFPR Journal, 17, 2 (1984), 303-309.

104. Fitch, E.C. and I.T.Hong,"Pump Contaminant Sensitivity -- Part 1 : An Overview of the Omega Theory", The FRH Journal, 6 (1985), 41-51.

105. Fitch, E.C. and I.T.Hong,"Pump Contaminant Sensitivity -- Part 2 : The Linear Omega Life Model", The FRH Journal, 6 (1985), 53-61.

106. Xuan, J.L.,"Pump Contaminant Sensitivity -- Part 3 : An Updated Pump Contaminant Sensitivity Analysis Program", The FRH Journal, 6 (1985), 63-68.

107. Hong, I.T. and E.C.Fitch,"Wear of Gear Pump under Abrasive Fluid Conditions", Proc.Nat.Conf.on Fluid Power, Chicago, (1986), 387-393.

108. Izawa, K. and S.Rao,"Servovalve Contaminant Sensitivity -- Part 1-4", The BFPR Journal, 17, 1 (1984), 113 -144.

109. Hong, I.T. and E.C.Fitch,"Contaminant Sensitivity of Electrohydraulic Servovalves", Proc.Int.Conf. on Fluid Power, Tampere University of Technology, Finland, (1987).

110. Fitch, E.C., "Hydraulic Component and System Assessment Manual", The BFPR Journal, 20 (1986).

111. Inoue, R.,"Antiwear Characteristics of Fire Resistant Fluids -- Results of The Gamma Falex Tests", The FRH Journal, 3, 1 (1982), 45-49.

112. Silva, G.,"A Study of the Synergistic Effect of Pump Wear", Research Proposal, Oklahoma State University, Feb., 1987.

113. Taylor, R. and Y.Y.Wang,"The Effect of Fluid Properties on Bearing Parameters : Part 1", The FRH Journal, 4, 2 (1983), 161-168.

114. Zhang, J. and Y.Y Wang,"Antiwear Characteristics of Hydraulic Fluids", The FRH Journal, 5, 1 (1984), 9-16.

115. Xuan, J.L.,"The Gamma System and Surface Contact Wear Investigation", The FRH Journal, 6 (1985),129-135.

116. Eleftherakis, J.G.,"The Sigma -- An Approach in Evaluating Fluid Synergistics", The TSF Journal, 7 (1986), 1-7.

117. Eleftherakis, J.G.,"Gamma System Qualification -- Part 1 : Surface Contact Gamma", The TSF Journal, 7 (1986), 8-14.

118. Eleftherakis, J.G.,"Identifying Fluid Antiwear Characteristics under Boundary Lubrication using the Gamma System", Proc.Nat.Conf.on Fluid Power, (1986), 395-400.

119. Inoue, R.,"Gamma Rating and Zeta Rating -- Effects of Fluid and Contaminant Abrasivity on Component Wear Life", The FRH Journal, 4, 2 (1984),

120. Xuan, J.L.,"The Zeta Concept -- Contaminant Abrasivity Rating", The BFPR Journal, 19 (1985), 29-35.

121. Halling, J., Principles of Tribology, Tinling Ltd., 1975.

122. Moore, D.F., Principles and Applications of Tribology, Pergamon Press, New York, 1975.

123. Raimondi, A.A. and J.Boyd,"A Solution for the Finite Journal Bearings and Its Application to Analysis and Design", Trans.ASCE, 1 (1958), 159-209.

124. Bell, F.G., Engineering Properties of Solid and Rocks, Whitstable Litho Ltd., 1983.

125. Kalpakjiam, S., Manufacturing Processes for Engineering Materials, Addison-Wesley Publishing Company, 1985.

126. Iwanaga, M.,"Contaminant Service Life and Cost of Hydraulic System",(Unpub.Ph.D. Dissertation, Oklahoma State University, Stillwater,OK, 1980)

127. McCarthy, D.F., Essentials of Soil Mechanics and Foundations, Reston Publishing Company, 1977.

128. Lambe, T.W. and R.V.Whitman, Soil Mechanics, John Wiley and Sons, Inc., 1969.

129. Boothroyd, G., Fundamentals of Metal Machining, Hemisphere Publishing, New York, 1985.

130. Hill, R., The Mathematical Theory of Plasticity, Oxford Press, Oxford, 1964.

131. Gringweig, J.T., M.Longman, and N.J.petch,"Calculations and Measurements of Wedge-Indentation", J. Mech. Phy.Solids, 2 (1954), 81-86.

132. Silva, G.,"Selection and Operation of Fixed Displace-ment Pumps for Different Fluids : Part 2 -- Selection and Operation Approach", The FRH Journal, 6 (1986), 77-80.

133. Smyrloglou, E.,"A Study on the Shape of AC Fine Test Dust", Research Report 3.3.1, Millipore Co., 1979.

134. Walker, D.L.,"Misconceptions about Automatic Counters", Contamination Control, Sept. (1969), 15-21.

APPENDIX A

THREE-BODY ABRASIVE WEAR TEST PROCEDURE

Procedure of Lubricated Three-body Abrasive Wear Test

1. Clean the fluid resevoir and circulating system. Remove all oil and water residue from the system.
2. Clean the test journal and bearings.
   2.1 Rinse journal and bearings with petroleum ether.
   2.2 Put journal in oven at 80 degree centigrade for 6 minutes.
   2.3 Put journal in cooling jar to remove moisture for 6 minutes.
3. Weight and record the initial weight of the journal to the nearest micrograms.
4. Measure the journal surface roughness in micrometers.
5. Install test journal and bearings.
6. Fill the resevoir with 350 milliliters of test fluid. This amount of fluiod will cover the load jaws so that the journal and the bearings are completely submerged.
7. Heat the test fluid and adjust temperature to the specified level plus or minus 2 degrees centigrade.
8. Circulate the clean test fluid through the test circuit while heating.
9. Put the specified amount of test abrasive particles in a clean glass container and inject into test fluid.
10. During test, circulate fluid in test circuit to maintain constant contaminant distribution throughout test fluid for the duration of the test.

11. Rotate the journal at 3000 revolutions per minute. Apply the desired load and maintain the test condition constant.
12. At the desired time interval or the end of 30 minutes, decrease the load to zero, stop the drive motor and pump, drain the test fluid, and remove the journal and bearings.
13. Clean the test journal according to step 2.
14. Reweigh the journal according to step 3. The weight loss of the test journal represents the amount of abrasive wear in 30 minutes.

APPENDIX B

PARTICLE COUNTING DATA

TABLE XXII

PARTICLE COUNTING DATA IN TEST USING ACFTD

Time / Size (um)	0 (min)	3	6	9	12	15	30
> 5	5940	6065	6141	6396	6902	6849	7022
> 10	1414	1438	1460	1583	1618	1640	1634
> 20	224	285	227	243	238	215	237
> 30	82	85	88	94	95	70	84
> 40	25	27	29	26	33	13	22
> 50	9	12	16	12	11	6	12
5-10	4526	4603	4681	4813	5284	5209	5388
10-20	1190	1211	1233	1340	1380	1425	1397
20-30	142	141	140	149	143	145	153
30-40	57	57	58	68	62	58	61
40-50	16	15	14	14	22	8	10

TABLE XXIII

PARTICLE COUNTING DATA IN TEST USING IRON POWDER

Size (um) \ Time (min)	0	3	6	9	12	15	30
> 5	7331	6316	5842	5956	5805	5917	6120
> 10	2385	1875	1644	1693	1660	1608	1675
> 20	310	225	206	206	204	188	214
> 30	65	48	54	54	47	47	53
> 40	18	17	18	22	19	18	22
> 50	7	7	10	8	10	9	10
5-10	4946	4441	4198	4263	4145	4309	4445
10-20	2075	1651	1438	1487	1456	1420	1461
20-30	245	177	153	151	157	141	161
30-40	47	30	35	32	28	29	31
40-50	12	10	9	14	10	10	12

TABLE XXIV

PARTICLE COUNTING DATA IN TEST USING GLASS BEADS

Size (um) \ Time (min)	0	3	6	9	12	15	30
> 5	3210	4065	4808	4925	5083	5386	6382
> 10	938	1065	1077	1178	1208	1243	1398
> 20	283	268	279	316	319	330	299
> 30	119	108	112	127	130	132	105
> 40	46	38	29	49	50	48	41
> 50	17	14	10	12	24	23	16
5-10	2272	3000	3731	3747	3875	4143	4984
10-20	655	797	798	862	889	913	1099
20-30	164	160	167	189	190	198	194
30-40	73	71	83	78	79	85	64
40-50	25	23	20	37	26	25	25

TABLE XXV

PARTICLE COUNTING DATA IN TEST USING Al_2O_3

Size (um) \ Time (min)	0	3	6	9	12	15	30
> 5	2728	3413	3765	3528	3342	3157	3673
> 10	628	803	819	641	631	622	702
> 20	148	166	172	117	105	94	98
> 30	96	98	107	69	61	53	49
> 40	80	80	90	62	53	44	38
> 50	58	58	72	48	41	33	29
5-10	2100	2610	2946	2887	2711	2535	2974
10-20	480	637	647	524	526	528	604
20-30	52	68	65	48	45	41	50
30-40	16	19	17	8	9	10	10
40-50	22	22	18	13	12	10	10

VITA

Jia-Luo Xuan

Candidate for the Degree of

Doctor of Philosophy

Thesis: THREE-BODY ABRASION SENSITIVITY OF TRIBO-MECHANICAL COMPONENTS UNDER FLUID FILM LUBRICATION

Major Field: Mechanical Engineering

Biographical:

Personal Data: Born in Changsha, China, November 25, 1950, the son of Mr. and Mrs.Sun-Tung Xuan; married in Shanghai, China, March, 1978, to Xing Zhou. Beget Lan Xuan, December 15, 1979.

Education: Graduated from The Shanghai Middle School, Shanghai, China, in June, 1966; received the Diploma (1979) and the Master of Engineering Science degree(1981) from Shanghai University of Technology, Shanghai, China, with a major in Mechanical Engineering; completed requirements for the Doctor of Philosophy degree at Oklahoma State University in May, 1988.

Professional Experience: Assistant Lecturer (11/1981 - 11/1982) and Lecturer (11/1982 - 11/1983) at the Mechanical Engineering Department,Shanghai University of Technology, Shanghai, China; Project Assistant (8/1984 - 8/1985), Project Associate (8/1985 - 12/1987), and Project Engineer (1/1988 - present) at Fluid Power Research Center, Oklahoma State University; Graduate Teaching Assistant (8/1986 - 5/1987) at the Mechanical and Aerospace Engineering School, Oklahoma State University, Stillwater, OK, 74078.

Professional and Academic Affiliations: Society of Tribologists and Lubrication Engineers; Fluid Power Society; American Society of Mechanical Engineers; National Society of Professional Engineers.